Pergamon

PII: S0079-6611(97)00012-8

Prog. Oceanog. Vol. 39, pp. 263–352, 1997

Printed in Great Britain
0079-6611/97 $32.00

On the total geostrophic circulation of the pacific ocean: flow patterns, tracers, and transports

JOSEPH L. REID

Marine Life Research Group, Scripps Institution of Oceanography, 9500 Gilman Dr., La Jolla, California 92093-0230, U.S.A.

Abstract – The large-scale circulation of the Pacific Ocean consists of two great anticyclonic gyres that contract poleward at increasing depth, two high-latitude cyclonic gyres, two westward flows along 10° to 15° north and south that are found from the surface to abyssal depths, and an eastward flow that takes place just north of the equator at the surface and at about 500m, but lies along the equator at all other depths.

This pattern is roughly symmetric about the equator except for the northward flow across the equator in the west and the southward flow in the east.

As no water denser than about 26.8 in σ_0 is formed in the North Pacific, the denser waters of the North Pacific are dominated by the inflow from the South Pacific. Salinity and oxygen in the deeper water are higher in the South Pacific and the nutrients are lower. These characteristics define recognizable paths as they move northward across the equator in the west and circulate within the North Pacific. Return flow is seen across the equator in the east. Part of it turns westward and then southward with the southward limb of the extended cyclonic gyre, and part continues southward along the eastern boundary and through the Drake Passage.

The important differences from earlier studies are that the equatorial crossings and the deep paths of flow are defined, and that there are strong cyclonic gyres in the tropics on either side of the equator.

CONTENTS

1. INTRODUCTION

This is the fourth of a series of studies of the large-scale circulation of the Atlantic and Pacific oceans. The first and second of these (REID, 1986, 1989) dealt with the South Pacific and South Atlantic, and the third (REID, 1994) with the North Atlantic.

The purpose of the present study is to estimate the general circulation of the entire Pacific Ocean in a manner that defines the flow at all depths and balances the total top-to-bottom geostrophic transport. The estimation is made through a new examination of the characteristics and the geostrophic shear. The method is the same as used in the earlier studies.

The two major assumptions used herein are that the flow is geostrophic and that both flow and mixing take place approximately along isopycnal surfaces. Characteristics acquired where the isopycnals outcrop, or in the case of the non-conservative characteristics by respiration or dissolution, are modified along the flow by both lateral and vertical diffusion. Some tracers show both lateral and vertical extrema in concentration and their patterns can be used to estimate the sense of flow.

The baroclinic flow is given by the density field, that is, the geostrophic flow relative to the bottom flow, which is estimated from examination of the various characteristics and taken as the reference velocity. The density field is defined fairly well over most of the Pacific Ocean by the present data set. While the flow is known to vary with time, the large-scale flow below the upper layer appears to be steady enough to allow data sets from different periods to be combined and the general circulation to be examined usefully.

The characteristics used as tracers have various sources and lie in various ranges of depth and density, and are spread throughout the ocean by both flow and mixing. Their patterns are examined along vertical sections and along isopycnal surfaces. In some density ranges the patterns are sharply defined and show features that appear to be the result of advection rather than horizontal diffusion alone. These and other patterns, both shallower and deeper, can in some places indicate flow components at different depths that are in opposite senses, and with the measured baroclinic component, constrain the value of the reference velocity to a narrow range.

The area studied is shown in Fig. 1 on a Mollweide projection, with the pertinent topographic features labeled. The array of stations used in determining the fields of adjusted steric height and volume transport (Table 1 and Fig. 2) is selected to include stations that reached near the bottom and, where it is possible, long lines made by a single ship roughly normal to major flows. Some combinations of stations from different expeditions are needed to complete lines. For the Pacific 2087 stations are selected for calculating the fields of flow, and they are identified in Table 1. A much larger set of stations (5258) is used on the isopycnal maps.

The work was carried out in two stages. First, on selected lines of stations (Fig. 2), components of geostrophic motion are calculated relative to the deepest common depth of each consecutive station pair and compared with the tracer patterns. If necessary a reference velocity is added to achieve the sense of flow assumed from the tracer patterns for that pair of stations. The adjusted flows normal to the station pairs along these lines define adjusted pressure gradients along the lines, and these are integrated horizontally to obtain the adjusted steric height.

A second stage is necessary because no constraint of continuity is used in the first stage, and the resulting transport across the line of stations may not be in balance. Transport into the Pacific Ocean south of Australia is taken to be $135 \times 10^6 m^3/sec$. The transport from the Pacific Ocean into the South Atlantic through the Drake Passage is taken to be $130 \times 10^6 m^3/sec$ (WHITWORTH *et al.*, 1982). Transport from the North Pacific into the Indonesian seas and the Indian Ocean is taken to be $3 \times 10^6 m^3/sec$ and through the Bering Sea into the Arctic Ocean is taken to be $2 \times 10^6 m^3/sec$. Further adjustments to match these constraints and to balance the transport at the intersections of the selected lines required very little change in the reference velocities and resulting flow patterns.

Except for the specified net transports through the Drake Passage, northward between the continents, and north and south of Australia, the only constraint applied herein is quite simple: that the large-scale flow should be qualitatively coherent with the tracer patterns. No constraint on heat or salt transport is applied and no Ekman transport accommodated.

2. THE DATA PRESENTATION

All of the illustrations have been placed after the text. As some of them will be referred to in different sections of the text it seems easier to have them grouped in order of surface maps, vertical sections, maps of geostrophic flow, and maps of characteristics along isopycnals. The isopycnals are labelled at different values as the depth varies, as in REID and LYNN (1971). Table 2 lists the range of numbers for each isopycnal. The figures are labelled with the densest (deepest) value for each isopycnal. The reader may wish to look at the figures before reading the sections that follow.

3. THE NEAR-SURFACE WATERS

The surface maps (Fig. 3a–3g) represent southern summer (November through April) as there was not enough southern winter data in the far south.

The maps of temperature and salinity are not significantly different from other versions. The highest density in the north is a little more than 26.6 in σ_0, off Kamchatka and in the Okhotsk Sea. In the south, in southern summer, the highest value is about 27.3, though winter values may exceed 27.5 near 60°S and 27.75 in the Ross Sea.

The oxygen pattern is dominated by the temperature field, with the highest oxygen in the colder waters in high latitudes and the lowest near the equator. The phosphate, nitrate, and silica are highest in the cyclonic gyres of high latitudes and along the upwelling zones near the equator and along the eastern boundary, and lowest within the anticyclonic gyres.

4. THE PRINCIPAL LAYERS

The deeper characteristics of the Pacific Ocean have been illustrated on other long top-to-bottom vertical sections (REID, 1965, 1986: STOMMEL *et al.*, 1973; GORDON and MOLINELLI, 1982; KENYON, 1983; SIEVERS and NOWLIN, 1984; TALLEY *et al.*, 1991; ROEMMICH *et al.*, 1991; TSUCHIYA and TALLEY, 1996), and others, from the World Ocean Circulation Experiment, are in preparation. Only one section, from Alaska to Antarctica is presented here.

The densest abyssal water found in the Pacific is not from the Weddell Sea but is formed in the Ross Sea (JACOBS *et al.*, 1970; GORDON, 1971), and is confined south of the Pacific Antarctic Rise. It is about 46.12 in σ_4, – 0.2° in potential temperature, and 34.70 to 34.71 in salinity, and 5.2 to 5.4 ml/l in oxygen (Fig. 4a–4g).

The densest waters north of the Pacific Antarctic Rise are about 46.00 in σ_4, 0° to 0.5° in potential temperature, 34.68 to 34.70 in salinity, and 5.0 to 5.1 ml/l in oxygen. They may contain waters from farther west or from the less-dense part of the Ross Sea that have flowed across the Rise near 160°E to 175°E. Waters as dense as 46.00 in σ_4 extend northward only to about 46°S just south of New Zealand.

Waters denser than 46.06 in σ_4 do not extend eastward through the Drake Passage. Instead they must recirculate in the South Pacific and mix with the less-dense overlying waters before departing. The densest waters leaving the Pacific through the Drake Passage are about 46.06 in σ_4, 0° to 0.1° in potential temperature, and 34.68 in salinity. They are denser, colder, and less saline than any waters north of the Pacific Antarctic Rise.

The water that reaches the North Pacific is much less dense. It has turned northward from the circumpolar current. As it reaches the equator its density is about 45.95 in σ_4, and its potential temperature and salinity are about 0.80°C and 34.71. This is denser, colder, and less saline than any of the water found at the saddle point near 40°N in the Atlantic, where dense waters from the Greenland Sea pour over the Denmark Strait and meet those from the Weddell Sea at the bottom. The density there is about 45.91 in σ_4 and the potential temperature and salinity about 1.80°C and 34.89, (MANTYLA and REID, 1983). The abyssal waters found at the equator in the Pacific must have a component of water from the colder, less saline, and denser Circumpolar Water to achieve these characteristics, though they have been mixing with the overlying warmer and more saline water from the northern North Atlantic. The abyssal temperatures and salinities have been raised, and those of the North Atlantic waters above have been lowered, by this mixing as they have passed from their Atlantic sources around Antarctica and into the Pacific

(REID and LYNN, 1971). Geothermal heating also contributes to the general warming of the abyssal waters (KNAUSS, 1962; GORDON and GERARD, 1970; SUDO, 1983; JOYCE *et al.*, 1986).

The deep salinity maximum that has originated in the Atlantic has also been eroded from the top. At 40°S in the Atlantic it is found at a density near 36.98 in σ_2 at about 2500 m and the density has changed to about 37.02 at 40°S in the Pacific. From there northward the maximum is found at successively greater densities and depths and at lower salinities to about 37.09 in σ_2, or 45.94 in σ_4 near 10°S at depths below 4000 m. It is last seen near 10°S. Vertical exchange with the overlying less-saline waters has depressed it in the column to a density greater than that of the saddle point in the Atlantic. Below the Intermediate Water in the North Pacific the salinity increases downward to the bottom everywhere: there is no deep vertical salinity maximum above the bottom in the North Pacific.

The mid-depth layer of low oxygen and high nutrients lying near 2000 m at 30°S is the most obvious signal of the return flow of the denser waters that enter the North Pacific. It takes place after diffusive exchange with the overlying waters has reduced their density to a value somewhere between that of the incoming deeper waters and that of the Intermediate Water. Respiration has lowered the oxygen concentration and raised the phosphate and nitrate concentration, and dissolution has raised the silica concentration.

Salinity is low at the surface in the high latitudes both north and south and extends equatorward as vertical minima beneath the less dense waters of lower latitudes. The salinity along these minima is raised away from the sources by vertical diffusion, and in the tropical zone they meet as a lateral maximum in salinity. Surface densities are much higher in the southern high latitudes and the extension from the south is denser, reaches greater depths, and covers a wider area in the tropics than the northern extension. There are shallower minima deriving from the surface at lower latitudes in both the North and South Pacific (REID, 1973b; YUAN and TALLEY, 1992) but they are of smaller lateral extent.

Sea-surface salinity is highest near the tropics and vertical diffusion raises the salinity of the waters in the thermocline. As these extend equatorward they appear as subsurface salinity maxima beneath the lower density surface water between the tropic circles.

5. SURFACE CIRCULATION

The major features of the surface circulation (Fig. 5a) are the two anticyclonic gyres with axes along about 20°N and 20°S, the cyclonic gyres along about 50°N and 65°S, and an eastward flow from coast to coast along about 5°N. There is a weaker eastward flow near 5°S west of about 175°W and a westward flow just south of Australia.

The map of adjusted steric height at the sea surface shows all of these features. It is not made up from averaged or synoptic data sets but from the sections chosen from the available data that reached the bottom (Fig. 2), and these are from different years and seasons. It will differ in some detail from maps using averaged, or where possible, synoptic data. It compares quite well with the flow at the surface relative to 1000 decibars made from the most nearly synoptic large-scale data sets available. These cover the area north of 20°N in the summer of 1955, the area between 20°N and 20°S and east of about 130°W in the fall of 1955, and the area between 20°N and 20°S west of 130°W in the summer of 1966 (REID, 1961).

One feature different from Reid's (1961) map is the high value of steric height seen herein at about 42°N, 148°E. This may indicate a large eddy broken off from the Kuroshio Current instead of the northward loop as contoured. The feature can be recognized down to about 3500 m.

6. FLOW BENEATH THE SURFACE (FIG. 5B–5M)

At 200 db (decibars) the axes of the eastern anticyclonic gyres have shifted poleward in the east, to about 25° latitude, and the eastward flow is no longer near 5°N to 10°N but takes place along the equator, between about 5°N and 5°S, as shown by TSUCHIYA (1968).

The flow pattern suggests that the tropical flow includes long and narrow cyclonic gyres on either side of the equator. This pattern is found everywhere down to 4000 m, except for the depth-range of about 300 m to 500 m, where the two cyclonic gyres are separated by a westward flow along the equator.

At 500 db the flow is westward along the equator between about 5°N and 2°S, and there are eastward flows just north of it (5°N to 10°N) and south of it (2°S to 6°S) as shown by REID (1965). Some of the westward flow along 10°S to 20°S in mid-ocean turns northward across the equator in the west and feeds the eastward flow between 5°N and 10°N.

Both of the high-latitude cyclonic gyres have been shown to extend to great depths (GORDON, 1971; REID and ARTHUR, 1975; REID, 1981; WARREN and OWENS, 1988). The northern cyclonic gyre extends into the Bering Sea, which receives its waters from the westward limb of the gyre (REID, 1961, 1965; HOOD and KELLEY, 1974; FAVORITE *et al.*, 1976; REED and STABENO, 1994; COKELET *et al.*, 1996). The characteristics within the Bering Sea are modified slightly by vertical diffusion, respiration, and dissolution (RODEN, 1995) and occasionally by winter spilling of water from the eastern shelf (WARNER and RODEN, 1995). The gyre also loops into the Okhotsk Sea, and there is evidence that on the northern shelf in winter some waters denser than 26.80 in σ_0 can be formed (KITANI, 1973; TALLEY and NAGATA, 1995).

Below the surface the northern cyclonic gyre loops slightly equatorward in the east, with narrow poleward flows along the eastern boundary. The rest of the mid-latitudes are filled by the great anticyclonic gyre.

But at 800 db the axes of the two anticyclonic gyres shift poleward to about 40° latitude in the east. The cyclonic gyre in the north expands southward in the east and then westward, and the equatorward branch of the great gyre contracts westward. The result is a smaller anticyclonic gyre and a larger cyclonic gyre that extends southward in the east and westward along 30°N to about 175°W.

In the South Pacific also the anticyclonic gyre does not extend so far equatorward or eastward at 800 db as in the layers above. Some of the equatorward flow in the east turns cyclonically eastward and then poleward, much as in the North Pacific. In this case the eastward turn takes place along about 30°S, just south of the Tuamotu-Easter Island-Sala y Gomez-Nazca ridges.

The flow is eastward along the equator at 800 m and at all depths down to about 4500 db. The cross-equatorial flow in the west turns eastward along 10°N to 12°N and then back to the west along about 20°N. There it joins the westward flow of the anticyclonic gyre, which feeds the Kuroshio Current.

The pattern at 1000 db in the North Pacific is much the same as at 800 db, though the great anticyclonic gyres do not reach so far east or equatorward. Part of the westward flow along 35°N to 40°N turns back from about 160°E, flows eastward to the boundary along 20°N to 25°N and northward to join the cyclonic gyre in the north.

In the South Pacific the great gyre is partly divided by the ridge extending northward from New Zealand and there is perhaps the beginning of a southward flow east of New Zealand.

At 1500 db the pattern in the north is simpler. Part of the water from the equatorial crossing in the west flows directly northward along the western boundary to feed the anticyclonic gyre and part of it turns eastward along 20°N. At the eastern boundary part of it turns northward to join the northern cyclonic gyre and part southward to join the westward flow along 10°N to 15°N. The westward-flowing limb of the anticyclonic gyre begins farther north in mid-ocean, about 45°N, and part of the westward flow turns back to join the cyclonic gyre.

The westward-flowing limb of the southern anticyclonic gyre has also shifted both poleward and westward, and its westward limb begins near 110°W. Part of the westward flow turns southward at the western boundary, part crosses the equator in the west, and part turns back eastward from about 150°W and then southward along the boundary to the Drake Passage. Its turn-back to the circumpolar current seems to take place along the southern side of the ridge extending from the Tuamotus (16°S, 145°W) to Easter Island and the Sala y Gomez Ridge.

In the western South Pacific there are several roughly meridional ridges and several possible western boundaries for the flow. At 1500 db part of the anticyclonic gyre turns southward east of the Tonga-Kermadec Ridge, but part continues westward past Fiji and turns southward along about 175°E to about 32°S and then southeastward north of New Zealand to the southern limb of the gyre.

The South Pacific anticyclonic gyre is almost completely divided by the ridges extending northward from New Zealand. There is southward flow along both sides of the Tonga-Kermadec Ridge and there is a separate anticyclonic gyre in the Tasman Sea.

At 2000 db the flow in both oceans is much like that at 1500 db in the central basins. However, the meridional ridges along about 140°E to 145°E in the north and from New Zealand to Fiji (about 15°S) have almost cut off the Philippine and Tasman seas from the ocean to the east. They have split each of the two anticyclonic gyres into eastern and western gyres.

The connection between the Philippine Sea and the central basin near 11°N, 140°E extends almost to 5000 db but is very narrow below 3500 db. The densest water found just west of the opening is about 45.87 in σ_4, and farther west, in the Philippine Trench, it is about 45.86 in σ_4.

In the South Pacific there are western boundary currents in the Tasman Sea along Australia and along the Tonga-Kermadec Ridge. Just east of the ridge the southward flow – part of the anticyclonic gyre – can be seen as deep as 3500 db, where it begins to turn offshore at about 25°S, as it meets the northward western boundary flow which has turned northward from the circumpolar current. In the Tasman Sea the anticyclonic gyre is seen only to about 2000 db. At greater depths the Tasman Sea is cut off from the north and is supplied directly from the circumpolar current.

The southern anticyclonic gyre is all east of the Tonga-Kermadec Ridges, and part of it turns back eastward near 20°S. A northward flow is seen along the Ridge up to about 30°S, where it turns back eastward with the anticyclonic gyre. The southern cyclonic gyre extends eastward to 80°E.

At 3000 db the Philippine Sea has a separate anticyclonic gyre. In the south the cyclonic gyre is divided by the East Pacific Rise into separate gyres. The southward limb of the southern anticyclonic gyre is turned offshore of the Tonga-Kermadec Ridge near 25°S as the deep northward flow east of New Zealand extends farther north and turns back eastward with the gyre.

At 3500 db the major change in pattern is caused by the East Pacific Rise. Below 3500 db all of the northward flow of the anticyclonic gyre takes place west of the Rise. There is still a small cyclonic gyre near 60°S, 170°W, north of the Rise. The cyclonic gyre east of the Rise (along about 100°W and south of 20°S) has no exit to the north.

At 4000 db the northern anticyclonic gyre still extends across the Emperor Seamounts and encloses the Shatski Rise. Part of its westward limb loops around the ridges near the Hess Rise and returns eastward north of the Hawaiian Islands. There is still an anticyclonic gyre in the Philippine Sea, and a very small connection to the open Pacific near 11°N, 140°E. There is no connection to the areas east of the East Pacific Rise at this depth. The cyclonic gyre between New Zealand and the Rise seems broader than at 3500 db, and the basin east of the Rise is smaller.

At 4000, 4500, and 5000 db there is a continuous northward flow along the western boundary from the plateau south of New Zealand along the Tonga-Kermadec Ridge and all the way to about 45°N, where it turns offshore of the southward flow of the cyclonic gyre.

7. TOTAL GEOSTROPHIC TRANSPORT (FIG. 6)

The total top-to-bottom transport into the Pacific Ocean from the Indian Ocean between Antarctica and Australia, is set at 135 × $10^6 m^3/sec$. The transport from the Pacific to the Atlantic through the Drake Passage is set at 130 × $10^6 m^3/sec$.

The transport integration begins from zero at Antarctica and reaches 135 × $10^6 m^3/sec$ at the coast of Australia and along the western boundary up to about 3°N. Between about 3°N and 6°N 3 of these 135 flow westward through the Indonesian Seas to the Indian Ocean. Northward from there the integral is 132 up to the western side of Bering Strait, where 2 flow into the Arctic Ocean. Along the eastern boundary the integral is everywhere 130 × $10^6 m^3/sec$.

The northward transport across the equator in the west is 35 × $10^6 m^3/sec$ (between the 135 at the western boundary and the 100 line near 157°E). Of these 35 × $10^6 m^3/sec$ crossing northward in the west, 3 are lost to the Indonesian Seas near 5°N. The remaining 32 (132 to 100) continue northward to Japan and then eastward with the anticyclonic gyre. They lose 2 to the northward flow along the eastern boundary and on through the Bering Strait (COACHMAN *et al.*, 1975). The other 30 (130 to 100) continue around the gyre and westward, and turn eastward between 24°N and 35°N with the extension of the cyclonic gyre. They turn back westward along 10°N to 15°N, eastward at 160°E along 0° to 8°N, and southward across the equator east of about 110°W.

The southward transport across the equator in the east is 30 × $10^6 m^3/sec$. About 20 (100 to 120) of this turn westward south of the equator and provide part of the northward crossing in the west. The other 10 (120 to 130) of the westward flow turn back eastward near 120°W and southward along the eastern boundary to join the circumpolar current. There are two low-latitude cyclonic gyres, with axes along about 8°N and 5°S. Both are seen in the total transport and on all of the maps of flow except that at the surface. The northern gyre near the equator appears clearly on the study by MUNK (1950) of the wind-driven circulation of the North Pacific. WELANDER (1959) maps of the Sverdrup transport show both of the gyres. HELLERMAN and ROSENSTEIN (1983) show maps that suggest both, but not very clearly.

The first clear evidence of a subsurface eastward flow just south of the equator, and of both cyclonic gyres, was seen at 300 to 400 db in Reid's (1965) study of the Intermediate Water, which showed cyclonic gyres north and south of the equator, with a westward flow between. The northern gyre is found at all depths, from the surface to 4000 db. TSUCHIYA (1968) has shown that the eastward flow south of the equator, which with the westward flow along about 10°S completes a cyclonic gyre, is not seen clearly at 100 db but is present at 200 db. The cyclonic feature is seen from there to 4000 db. Only at about 300 to 500 db are the two features separated by a westward flow along the equator.

The largest meridional transports do not take place at the equator but at about 5°S, where the two cross-equatorial flows in the west and east add 40 × $10^6 m^3/sec$ to the flow of each gyre. Across 5°S the northward flow in the west is about 75 × $10^6 m^3/sec$ (between the 135 at the boundary and the 60 at about 165°E). However, the northward flow across the equator in the west is only 35, because 40 of the northward flow across 5°S turn eastward before reaching the equator, cross 5°S in the east and return westward. This leaves a gyre just south of the equator, with its axis along about 5°S, that recirculates about $40 \times 10^6 m^3/sec$.

The cyclonic gyre just north of the equator is centered along about 7°N to 8°N. Between about 160°E and 165°E it transports $30 \times 10^6 m^3/sec$ southward and then eastward north of the equator. East of 165°E another $10 \times 10^6 m^3/sec$ also turns southward and then eastward. Of this total of $40 \times 10^6 m^3/sec$ of eastward flow 10 turn northward at the eastern boundary and 30 turn southward across the equator.

The total flow southward across 5°S in the east is $70 \times 10^6 m^3/sec$, 40 from the southward flow of the southern gyre and 30 from across the equator.

Of course the isopleths of total flow are not streamlines of flow at any depth. While they reflect all of the features of the flow at the surface - the anticyclonic and cyclonic gyres, the eastward flow near the equator, and the circumpolar current, some of the gyres have been reshaped. The total transport pattern is much more like the pattern of flow at 1500 m and below.

8. TRACERS

The bottom velocities chosen for each of the station pairs along the lines shown in Fig. 2 were selected to match the pattern of flow to the patterns of characteristics. The patterns of tracers that suggested those choices are shown here along isopycnals. They range from 26.0 in σ_0, which outcrops at both high latitudes and has a maximum depth of about 500 m north of the equator, to 45.90 in σ_4, which outcrops only in the far south and intersects the bottom at about 5600 m near 35°N in the western North Pacific.

The densest water formed in the North Pacific Ocean is about 26.8 in σ_0. All water of greater density in the north must have a component from the South Pacific. During their passage through the North Pacific these denser waters are made less saline and less dense, their high oxygen concentrations are lowered and their nutrient content raised by respiration or dissolution. The ranges of these characteristics over the whole Pacific are quite large, and the large-scale circulation leaves patterns that indicate the various paths of flow.

Of these tracers the vertical extrema of salinity include the surface highs and lows, the shallow lateral extensions from the great evaporation cells toward the equator in the west, the minima from high latitudes that extend beneath the surface toward the equator, and the deep maximum from the circumpolar water.

In the deeper waters of the North Pacific, well north of the direct effect of the hydrothermal vents along the East Pacific Rise, the lateral gradients of temperature and salinity are very weak, and the salinity/temperature along isopycnals (and along surfaces of constant depth) give little detail, though they do indicate the general northward flow. In the equatorial and North Pacific the non-conservative tracers give much clearer indications of the flow pattern beneath the Intermediate Water.

Of the non-conservative tracers oxygen is most useful. Phosphate and nitrate, as near-images of oxygen, would serve about as well except for the limited number and spacing of the high-quality data. Silica, as the product of dissolution rather than respiration, gives a slightly different signal and is a useful augmentation of the information from oxygen. A few maps of these tracers are included to show their general coherence with the oxygen field.

These tracer patterns indicate a northward flow across the equator in the west on all isopycnals from 26.8 in σ_0 (about 400 m) to the bottom. They do not give such an obvious pattern of southward flow across the equator in the east, but it can be inferred from the values found just south of the equator in the east.

These crossings are clearly evident from the field of total transport. Isopleths of steric height cannot show trans-equatorial flow, but it can be shown by the convergence of the geostrophic flow near the equator at the boundaries.

9. THE SALINITY PATTERNS

9.1. The isopycnals where σ_0 is 26.0 and 26.8 (Figs 7 and 8)

The two shallowest isopycnals lie above the vertical salinity minimum of the equatorial zone (Fig. 4b and Fig. 4c). Each shows a salinity/temperature maximum along about 2°S to 9°S. On the shallowest isopycnal (26.00 in σ_0) two tongues of lower salinity extend from the high latitude sources around the anticyclonic gyres and turn westward along about 10° to 20° latitude. The source of the higher salinity in between, along about 5°S, is of course the overlying water. It has been traced by TSUCHIYA (1968, 1981) to the vertical exchange within the South Pacific anticyclonic gyre, where the highest salinity along these two isopycnals is found. It derives from the convergence within that gyre and the downward diffusion of heat and salt there. The westward flow of the northern limb carries the high salinity and temperature northwestward to the north of the Solomon Islands. Along 26.00 in σ_0 the flow turns back eastward near the equator at about 150°E and extends as a broad tongue of warm saline water between about 2°S and 9°S all the way to the eastern boundary.

Near 200 m flow is eastward on both sides of the equator, but the salinity maximum is centered well south of the equator because the temperature and salinity on this isopycnal are so much higher in the South Pacific. The southern part of the eastward flow carries the much more saline water of the western South Pacific, and accounts for the asymmetry of the pattern.

Along the deeper isopycnal (26.80 in σ_0) the lateral salinity maximum along about 5°S is isolated laterally from the high salinity of the western South Pacific by the westward flow of less saline water from the circumpolar current, flowing around the anticyclonic gyre and westward along about 15°S. The source of the maximum must be diffusion from the overlying much warmer and more saline water found just above (REID, 1965).

The vertical minimum in salinity in the North Pacific is found near 26.8 in σ_0 between about 20°N and 45°N. This has been called the North Pacific Intermediate Water (REID, 1965; TALLEY, 1993).

North of 45°N there is a lateral salinity minimum along the axis of the cyclonic gyre. The values are lowest in the Okhotsk Sea. The westward limb of the gyre carries more saline (warmer) water from the eastern Pacific along the Aleutian Islands.

9.2. The isopycnal where σ_1 is 31.8 (Fig. 9)

The only sources of water of low salinity that can account for the vertical minimum in salinity found near 750 m (31.8 in σ_1) in the tropical zone (Fig. 4b and Fig. 4c) are in the high latitude surface layers. On this isopycnal and down to 41.44 in σ_3 (about 3000 m) temperature and salinity are lateral maxima in that zone, but unlike the shallower layers, the highest values are in the east, and east of about 120°W are split by an eastward flow of less saline water along the equator.

In an earlier study (REID, 1965) the lateral maximum in salinity near the equator was described, but it appeared to be almost uniform zonally between about 15°S and 20°N. The data available at that time did not determine the difference of only about 0.025 in salinity now seen between the eastern and western boundaries. Therefore it was assumed that the lateral maximum in salinity along the vertical minimum near the equator was the result of the vertical diffusion taking place throughout the entire basin. No localized source of intensification was indicated and the widespread warming from the overlying layers and increase of salinity from the more saline waters above and below appeared to be enough to account for the maximum.

The lateral maxima in salinity (and thus temperature) seen here in the tropical Pacific are also found down to 3000 m, in much more saline waters. They are highest in the east and indicate a source near that depth. Measurements of heat flow through the bottom had found high values along the East Pacific Rise near 5°S to 30°S (VON HERZEN, 1959). KNAUSS (1962) had noted higher water temperatures at 3000 m in that area and proposed that they were caused by the high geothermal heat flow along the Rise. He noted that the pattern of temperature at 3000 to 3500 m indicated an eastward flow of colder water along the equator at that depth. The data he had did not extend far enough to the west for him to suggest westward flow near 5°N to 10°N and 15°S to 20°S, but are consistent with such flows. However, it was not until more temperature and salinity data had been collected, and the discoveries of the hydrothermal vents both north and south of the equator, that an obvious effect of the heating upon the water characteristics was recognized.

A tongue of high ^{3}He extending westward from the Rise along 15°S near 2500 to 2700 m was reported by LUPTON and CRAIG (1981), and a corresponding tongue of high temperature by REID (1982). Westward flow south of the equator from the sea surface to 4000 m was found by REID (1986). Volume 7 of the GEOSECS reports showed deep maxima in ^{3}He both north and south of the equator near 2000 to 2500 m (OSTLUND *et al.*, 1987). In three abstracts CRAIG (1990a, b) CRAIG, 1991), with more data, described these features as two westward jets, with an eastward flow between, as KNAUSS (1962) had proposed.

TALLEY and JOHNSON (1994) reported another tongue of high temperature north of the equator extending westward from the East Pacific Rise along 5°N to 7°N, separated from the high temperature south of the equator by cooler water. They proposed westward flow from the Rise for the warm tongues and eastward flow for the cooler water in between.

Such warming lowers the density, and isopycnals will be found at higher temperatures and salinities as the water flows past the sources. In the depth range of the tropical Pacific salinity increases downward from about 800 m, and potential temperature decreases at all depths. As the warming takes place the isopycnal is found at a higher salinity. Both temperature and salinity are raised along the path through the area of warming.

The higher temperatures are here represented on isopycnals by their associated higher salinities. They were first noted only on isopycnals near 2500 m to 3000 m in the South Pacific by REID (1981, 1982, 1986) and in the North Pacific by TALLEY and JOHNSON (1994). They are separated in the east by the less saline (and colder) water flowing eastward along the equator.

9.3. The isopycnals where σ_1 is 32.0 (about 1050 m) and σ_2 is 36.76 (about 1550 m) (Figs 10 and 11)

On these isopycnals there is an eastward flow of lower-salinity water along the equator. East of about 110°W this splits the lateral salinity maximum into two westward extensions. They merge across the equator west of about 100°W.

9.4. *The isopycnals where σ_2 is 36.88 and 36.94 (Figs 12 and 13)*

Along these isopycnals the pattern is much the same as above near the equator, and in the north, but there is a new feature in the south.

At these densities the water in the circumpolar current does not enter the southern anticyclonic gyre as a lateral minimum in salinity and temperature, as seen in the upper layers. Instead it shows the higher salinity and temperature characteristic of a North Atlantic source, and is a lateral maximum in salinity along about 55°S. Along 36.94 in σ_2 these more saline waters from the south extend north partway along the Tonga-Kermadec Ridge, but near 30°S they turn back southeastward with the anticyclonic gyre.

This leaves an isolated lateral salinity minimum within the gyre. This results from vertical diffusive exchange with the overlying less saline water, as in the band of low salinity near 50°N, within the subarctic gyre. The minimum is bounded in the north by the more saline water near the hydrothermal vents. A similar feature is also seen in the Indian Ocean (REID, 1981; MANTYLA and REID, 1995).

On these isopycnals the salinity is still lowest north of 45°N but there is no obvious contribution from the Okhotsk Sea. In the west the anticyclonic gyre carries more saline water from the tropics northward across 30°N.

9.5. *The isopycnal where σ_3 is 41.44 (Fig. 14)*

This is the deepest of the isopycnals that shows the effect of the hydrothermal vents. It lies near 2800 to 3000 m north of 50°S, and rises to less than 400 m south of 70°S. It outcrops in winter in the Ross Sea, and probably at other places along the coast of Antarctica. The lateral salinity minimum within the southern anticyclonic gyre is still present at this depth. As part of the gyre turns back eastward near 25°S to 30°S some of the lower salinity water extends eastward and southward along the boundary and through the Drake Passage.

In the north there is a southwestward extension of low-salinity water from the Bering Sea along the western boundary. Offshore the more saline waters from the tropics appear to extend farther north than in the overlying waters.

9.6. *The isopycnal where σ_4 is 45.85 (Fig. 15)*

Along 45.85 in σ_4, which is deeper than 3500 m north of about 30°S, no direct effect of the hydrothermal vents is seen.

The higher salinity from the circumpolar current extends northward along the Tonga-Kermadec Ridge with the deep northward flow. It decreases monotonically northward from the deep salinity maximum of the circumpolar current to the narrow zone of low salinity near 45°N to 50°N, along the axis of the cyclonic gyre.

9.7. *The isopycnals where σ_4 is 45.87 and 45.90 (Figs 16 and 17)*

This isopycnal where σ_4 is 45.87 lies below 4000 m north of 20°N and reaches 4400 m at 50°N. It probably outcrops only in the Ross Sea. The high salinity of the deep saline layer is still seen, though this isopycnal lies below the maximum value. Higher salinities extend from the entering circumpolar water all along the western boundary and across the equator and into the anticyclonic gyre.

The pattern is much the same where σ_4 is 45.90, but the isopycnal incrops south of 40°N. The higher salinity values from the far south extend northward across the equator in the west and diminish toward the east.

On 45.94 in σ_4 (not shown), which reaches the bottom near 5000 m near 10°N, the patterns are about the same as at 45.90, but on still deeper isopycnals the data show no significant tracer patterns north of about 40°S.

10. THE LATERAL EXTREMA IN OXYGEN

The oxygen concentration at the sea surface (Fig. 3d) is roughly symmetrical about the equator, with the highest concentrations in the colder waters of high latitudes and the lowest in the warm waters of the tropics. The symmetry holds, however, only above the density of the salinity minimum of the North Pacific Intermediate Water, about 26.8 in σ_0. Convection does not extend to this density in the North Pacific and the oxygen decreases and nutrients increase near the salinity minimum.

10.1. The isopycnal where σ_0 is 26.0 (Fig. 7)

The shallowest isopycnal (26.0 in σ_0) outcrops in both high latitudes, and the lowest values of oxygen are in the eastern tropical zone. This is because the oxygen-rich waters of high-latitudes do not flow directly to this zone, but must follow long and circuitous paths. During this flow respiration decreases the concentration of oxygen and increases the phosphate and nitrate. The flow of the high oxygen water begins at the outcrops and extends first around the anticyclonic gyres and then westward just north of 10°N and south of 10°S. The flows at 200 m turn back at the western boundary and eastward near the equator. They flow around the two zones between the eastward flow along the equator and the two westward flows. These are also zones of upwelling (HELLERMAN and ROSENSTEIN, 1983). This pattern of flow limits the direct lateral advection of the newer waters, and leaves the zones lower in oxygen and higher in nutrients than the waters poleward of the zones and in the eastward flow in between.

High values of phosphate (and nitrate and silica, not shown) are found in both high latitudes, but the highest are found in the two zones of low oxygen near the equator. The lowest values are found within the anticyclonic gyres.

The salinity, oxygen, and nutrient patterns indicate that the waters at this density that enter the Celebes Sea are from the North Pacific. WYRTKI (1956) proposed that waters from both the North and South Pacific flow into the Celebes Sea, with the northern waters at shallower depths. REID (1965) showed that at 26.8 and 27.28 in σ_0 high salinity and oxygen from the South Pacific enter from the south. Later studies using more recent data have clarified the flow patterns in the western Pacific and the sources of eastward flow along the equator and the waters entering the Celebes Sea (TSUCHIYA *et al.*, 1989; LUKAS *et al.*, 1991; FINE *et al.*, 1994; HAUTALA *et al.*, 1996).

10.2. The isopycnal where σ_0 is 26.8 (Fig. 8)

The isopycnal where σ_0 is 26.8 lies at 400 to 500 m near the equator. It does not outcrop in the North Pacific, and the oxygen there is much lower and the nutrients higher than in the South Pacific. The highest value in the North Pacific is about 4.5 ml/l in the Okhotsk Sea where the silica is quite low. In the earlier study of the Intermediate Waters (REID, 1965) some of the oxygen measurements off Kamchatka and northern Japan were as high as 6 ml/l at 26.8 in σ_0. These now appear to be wrong. An expedition to that area February and March of 1966 found much lower values. Those were shown in a later study (REID, 1973a) and are used herein.

The pattern along 26.8 in σ_0 differs from that along 26.0 in σ_0 in having a third westward extension of lower oxygen and higher nutrients along the equator. The tongue of high oxygen extending eastward seen along the equator at 26.0 in σ_0 has broadened and is split into two tongues by a westward flow in between, carrying low oxygen westward along the equator. This was shown in an earlier presentation of the geostrophic shear and the oxygen (REID, 1965), by HISARD and RUAL (1970), TAFT *et al.* (1974), GOURIOU and TOOLE (1993), WIJFFELS (1993), and more recently by Acoustic Doppler Current Profiler measurements (ELDIN *et al.*, 1992; DELCROIX and ELDIN, 1996). It appears only in the depth range from about 300 to 600 m. It is seen clearly on the oxygen, phosphate, and nitrate patterns where σ_0 is 26.8 (not shown), but not where σ_0 is 26.0 (200 m) or where σ_1 is 31.8 (750 m) or deeper.

10.3. The isopycnals where σ_1 is 31.8 and 32.00 (Figs 9 and 10)

Along the isopycnal where σ_1 is 31.8 (about 750 m in the tropics) the waters flowing westward near 10°S in mid-ocean turn northward at the western boundary. They carry the higher oxygen and lower nutrient of the South Pacific to the equator. Part of the flow turns back eastward along the equator. Part of it continues northward across the equator and turns eastward along 10°N to 15°N, and part extends farther north along the western boundary and joins the anticyclonic gyre. This raises the oxygen values well above the other values in the far north, where there is no renewal of oxygen by convection, and lowers the concentration of nitrate and other nutrients. There are thus three eastward extensions of high oxygen and low nutrients: along the equator, along about 15°N to 20°N, and along 35°N to 45°N with the anticyclonic gyre, as noted by REID and MANTYLA (1978).

Along 32.00 in σ_1 the oxygen and nutrient patterns are much the same as at 31.8 in σ_1 except that the eastward extension of high oxygen and low nutrients along the equator is not so strong.

In the north the zone of low oxygen and high nutrients near 30°N in the east results from the northward and westward retreat of the anticyclonic gyre. The gyre receives high oxygen and low nutrients from the northward flow along the western boundary, but they do not reach the eastern boundary. Instead the lower-oxygen waters from the cyclonic gyre turns southward and westward along 30°N. They fill the space between the high oxygens of the anticyclonic gyre and of the eastward flow along 20°N. This feature of the oxygen pattern, the result of the flow pattern, is seen also in the nutrient patterns, and is found in the northeastern area at all depths below 800m.

No such feature occurs in the South Pacific, even though the cyclonic gyre performs the same loop. Because this isopycnal outcrops in the south, the oxygen within the extension from the cyclonic gyre is high and the nutrients low. They mix with the westward flow of opposite character near 10°S to 15°S, and the western limb of the anticyclonic gyre, along the coast of Australia, is lower in oxygen and higher in nutrients than the waters to the east.

On the deeper isopycnals the oxygen patterns in the north change gradually with increasing depth. The two oxygen minima and the corresponding nutrient maxima near the equator weaken with depth and disappear at about 2000 m. The northern oxygen minimum, at about 35°N at 31.8 in σ_1 (about 800 m), lies near 40°N at 32.00 in σ_1 (about 1050 m).

10.4. The isopycnal where σ_2 is 36.76 (Fig. 11)

Along 36.76 in σ_2 (about 1500 m) north of 40°S the southward and westward loop of lower-oxygen water from the northern cyclonic gyre begins farther north, and the minimum lies near 45°N. Slightly higher oxygen values from the eastward flow between 20°N and 30°N extend northward along the eastern boundary. This leaves the minimum in oxygen laterally isolated. The nutrient patterns may have isolated maxima that correspond to the oxygen minima, but the signals in the present data are not strong enough to be certain.

In the western South Pacific the various ridges west of 170°W divert part of the anticyclonic gyre southward east of the New Hebrides.

The waters that cross the equator northward in the west have come directly from the circumpolar current and are much higher in oxygen than those they pass by, and give a clear signal of the crossing. But those waters crossing the equator southward have not come directly from the area of extremely low values in the far northeast Pacific. Instead they have taken a long path westward, eastward, and westward again before joining the eastward flow near the equator. Along the path they have mixed laterally with the incoming waters. As they cross the equator they have reached nearly the same concentration of oxygen as the waters they enter. As they extend farther southward along the eastern boundary, however, the signal becomes clear.

10.5. The isopycnal where σ_2 is 36.88 (Fig. 12)

Along 36.88 in σ_2 at about 2000 m, the oxygen minimum and nutrient maxima just north of the equator have disappeared. There are still extrema in both oxygen and silica just south of the equator in the east, but the flow pattern suggests that this is from water that has crossed the equator from the north. The low oxygen and high nutrients south of 20°S along the eastern boundary suggests a southward flow.

The low oxygen and high nutrients near 45°N in the east are present all the way to the bottom, but higher-oxygen water is seen at the coast, just as where σ_2 is 36.76 (about 1500 m). The Tasman Sea is almost cut off from the north, and shows the higher oxygen and lower nutrients of the circumpolar current.

10.6. The isopycnals where σ_2 is 36.94 and σ_3 is 41.44 (Figs 13 and 14)

Along 36.94 in σ_2 (about 2400 m north of 20°S) and 41.44 in σ_3 (2800 to 3000 m north of 30°S) the Coral and Tasman seas are almost closed to the north and have only a narrow connection with each other. The Tasman Sea receives the high oxygen and low nutrients of the circumpolar flow but the Coral Sea is almost cut off from that source.

The mixture along 10°S of waters from the circumpolar current and the eastern tropical zone extends southward along the Tonga-Kermadec Ridge as part of the anticyclonic gyre. The southward flow along the Ridge turns offshore near 30°S as it meets a northward flow of higher-oxygen and lower nutrients from the circumpolar current.

Along the isopycnal 41.44 in σ_3 the northwestern Philippine Sea oxygen is higher and silica lower than in the waters entering and leaving. As this isopycnal lies well below the oxygen minimum this must result from vertical diffusion from the deeper more oxygen-rich waters (Reid and Mantyla, 1980; Kawabe, 1993).

10.7. *The isopycnal where σ_4 is 45.85 (Fig. 15)*

The isopycnal where σ_4 is 45.85 incrops along the East Pacific Rise just south of 50°S. It lies near 3500 m north of 30°S and does not extend into the Coral Sea. Waters with the high-oxygen characteristics of the circumpolar current extend into the central basin along the Tonga-Kermadec Ridge. They also fill the Tasman Sea and the basin south of the Chile Rise. The southward flow of lower-oxygen tropical water along the Tonga-Kermadec Ridge turns offshore near 20°S, as the Circumpolar Water turns northward along the Ridge and then, near 30°S, turns eastward with the anticyclonic gyre.

10.8. *The isopycnal where σ_4 is 45.87 (Fig. 16)*

Although the flow field at 4000 db in the south indicates a vestige of the strong overlying anticyclonic gyre in the central basin, the fields of characteristics show only the northward flow along the Tonga-Kermadec Ridge. Their ranges are too small to leave a clear signal there.

In the north the pattern is about the same as in the overlying waters. Water of higher oxygen and lower silica flows along the western boundary across the equator, and extends both eastward along 24°N and northward to Japan along the boundary, continuing northward to 50°N offshore of the southward flow along the boundary, and then eastward near 50°N.

10.9. *The isopycnal where σ_4 is 45.90 (Fig. 17)*

The isopycnal where σ_4 is 45.90 lies between 3500 m and 4200 m south of the equator and between 4200 and 5200 m in the north. The pattern simply shows the northward flow of higher-oxygen water from the circumpolar current along the western boundary into the North Pacific.

11. PATHS OF FLOW

Waters that leave the circumpolar current and enter the Pacific Ocean are caught up in its gyral patterns and can extend throughout the whole Pacific before returning. The paths along which they circulate in the South Pacific before crossing the equator, and those they follow in the North Pacific before returning at lower density, are revealed by the patterns of tracers. The patterns are displayed here on isopycnal surfaces, but they indicate that there is significant vertical exchange by diffusion. The isolated lateral maximum in salinity along the equator in the density range of the Intermediate Water, and the lateral minima at greater densities in both the North and South Pacific, make this plain. This must affect the patterns of non-conservative characteristics also, though the results are not so obvious. It is clear that not all mixing is lateral, and as this applies to density also, then the flow is not restricted to isopycnals. Some of the waters that enter the North Pacific are denser than any that depart. The denser waters must mix with less dense water before they leave.

In the upper 400 m the flow is nearly symmetric about the equator and the isopycnal maps show no clear evidence of cross-equatorial flow. At greater depths and densities, more than 400 m and 26.8 in σ_0, the tracer patterns indicate northward flow across the equator in the west and southward flow in the east. Between about 31.8 in σ_1 (about 750 m) and 45.85 in σ_4 (about 3500 m north of 40°S) the waters crossing the equator in the west and circulating through the North Pacific have come from the circumpolar current by passing around the southern anticyclonic gyre. Along their westward flow between about 10°S and 20°S they have been joined by and mixed with the tropical waters recirculating in the zonal flows near the equator. Some of the flow has continued around the gyre to the Tasman Sea, some has turned back eastward along the equator, and some has crossed the equator in the west.

At densities higher than 45.85 in σ_4 the waters that cross the equator have come directly northward from the circumpolar current along the Tonga-Kermadec Ridge, beneath the anticyclonic gyre. North of the Ridge the flow continues northward east of the Solomon Rise and Mariana ridges. It joins the overlying northward flow near 30°N.

At and below 45.85 in σ_4 the northward flow in the South Pacific is confined between the Tonga-Kermadec Ridge and the Tuamotu Islands. The greater part of the denser water flows through the Samoan Passage, a narrow channel along about 169°W across 10°S. It was identified by Wüst (1937) and a few current measurements reported by Reid and Lonsdale (1974) showed strong northward flow near the bottom there. More detailed studies by Taft *et al.*, 1991, and Rudnick (1997) extended the data. Roemmich *et al.*, 1996 found about $12 \times 10^6 m^3/sec$ of water below 1.2° in potential temperature (about 45.85 in σ_4) flowing northward between Fiji and the Tuamotu Islands, with most of this through the Samoan Passage. The maps at 4000 decibars and deeper illustrate the paths of flow in that area.

From about 32.00 in σ_1 (about 1100 m north of 20°S) down to the depth of the east Pacific Rise the tracer patterns indicate a southward or southwestward flow across the equator in the east. This is water that has flowed eastward between about 5°N and 5°S and divides at the coast, with some of the northern water crossing the equator southward.

The water that crosses the equator in the east turns westward north of 10°S. Water shallower than the Rise crest (between 3000 and 3500 m) then turns south and eastward across the Rise to the coast, and then southward to the Drake Passage. Water deeper than about 3500 m cannot cross the Rise, but continues westward to join the northward flow across the equator.

Through this system of flows the characteristics of the several layers of denser water from the circumpolar current are spread throughout the Pacific. They are altered there by diffusive vertical exchange with overlying layers of less saline and warmer waters and the heat flux from the sea floor, and by the heat added by the hydrothermal vents. Their non-conservative characteristics are modified by the respiration and dissolution along their paths.

Except for the addition of heat from the hydrothermal vents along the East Pacific Rise and the more widespread but weaker geothermal warming the deeper waters that come in from the south are not entering a different ocean — one with different sources of deep water. Instead they are entering a less-stratified version of the original temperature, salinity, and density structure. These are modified in the North Pacific only by vertical and lateral diffusive exchange. Only respiration and dissolution can create new features there.

12. CONCLUSION

The fields of flow and characteristics are presented here. The flow patterns at the surface have been known for a long time, and the flow along the bottom had been inferred from the abyssal temperature and salinity fields. But at the least-known and least-studied layers, those at mid-depth, the temperature and salinity have patterns less distinct than those above and below. In those layers it is the non-conservative characteristics, particularly oxygen in this study, that give the clearest signals of sense and path of flow.

Many of the flow patterns shown here, especially those for the upper few hundred meters in the tropics, are much like those of recent more localized studies, but at greater depths and high latitudes there are no large-scale studies with which these flow patterns can be compared.

The major differences between this work and earlier studies are that the equatorial crossings and the paths of flow are defined at all depths, and that the tropical cyclonic gyres on either side of the equator are shown to be very strong and to extend to great depth.

The poleward shift of the westward component of the anticyclonic gyres was made clear in the density field in earlier work and is shown here, as in the Atlantic (REID, 1994) to extend to great depths and to be consonant with the tracer patterns.

The equatorward and westward extension of the high-latitude cyclonic gyres in both the North and South Pacific is much as seen in the North Atlantic: it is not seen in the South Atlantic Ocean, possibly because Africa does not extend poleward as far as South America, and does not reach close enough to the latitude of the cyclonic gyres to offset its flow.

13. ACKNOWLEDGEMENTS

The work reported here represents one of the results of research supported by the National Science Foundation and the Marine Life Research Program of the Scripps Institution of Oceanography. I wish to acknowledge the assistance given by Arnold Mantyla in selecting the data and by David Newton for writing the various programs. I thank Gunnar Roden for giving me an early look at his data from the WOCE line P14 North, along 180° longitude.I wish to acknowledge especially Sarilee Anderson for the great skill in handling the various data formats, in arranging the data and calculating and plotting the data points along the isopycnals and on the fields of steric height and for her patience in the long succession of adjustments.

14. REFERENCES

COACHMAN L.K., AAGAARD K. and TRIPP R.B. (1975) *Bering Strait. The regional physical oceanography.* University of Washington Press, Seattle. 172 pp.

COKELET E.D., SCHALL M.L. and DOUGHERTY D.M. (1996) ADCP-referenced geostrophic circulation in the Bering Sea basin. *Journal of Physical Oceanography* **26**(7), 1113–1128.

CRAIG H. (1990a) The HELIOS helium 3 section: Implications for the deep water circulation in the North and South Pacific. *EOS, Transactions, American Geophysical Union*, **71**(28), 882 (abstract).

CRAIG H. (1990b) The HELIOS helium 3 jets in the North and South Pacific. *EOS, Transactions, American Geophysical Union*, **71**(43), 1396 (abstract).

CRAIG H. (1991) Hydrothermal plumes at 5 and 9 degrees north on the EPR and the origin of the northern hemisphere zonal helium jet. *EOS, Transactions, American Geophysical Union*, **72**(44), 491 (abstract).

DELCROIX T. and ELDIN G. (1996) Observations hydrologiques dans l'Ocean Pacifique tropical ouest. *Campagnes SURTROPAC la 17, de Janvier 1984 a aout 1992, Campagnes COARE156 la 3, a aout 1991 a octobre 1992.* ORSTOM, N°141 F3, 88 pp.

ELDIN G., MORLIÈRE A. and REVERDIN G. (1992) Acoustic Doppler current profiling along the Pacific equator from 95°W to 165°E. *Geophysical Research Letters* **19**(9), 913–916.

FAVORITE F., DODIMEAD A.J. and NASU K. (1976) Oceanography of the subarctic Pacific region, 1960-71. *International North Pacific Fisheries Commission, Bulletin*, **3**, 187 pp.

FINE R.A., LUKAS R., BINGHAM F.M., WARNER M.J. and GAMMON R.H. (1994) The western equatorial Pacific: A water mass crossroads. *Journal of Geophysical Research*, **99**(C12), 25,063-25,080.

GORDON A.L. (1971) Oceanography of Antarctic waters. In: *Antarctic Oceanology I, Antarctic Research Series*, **15**, J. L. Reid, editor, American Geophysical Union, Washington, DC, 169-203.

GORDON A.L. and GERARD R.D. (1970) North Pacific bottom potential temperature. In: *Geological Investigations of the North Pacific*, **126**, J. D. Hays, editor, The Geological Society of America, Boulder, CO, 23-39.

GORDON A.L. and MOLINELLI E.J. (1982) Thermohaline and chemical distributions and the atlas data set. In: *Southern Ocean Atlas*, Columbia University Press, New York, 11 pp, 233 plates.

GOURIOU Y. and TOOLE J. (1993) Mean circulation of the upper layers of the western equatorial Pacific Ocean. *Journal of Geophysical Research*, **98**(C12), 22,495-22,520.

HAUTALA S.L., REID J.L. and BRAY N. (1996) The distribution and mixing of Pacific water masses in the Indonesian Seas. *Journal of Geophysical Research*, **101**(C5), 12,375-12,390.

HELLERMAN S. and ROSENSTEIN M. (1983) Normal monthly wind stress over the World Ocean with error estimates. *Journal of Physical Oceanography* **13**(7), 1093–1104.

HISARD P. and RUAL P. (1970) Courant Equatorial Intermédiare de l'Océan Pacifique et contre-courants adjacents. *Cahiers Océanographique*, **VIII**(1), 21-45.

HOOD D.W. and KELLEY E.J. [editors] (1974) Oceanography of the Bering Sea with emphasis on renewable resources. Proceedings of International Symposium for Bering Sea Study, 31 January-4 February 1972, Hokodate, Japan, Occasional Publication No. 2, Institute of Marine Sciences, University of Alaska, Fairbanks, 623pp.

JACOBS S.S., AMOS A.F. and BRUCHHAUSEN P.M. (1970) Ross Sea oceanography and Antarctic bottom water formation. *Deep-Sea Research* **17**, 935–962.

JOYCE T.M., WARREN B.A. and TALLEY L.D. (1986) The geothermal heating of the abyssal subarctic Pacific Ocean. *Deep-Sea Research* **33**(8A), 1003–1015.

KAWABE M. (1993) Deep water properties and circulation in the western North Pacific. In: *Deep Ocean Circulation, Physical and Chemical Aspects*, T. Teramoto, editor, Elsevier Science Publishers. B.V., Netherlands, 17-37.

KENYON K.E. (1983) Sections along 35°N in the Pacific. *Deep-Sea Research* **30**(4A), 349–369.

KITANI K. (1973) An oceanographic study of the Okhotsk Sea - particularly in regard to cold waters. *Bulletin Far Seas Fisheries Research Laboratory* **9**, 45–77.

KNAUSS J.A. (1962) On some aspects of the deep circulation of the Pacific. *Journal of Geophysical Research* **67**(10), 3943–3954.

LUKAS R., FIRING E., HACKER P., RICHARDSON P.L., COLLINS C.A., FINE R. and GAMMON R. (1991) Observations of the Mindanao Current during the Western Equatorial Pacific Ocean Circulation Study. *Journal of Geophysical Research* **96**(C4), 7089–7104.

LUPTON J.E. and CRAIG H. (1981) A major helium-3 source at 15°S on the East Pacific Rise. *Science* **214**(4516), 13–18.

MANTYLA A.W. and REID J.L. (1983) Abyssal characteristics of the World Ocean waters. *Deep-Sea Research* **30**(8A), 805–833.

MANTYLA A.W. and REID J.L. (1995) On the origins of deep and bottom waters of the Indian Ocean. *Journal of Geophysical Research* **100**(C2), 2417–2439.

MUNK W.H. (1950) On the wind-driven ocean circulation. *Journal of Meteorology* **7**(2), 79–93.

OSTLUND H.G., CRAIG H., BROECKER W.S. and SPENCER D. (1987) *GEOSECS Atlantic, Pacific and Indian Ocean Expeditions, Shorebased Data and Graphics*. **7**, National Science Foundation, Washington, DC, 200 plates.

REED R.K. and STABENO P.J. (1994) Flow along and across the Aleutian Ridge. *Journal of Marine Research* **52**(4), 639–648.

REID J.L. (1961) On the geostrophic flow at the surface of the Pacific Ocean with respect to the 1000-decibar surface. *Tellus* **13**(4), 489–502.

REID J.L. Jr. (1965) Intermediate waters of the Pacific Ocean. *The Johns Hopkins Oceanographic Studies*, **2**, The Johns Hopkins Press, Baltimore, 85 pp. 32 Figs.

REID J.L. (1973a) Northwest Pacific Ocean water in winter. *The Johns Hopkins Oceanographic Studies*, **5**, The Johns Hopkins Press, Baltimore, 96 pp.

REID J.L. (1973b) The shallow salinity minima of the Pacific Ocean. *Deep-Sea Research* **20**(1), 51–68.

REID J.L. (1981) On the mid-depth circulation of the world ocean. In: *Evolution of Physical Oceanography*, B. A. Warren and C. Wunsch, editors, The MIT press, Cambridge, MA and London England, 70-111.

REID J.L. (1982) Evidence of an effect of heat flux from the East Pacific Rise upon the characteristics of the mid-depth waters. *Geophysical Research Letters* **9**(4), 381–384.

REID J.L. (1986) On the total geostrophic circulation of the South Pacific Ocean: Flow patterns, tracers and transports. *Progress in Oceanography* **16**(1), 1–61.

REID J.L. (1989) On the total geostrophic circulation of the South Atlantic Ocean: Flow patterns, tracers and transports. *Progress in Oceanography* **23**(3), 149–244.

REID J.L. (1994) On the total geostrophic circulation of the North Atlantic Ocean: Flow patterns, tracers and transports. *Progress in Oceanography* **33**(1), 1–92.

REID J.L. and ARTHUR R.S. (1975) Interpretation of maps of geopotential anomaly for the deep Pacific Ocean. *Journal of Marine Research*, **33**, (Suppl.), 37-52.

REID J.L. and LONSDALE P.F. (1974) On the flow of water through the Samoan Passage. *Journal of Physical Oceanography* **4**(1), 58–73.

REID J.L. and LYNN R.J. (1971) On the influence of the Norwegian-Greenland and Weddell seas upon the bottom waters of the Indian and Pacific oceans. *Deep-Sea Research* **18**(11), 1063–1088.

REID J.L. and MANTYLA A.W. (1978) On the mid-depth circulation of the North Pacific Ocean. *Journal of Physical Oceanography* **8**(6), 946-951.

REID J.L. and MANTYLA A.W. (1980) On the vertical exchange within the Philippine Sea. *EOS, Transactions, American Geophysical Union*, **61**(17), 274 (abstract).

RODEN, G. (1995) Aleutian Basin of the Bering Sea: Thermohaline, oxygen, nutrient, and current structure in July 1993. *Journal of Geophysical Research*, **100**(C7), 13,539-13,554.

ROEMMICH D., HAUTALA S. and RUDNICK D. (1996) Northward abyssal transport through the Samoan Passage and adjacent regions. *Journal of Geophysical Research*, **101**(C6), 14,039-14,056.

ROEMMICH D., MCCALLISTER T. and SWIFT J. (1991) A trans-Pacific hydrographic section along latitude 24°N: The distribution of properties in the subtropical gyre. *Deep-Sea Research* **38**, S1–20.

RUDNICK D.L. (1997) Direct velocity measurements in the Samoan Passage. *Journal of Geophysical Research* **102**(C2), 3293-3302.

SIEVERS H.A. and NOWLIN W.D. Jr. (1984) The stratification and water masses at Drake Passage. *Journal of Geophysical Research*, **89**(C6), 10,489-10,514.

STOMMEL H., STROUP E.D., REID J.L. and WARREN B.A. (1973) Transpacific hydrographic section at Lats. 43°S and 28°S: the SCORPIO Expedition - I. *Preface. Deep-Sea Research* **20**(1), 1–7.

SUDO H. (1983) Deep water isopleth distributions in the western North Pacific. *La Mer* **21**(2), 61–74.

TAFT B.A., HICKEY B.M., WUNSCH C. and BAKER D.J. (1974) Equatorial undercurrent and deeper flows in the central Pacific. *Deep-Sea Research* **21**(6), 403–430.

TAFT B.A., HAYES S.P., FRIEDERICH G.E. and CODISPOTI L.A. (1991) Flow of abyssal water into the Samoa Passage. *Deep-Sea Research*, **38** (Supp. 1A), 5103-5128.

TALLEY L.D. (1993) Distribution and formation of North Pacific intermediate water. *Journal of Physical Oceanography* **23**(3), 517–537.

TALLEY L.D., JOYCE T.J. and DESZOEKE R.A. (1991) Trans-Pacific sections at 47°N and 152°W: Distribution of properties. *Deep-Sea Research* **38**, S63–82.

TALLEY L.D. and JOHNSON G.C. (1994) Deep, zonal subequatorial currents. *Science* **263**, 1125–1128.

TALLEY L.D. and NAGATA Y. [editors] (1995) PICES Scientific Report no. 2, 1995. The Okhotsk Sea and Oyashio Region. North Pacific Marine Science Organization (PICES), 227 pp.

TSUCHIYA M. (1968) Upper Waters of the Intertropical Pacific Ocean. *The Johns Hopkins Oceanographic Studies*, **4**, The Johns Hopkins Press, Baltimore, 50 pp.

TSUCHIYA M. (1981) The origin of the Pacific equatorial 13° water. *Journal of Physical Oceanography* **11**(6), 794–812.

TSUCHIYA M., LUKAS R., FINE R.A., FIRING E. and LINDSTROM E. (1989) Source waters of the Pacific Equatorial Undercurrent. *Progress in Oceanography* **23**, 101–147.

TSUCHIYA M. and TALLEY L.D. (1996) Water-property distributions along an eastern Pacific hydrographic section at 135°W. *Journal of Marine Research* **54**, 541–564.

VON HERZEN R. (1959) Heat-flow values from the southeastern Pacific. *Nature* **183**, 882–883.

WARNER M.J. and RODEN G.I. (1995) Chlorofluorocarbon evidence for recent ventilation of the deep Bering Sea. *Nature* **373**, 409–412.

WARREN B.A. and OWENS W.B. (1988) Deep currents in the central subarctic Pacific Ocean. *Journal of Physical Oceanography* **18**(4), 529–551.

WELANDER P. (1959) On the vertically integrated mass transport in the oceans. In: *The Atmosphere and the Sea in Motion*, B. Bokin, editor, The Rockefeller Institute Press, 509 pp.

WHITWORTH T., III, NOWLIN W.D. Jr. and WORLEY S.J. (1982) The net transport of the Antarctic Circumpolar Current through Drake Passage. *Journal of Physical Oceanography*, **12**(9), 960-971.

WIJFFELS S.E. (1993) Exchanges between hemispheres and gyres: A direct approach to the mean circulation of the Equatorial Pacific. Doctoral dissertation, Woods Hole Oceanographic Institution, 267 pp.

WÜST G. (1937) Bodentemperatur und bodenstrom in der Pazifischen Tiefsee. *Veröffentlichungen des Instituts für Meereskunde an der Universität Berlin*, **35**, 1-56.

WYRTKI K. (1956) The subtropical lower water between the Philippines and Irian (New Guinea). *Marine Research in Indonesia* **1**, 21–52.

YUAN X. and TALLEY L.D. (1992) Shallow salinity minima in the North Pacific. *Journal of Physical Oceanography* **22**(11), 1302–1316.

Table 1. Expeditions from which stations were chosen to calculate the adjusted steric height

Expedition/Ship	Dates	NODC #	Source
ARIES	Jan.–Feb. 1971	311224	SIO (1977)
Atlantis II	Sept. 1965	310247	Warren and Owens (1988)
Burton Island	Feb.–Apr. 1968	311214	SIO (1971)
Eltanin Cr. 41	Dec. 1969–Feb. 1970	311213	SIO, Horace Lamb Centre and Johns Hopkins Univ (1972)
Eltanin Cr. 45	Sept.–Oct. 1970	31	Lamont-Doherty (1972)
Franklin Cr. 10/89	Aug.–Sept. 1989	099114	CSIRO
Franklin Cr. 2/90	Feb.–Mar. 1990	099117	CSIRO
G1/60	Feb.–Mar. 1960	090005	CSIRO (1962)
G2/60	Mar.–Apr. 1960	090005	CSIRO (1962)
G1/61	Jan.–Feb. 1961	090008	CSIRO (1963)
G3/61	Aug.–Oct. 1961	090033	CSIRO (1967)
G3/63	Jul.–Aug. 1963	090059	CSIRO (1968)
GEOSECS	Dec. 1973–May 1974	318488-97	Broecker, Spencer and Craig (1982)
GREAT BEAR KH-70-2	Apr.–Jun. 1970	490785	Horibe (1971)
INDOPAC I, II, III, XVI	Mar. 1976–Jul. 1977	312998-3000/3004	SIO (1978)
JUNO I	Oct.–Nov. 1992	316N138/9	SIO WOCE
KIWI	Sept.–Nov. 1969	312701	Warren and Voorhis (1970)
MARATHON 2	May–Jun. 1984	318817	Oregon State Univ. (1987)
Moana Wave Cr. 89-3-4-6	Feb.–May 1989	329646	WHOI (1991)
NEMO	Feb. 1972	311225	SIO (1974a)
PHOENIX KH-71-5	Nov. 1971–Feb. 1972	490765	Tsubota (1973)
PIQUERO Leg 3	Dec.–Apr. 1969	311221	SIO (1974b)
SCORPIO	Mar.–Jul. 1967	311212	SIO, WHOI, and MIT (1969)
SOUTHERN CROSS KH-68-4	Nov.1968–Mar.1969	498001	Horibe (1970)
STEP I	Sept.–Dec. 1960	310876	SIO (1961)
STYX	Apr.–Aug. 1968	311222	SIO (1971)
TPS 24N	Mar.–Jun. 1985	313186	SIO (1990)
TPS 47N	Aug.–Sept. 1985	313453	SIO (1988)
TUNES 1	Jun.–Jul. 1991	31WTTUNES/1	SIO
TUNES 2	Jul.–Aug. 1991	31WTTUNES/2	SIO
TUNES 3	Sept. 1991	31WTTUNES/3	SIO
WEPOCS 2	Jan.–Feb. 1986	329633	SIO (1987)

Table 2. Specifications of the isopycnal surfaces. The potential density is expressed as σ_0 from 0–500 db, as σ_1 from 500–1500 db, as σ_2 from 1500–2500 db, as σ_3 from 2500–3500 db, as σ_4 from 3500–4500 db, and as σ_5 from 4500 db to the bottom. The potential density is given in units of σ, which is ρ-1000, where ρ is in kg m^{-3}. This table lists the different numbers used for each isopycnal as it extends to the different pressure ranges. The numbers in bold-face type are those used in the text and figures to identify each isopycnal

North Pacific

Lat.	σ_0	σ_1	σ_2	σ_3	σ_4	σ_5
	26.000					
	26.800					
	27.182	**31.800**				
	27.360	**32.000**	36.523			
		32.220	**36.760**			
		32.340	**36.880**	41.332		
			36.940	41.397	45.750	
				41.440		
				41.485	**45.850**	
					45.870	50.135
					45.900	50.170

South Pacific

Lat.	σ_0	σ_1	σ_2	σ_3	σ_4	σ_5
	26.000					
	26.800					
	27.201	**31.800**				
40-50E	27.332					
50-60E	27.375	**32.000**	36.512			
60-70E	27.368					
	27.573	32.226	**36.760**			
	27.671	32.337	**36.880**	41.325		
	27.726	32.392	**36.940**	41.392		
	27.765	32.430	36.985	**41.440**		
	27.784	32.464	37.030	41.488	**45.850**	
	27.801	32.472	37.041	41.505	**45.870**	50.135
	27.823	32.496	37.066	41.533	**45.900**	50.169

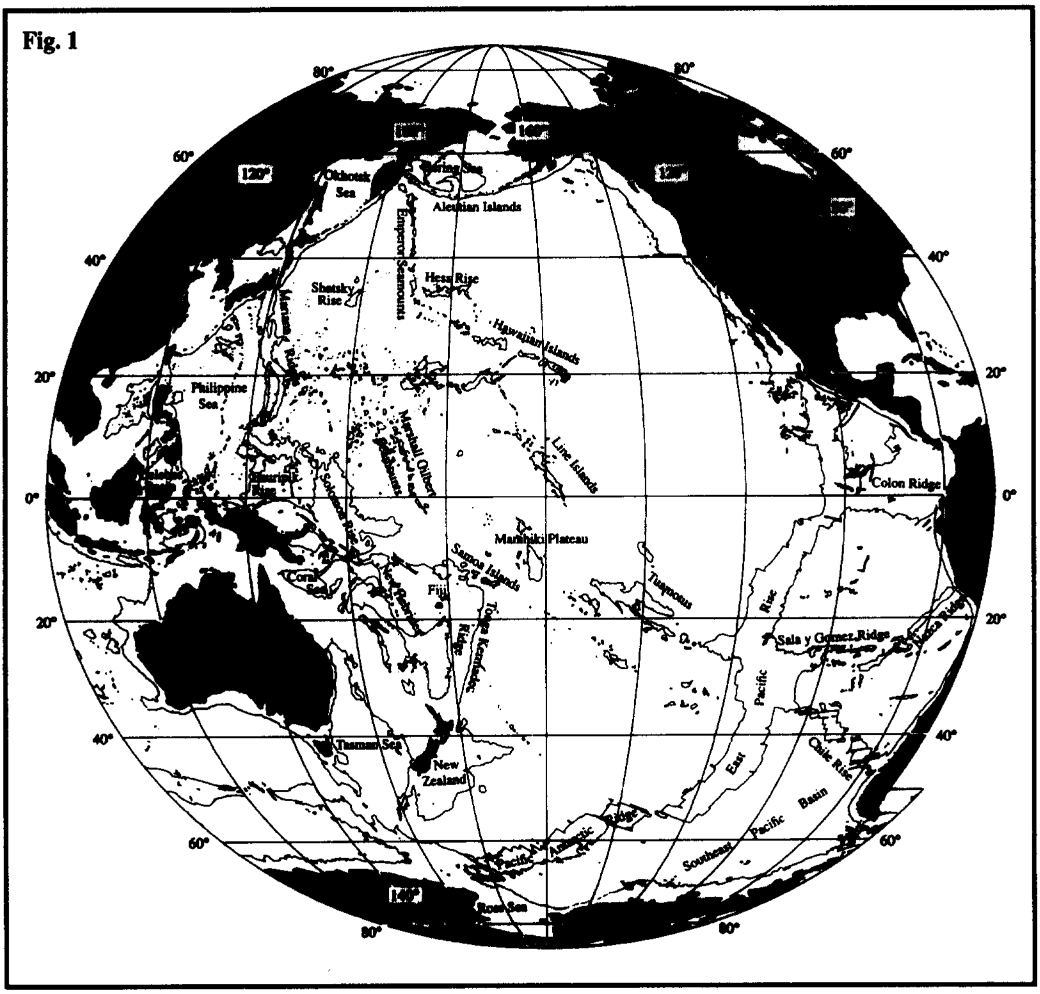

Fig. 1. Principal topographic features referred to in the text, shown on a Molleweide projection. The 3500 m depth contour is indicated.

Fig. 2

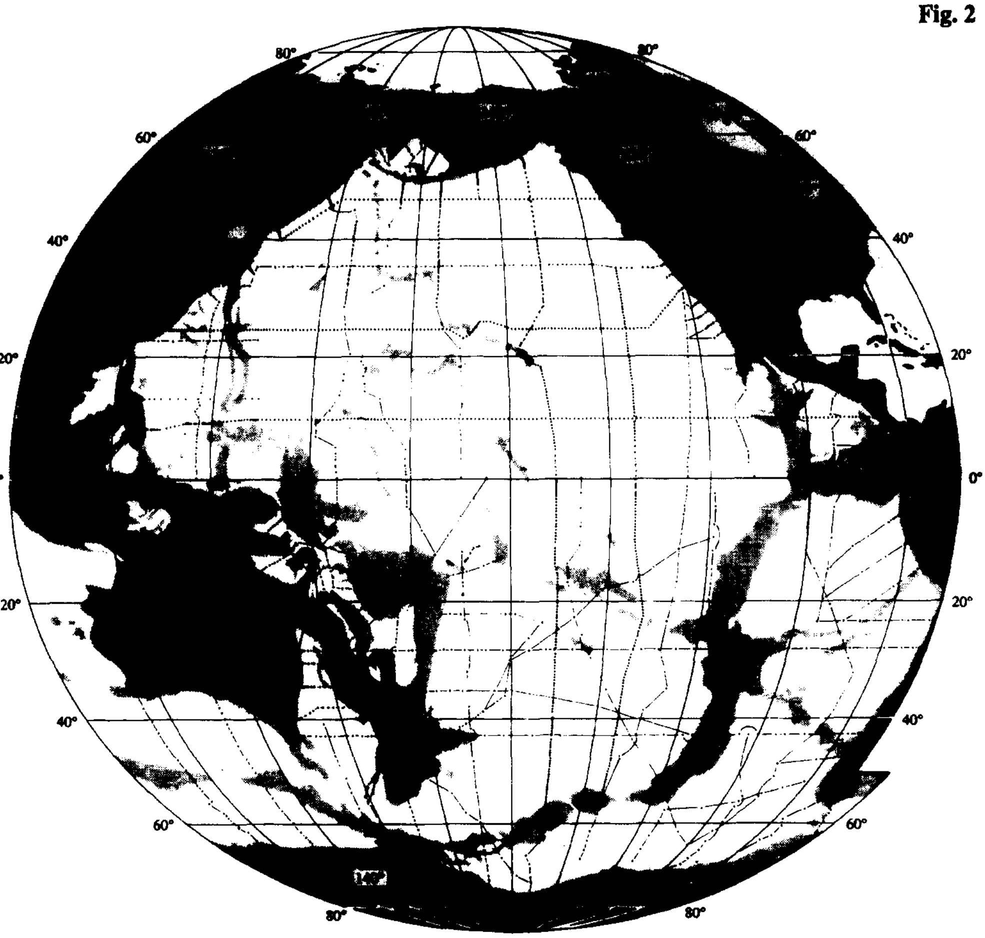

Fig. 2. Lines of stations used in the calculation of the geostrophic flow. Lines connecting stations indicate the paths along which the geostrophically-balanced slopes of the isobars were integrated to provide the adjusted geopotential (steric height) of the isobars with respect to a level surface. Depths less than 3500 m are shaded.

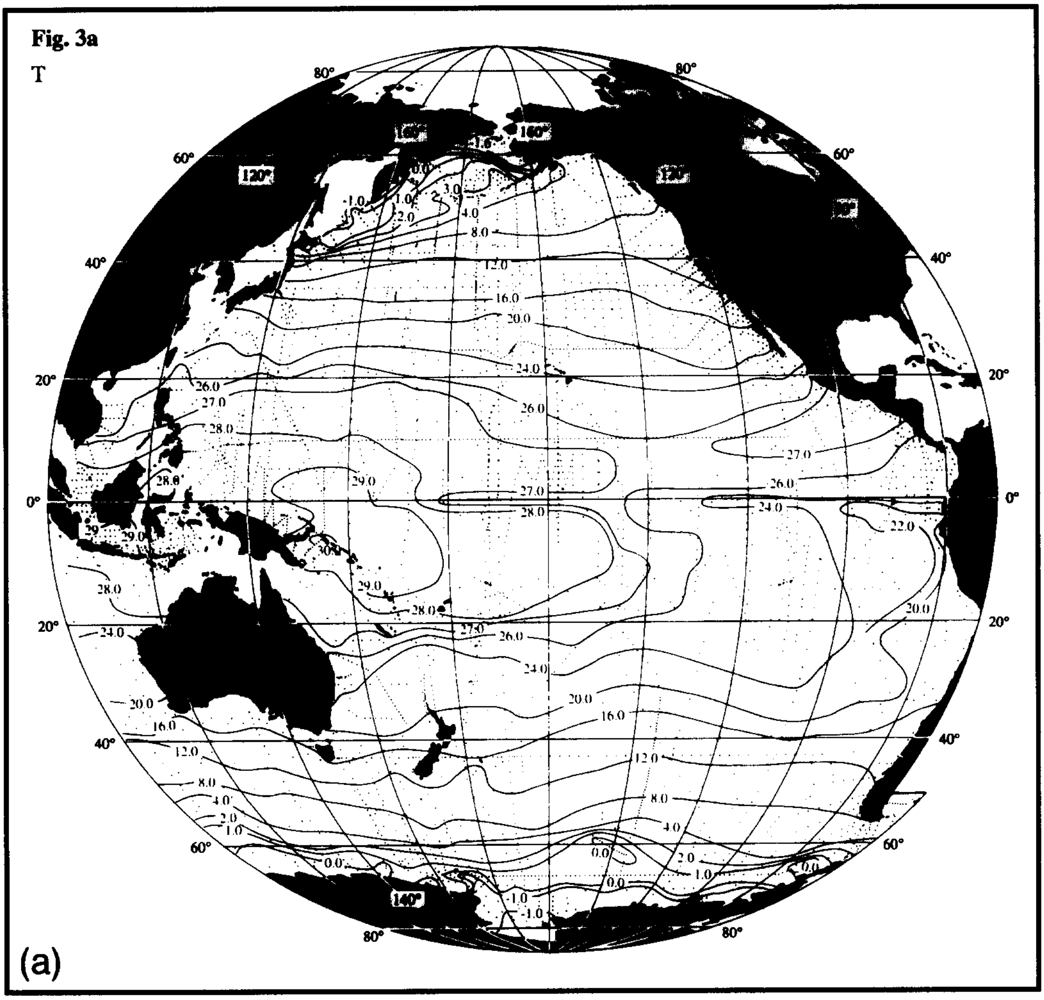

Fig. 3. (a), Northern winter (Nov–Apr) temperature (°C) at the sea surface.

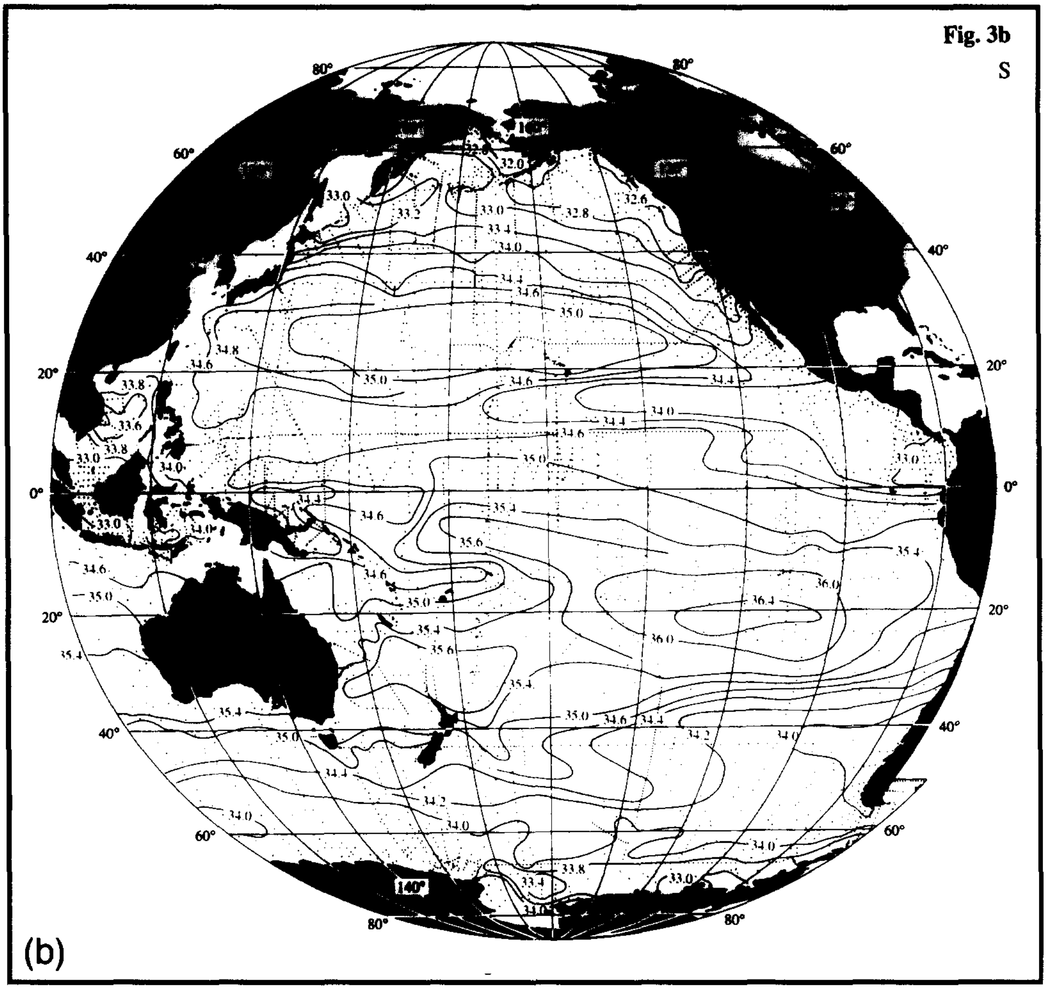

Fig. 3. (b), Northern winter (Nov–Apr) salinity at the sea surface.

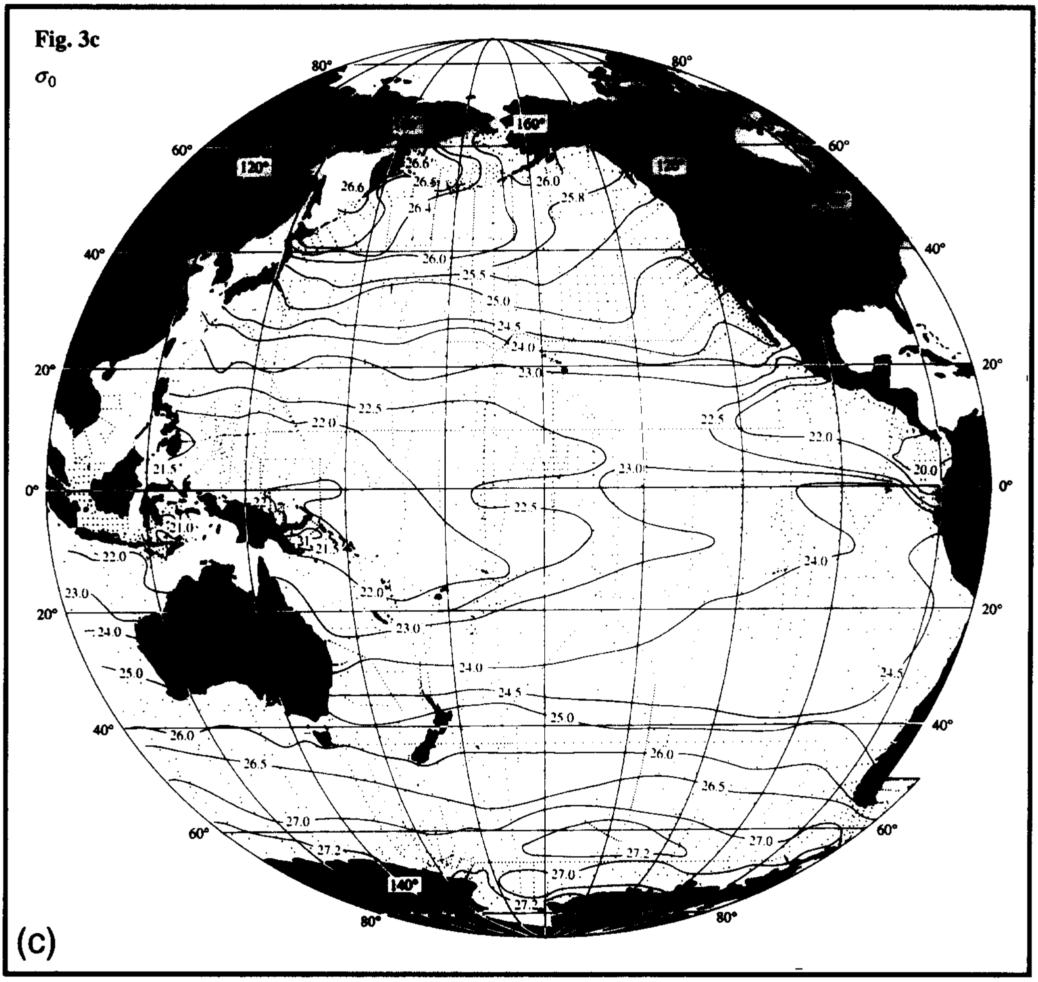

Fig. 3. (c), Northern winter (Nov–Apr) potential density (σ_0) at the sea surface.

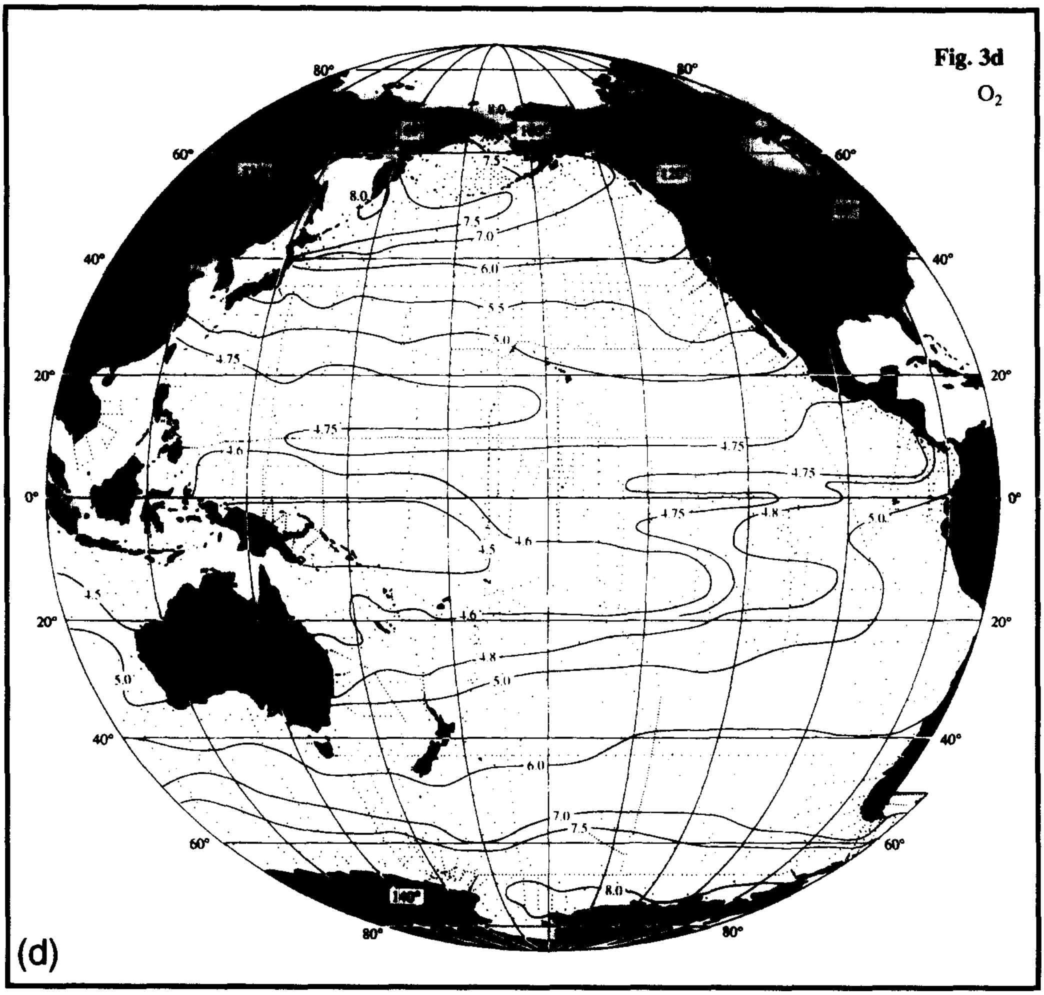

Fig. 3. (d), Northern winter (Nov–Apr) oxygen (ml/l) at the sea surface.

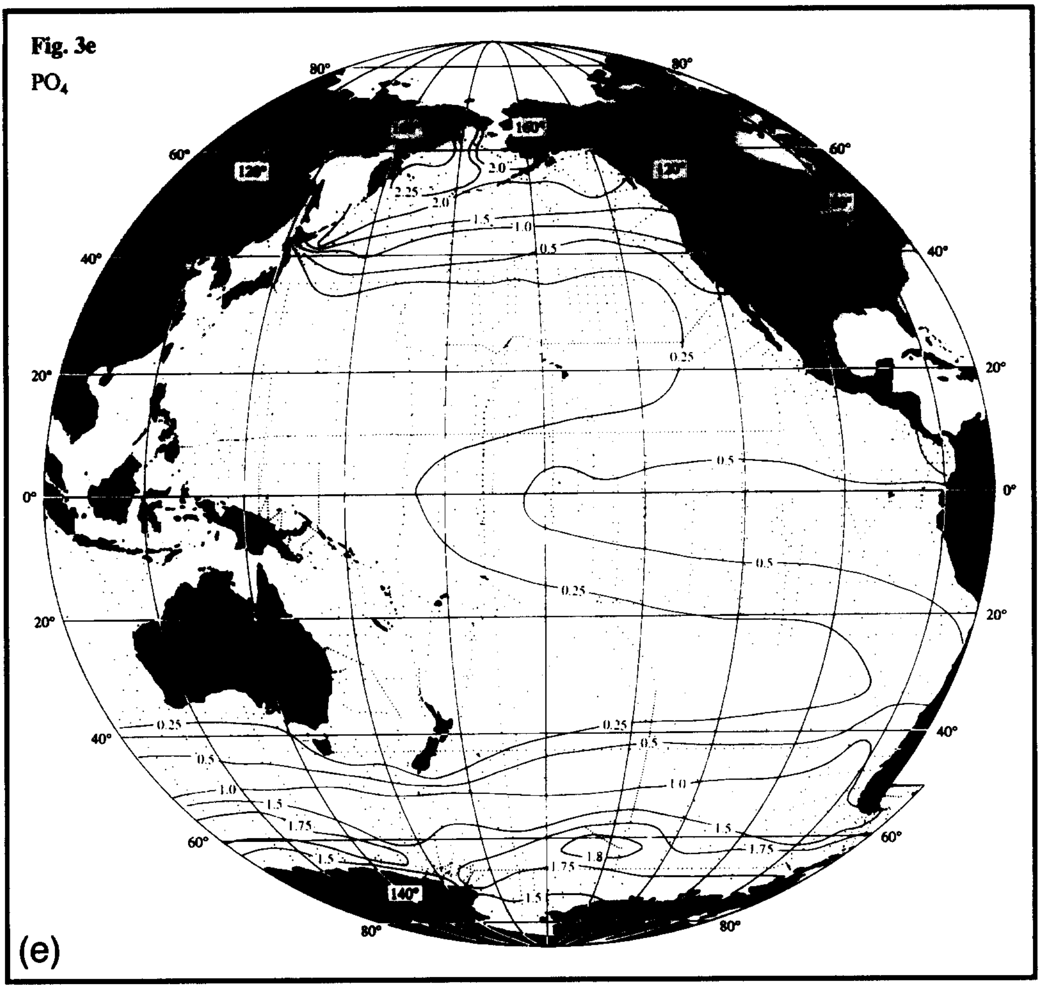

Fig. 3. (e), Northern winter (Nov–Apr) phosphate (μm kg^{-1}) at the sea surface.

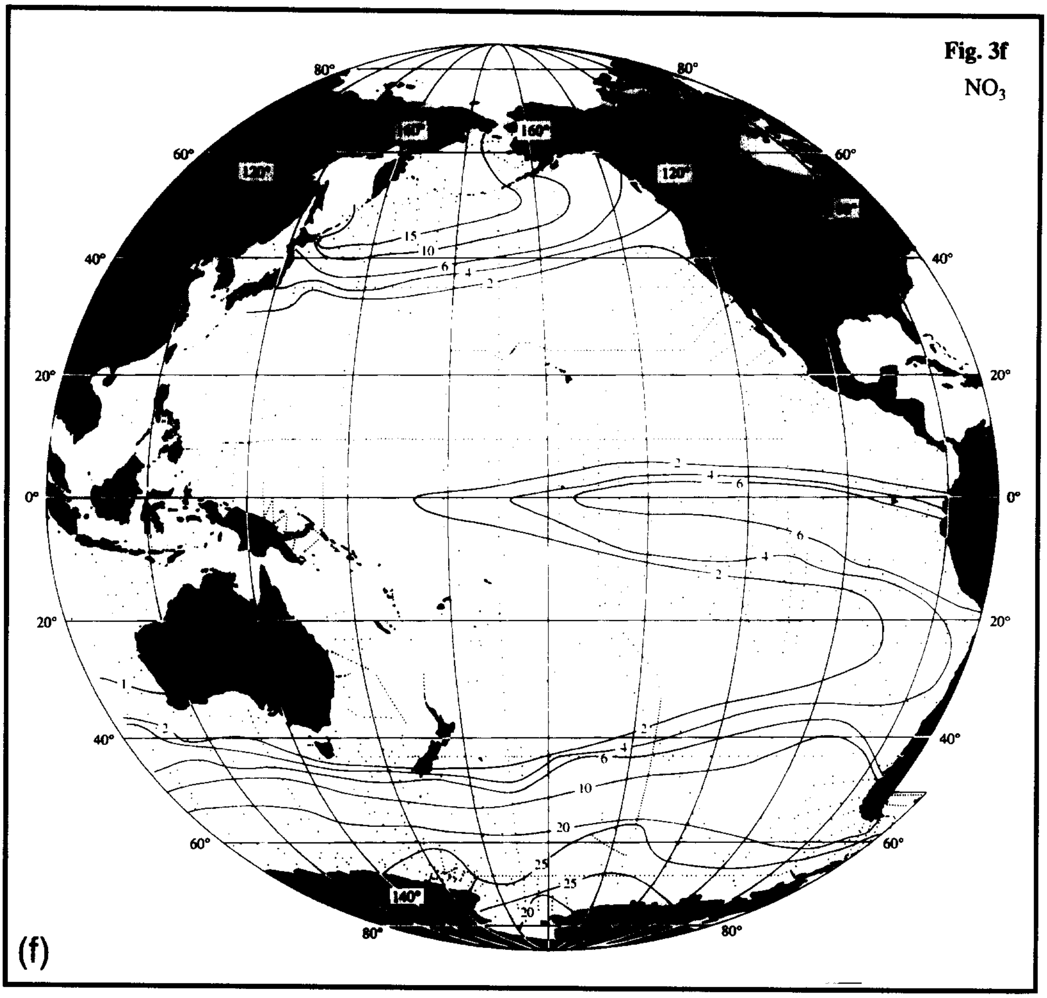

Fig. 3. (f), Northern winter (Nov–Apr) nitrate (μm kg^{-1}) at the sea surface.

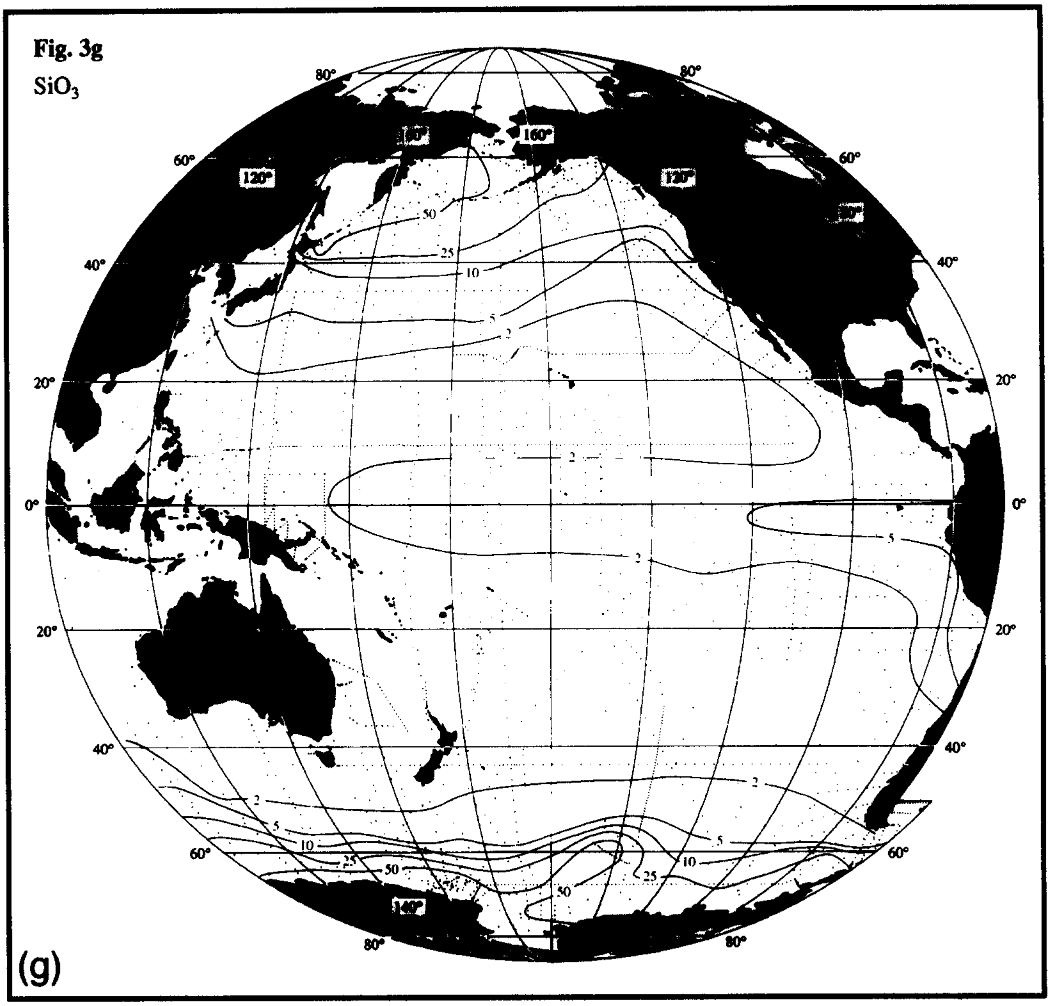

Fig. 3. (g), Northern winter (Nov–Apr) silica (μm kg^{-1}) at the sea surface.

Fig. 4a, 4b
θ, S

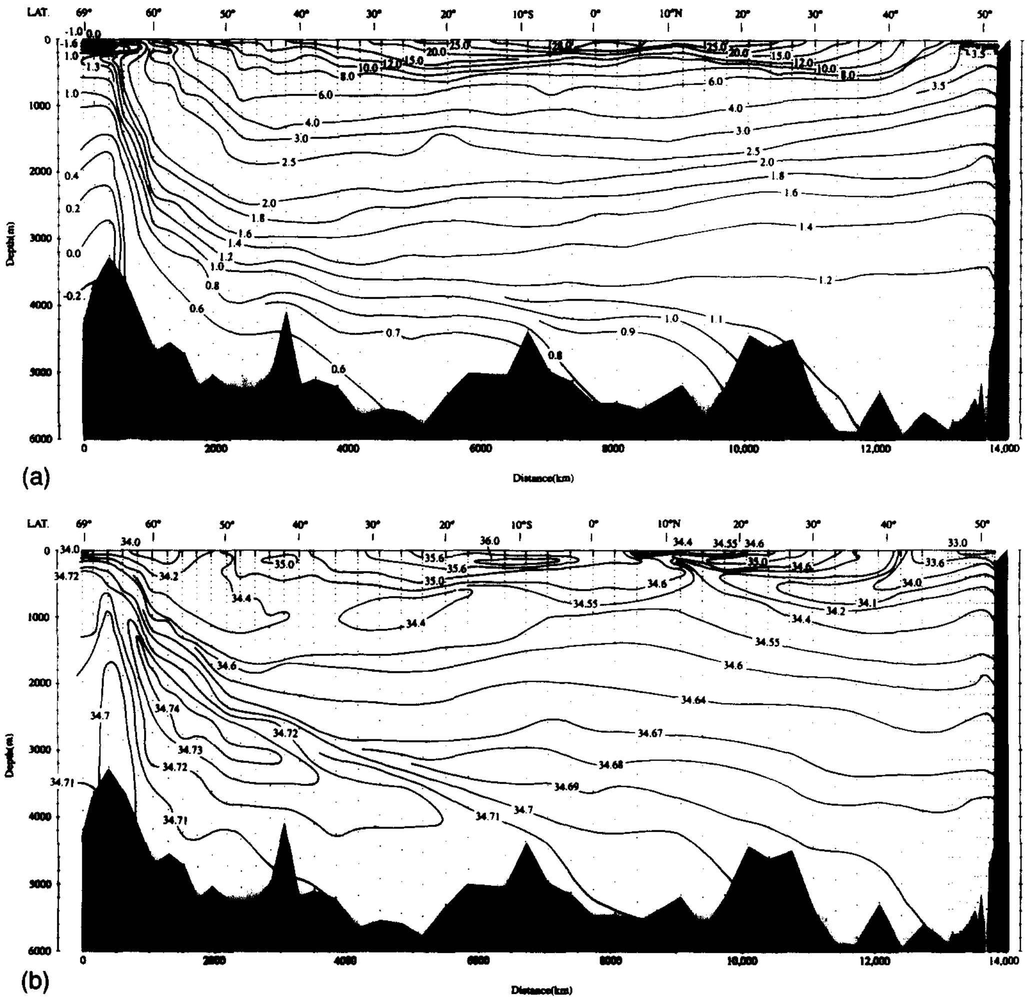

Fig. 4. (a) Potential temperature (°C) on a vertical section along 170°W. (b), Salinity on a vertical section along 170°W.

Fig. 4c, 4d

$\sigma_0 - \sigma_4$, O_2

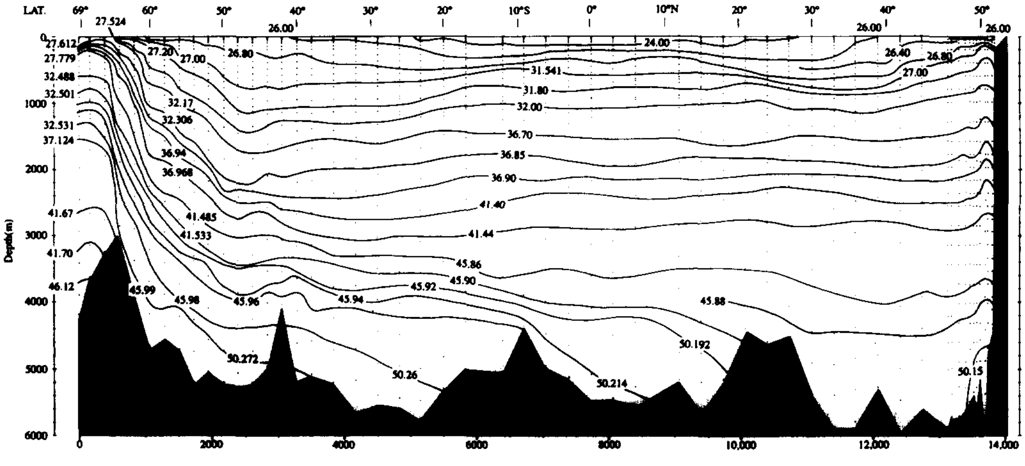

(c)

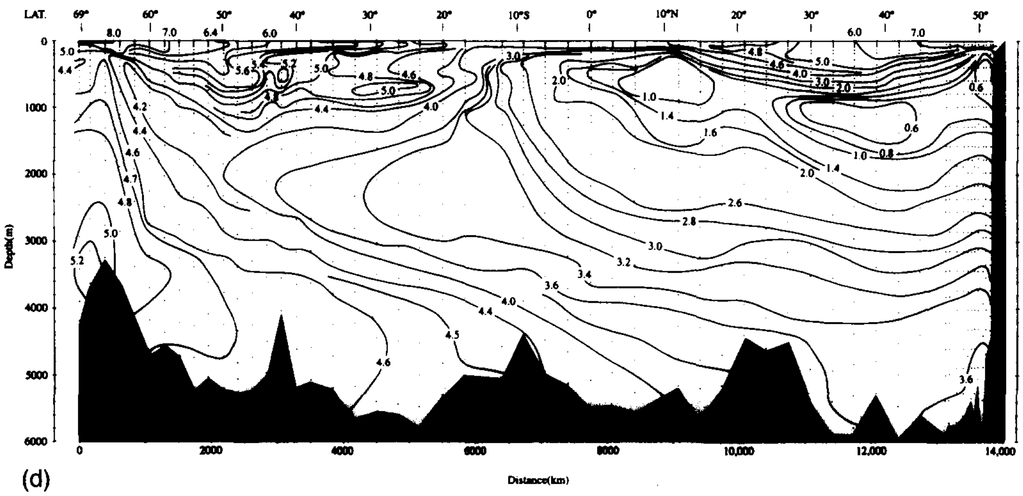

(d)

Fig. 4. (c), Potential density (σ_0–σ_5) on a vertical section along 170°W. (d), Oxygen (ml/l) on a vertical section along 170°W.

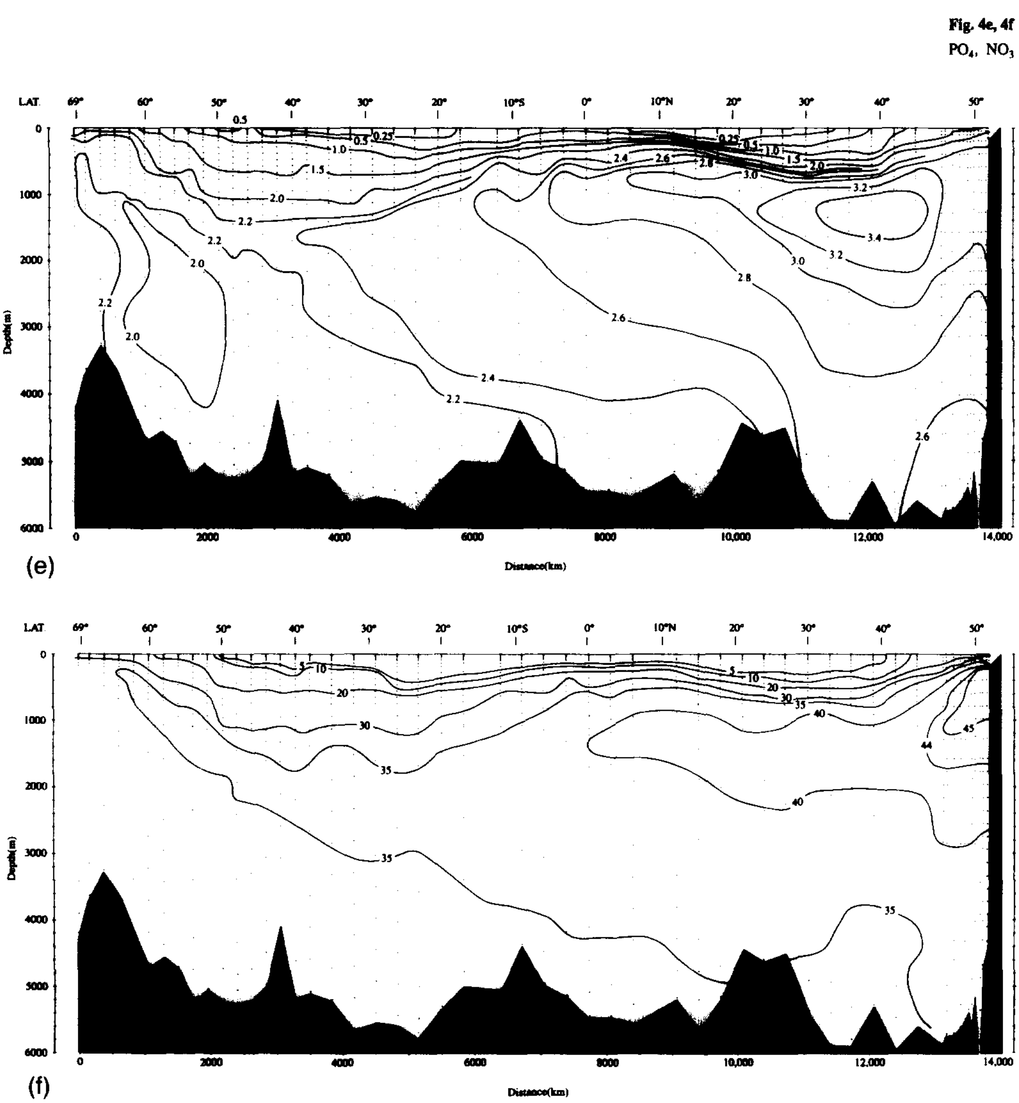

Fig. 4. (e), Phosphate (μm kg^{-1}) on a vertical section along 170°W. (f), Nitrate (μm kg^{-1}) on a vertical section along 170°W.

Fig. 4g
SiO_3

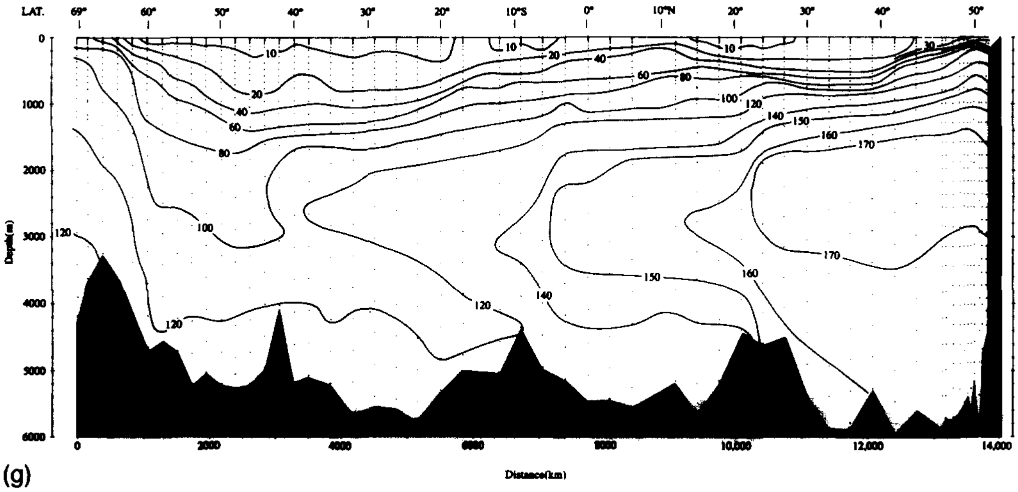

Fig. 4. (g), Silica (μm kg^{-1}) on a vertical section along 170°W.

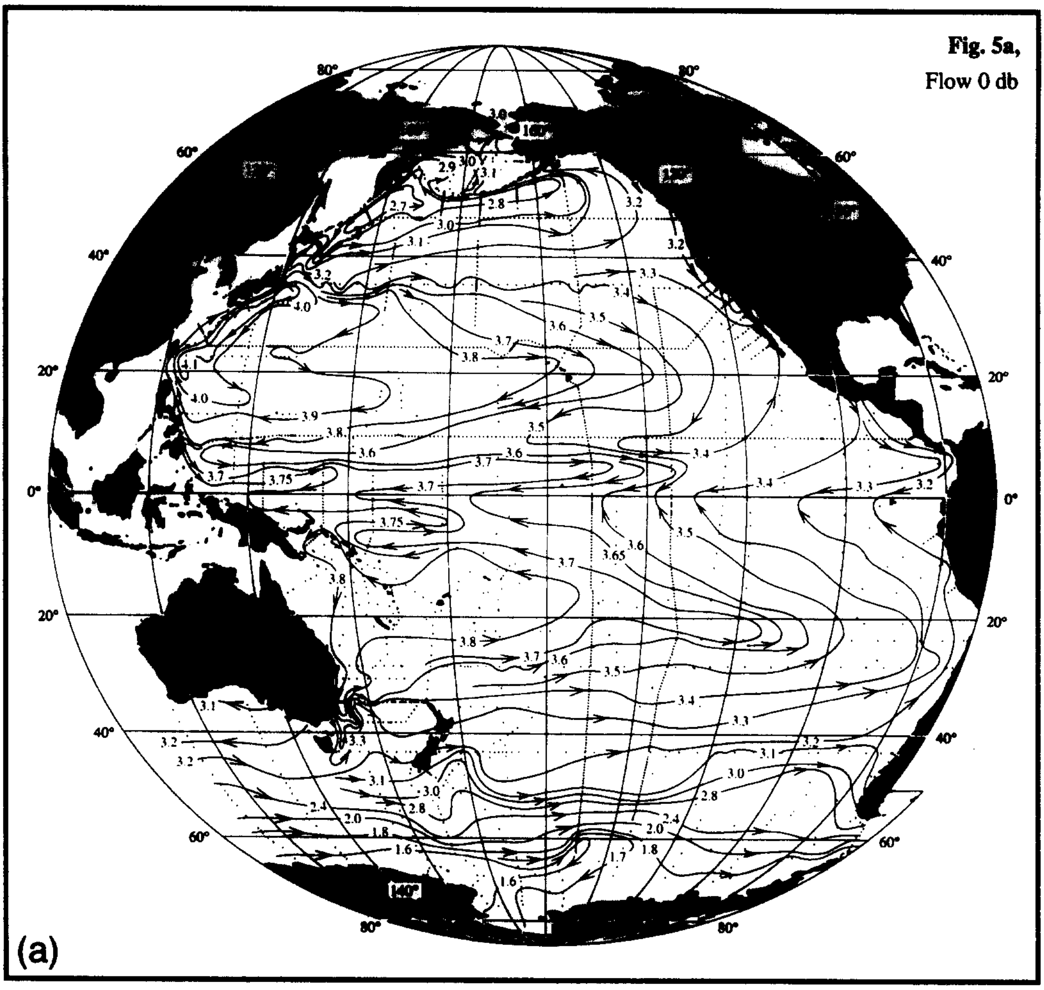

Fig. 5. (a) Adjusted steric height at 0 db (10 m^2s^{-2} or 10 Jkg^{-1}).

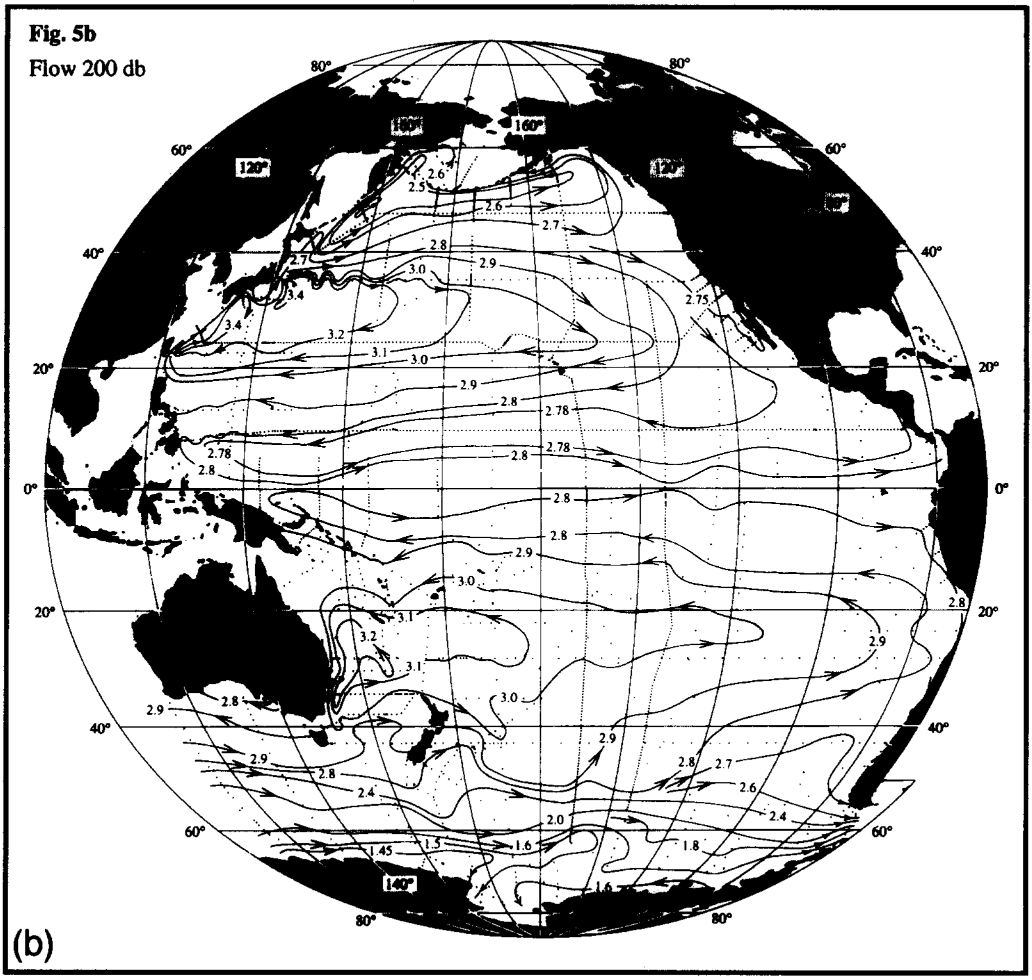

Fig. 5. (b), Adjusted steric height at 200 db (10 m^2s^{-2} or 10 Jkg^{-1}).

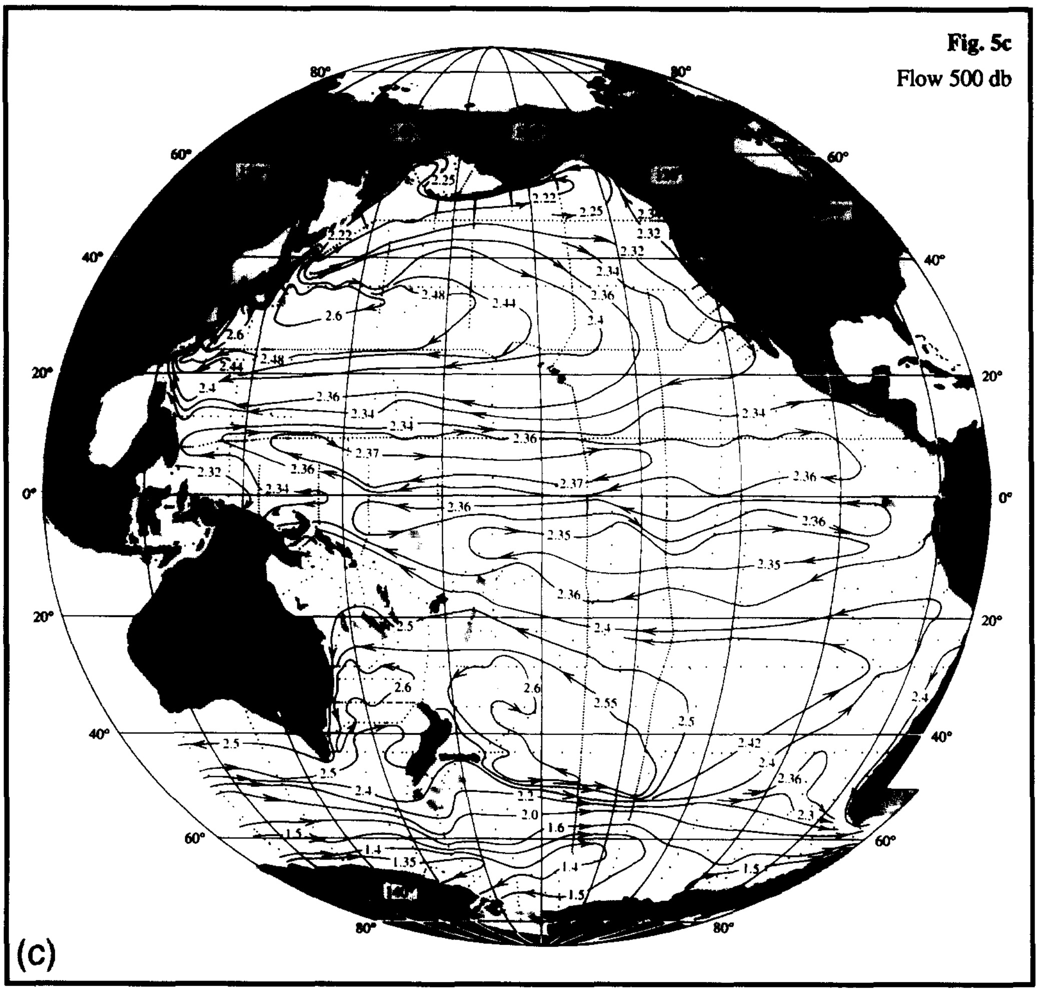

Fig. 5. (c), Adjusted steric height at 500 db (10 m^2s^{-2} or 10 Jkg^{-1}). Depths less than 500 m are shaded.

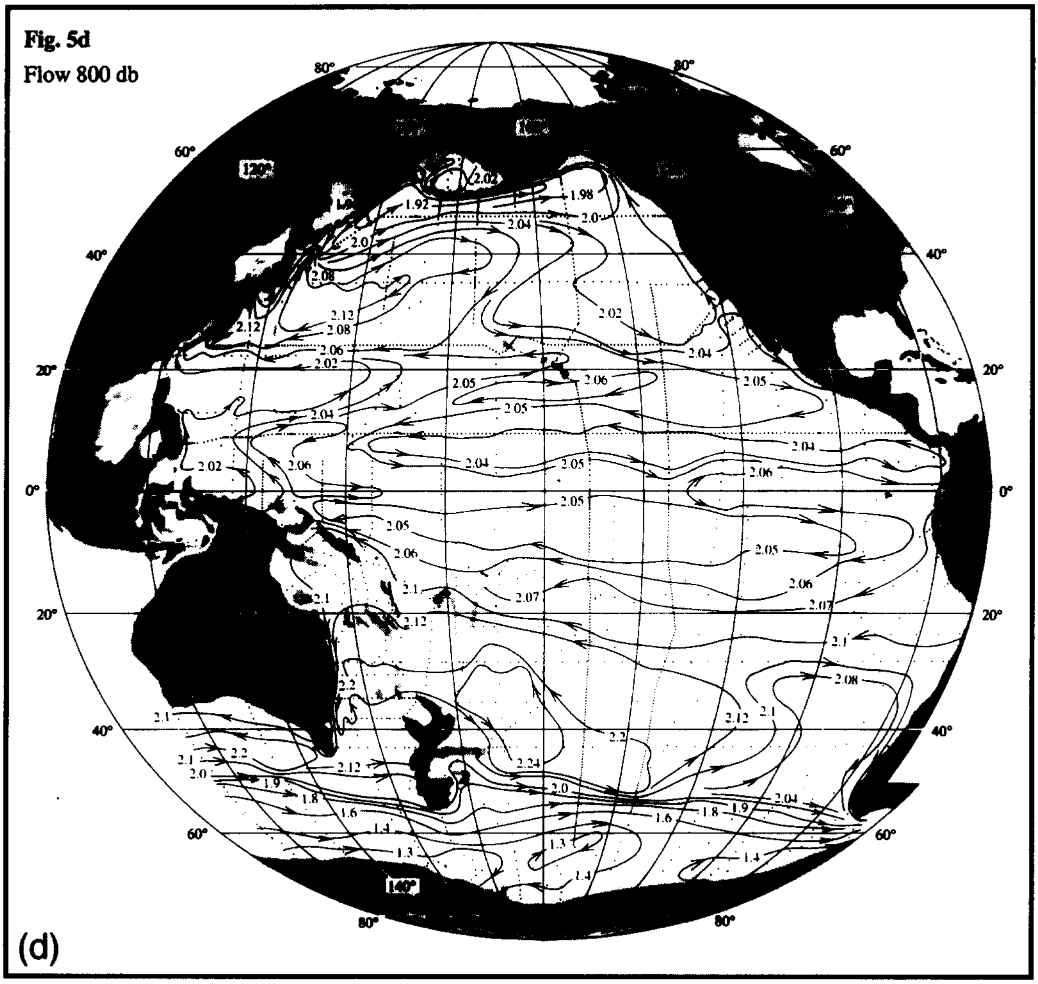

Fig. 5. (d), Adjusted steric height at 800 db (10 m^2s^{-2} or 10 Jkg^{-1}). Depths less than 1000 m are shaded.

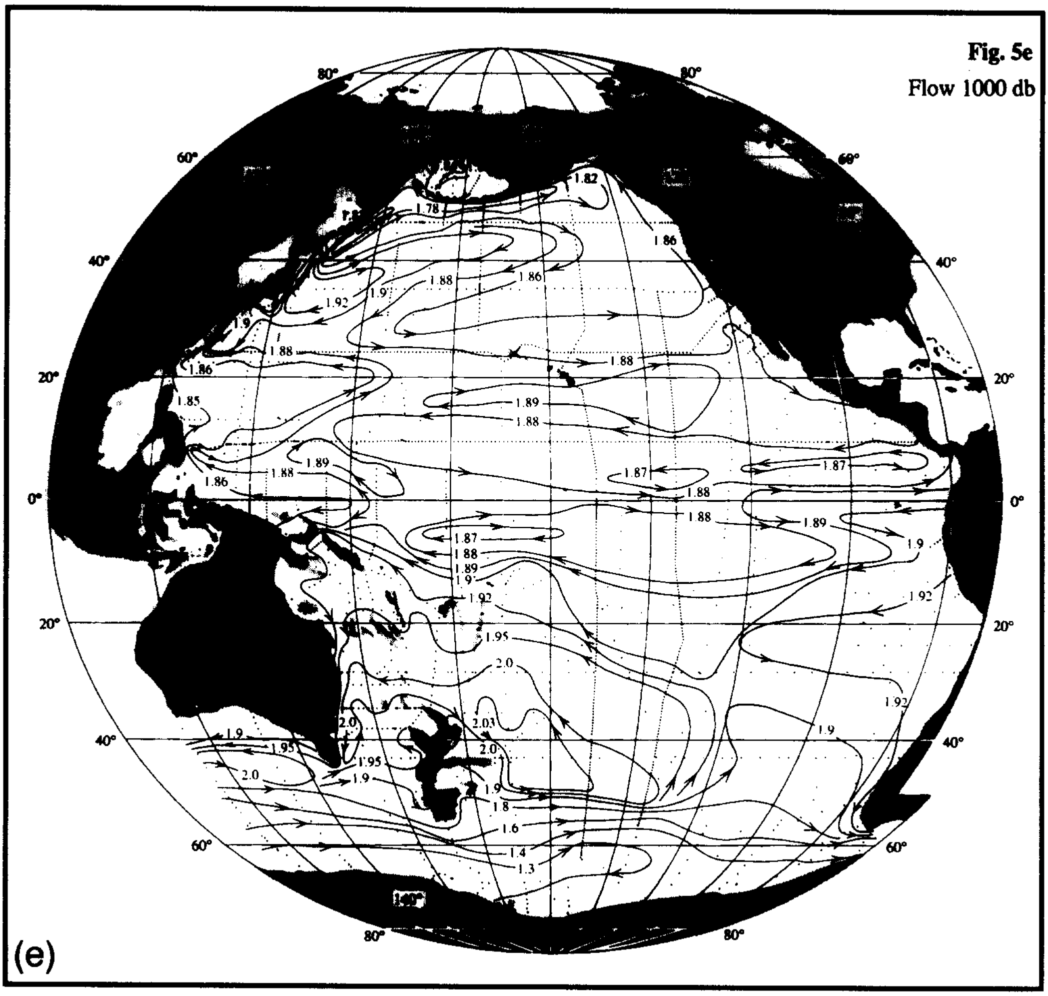

Fig. 5. (e), Adjusted steric height at 1000 db ($10\ m^2s^{-2}$ or $10\ Jkg^{-1}$). Depths less than 1000 m are shaded.

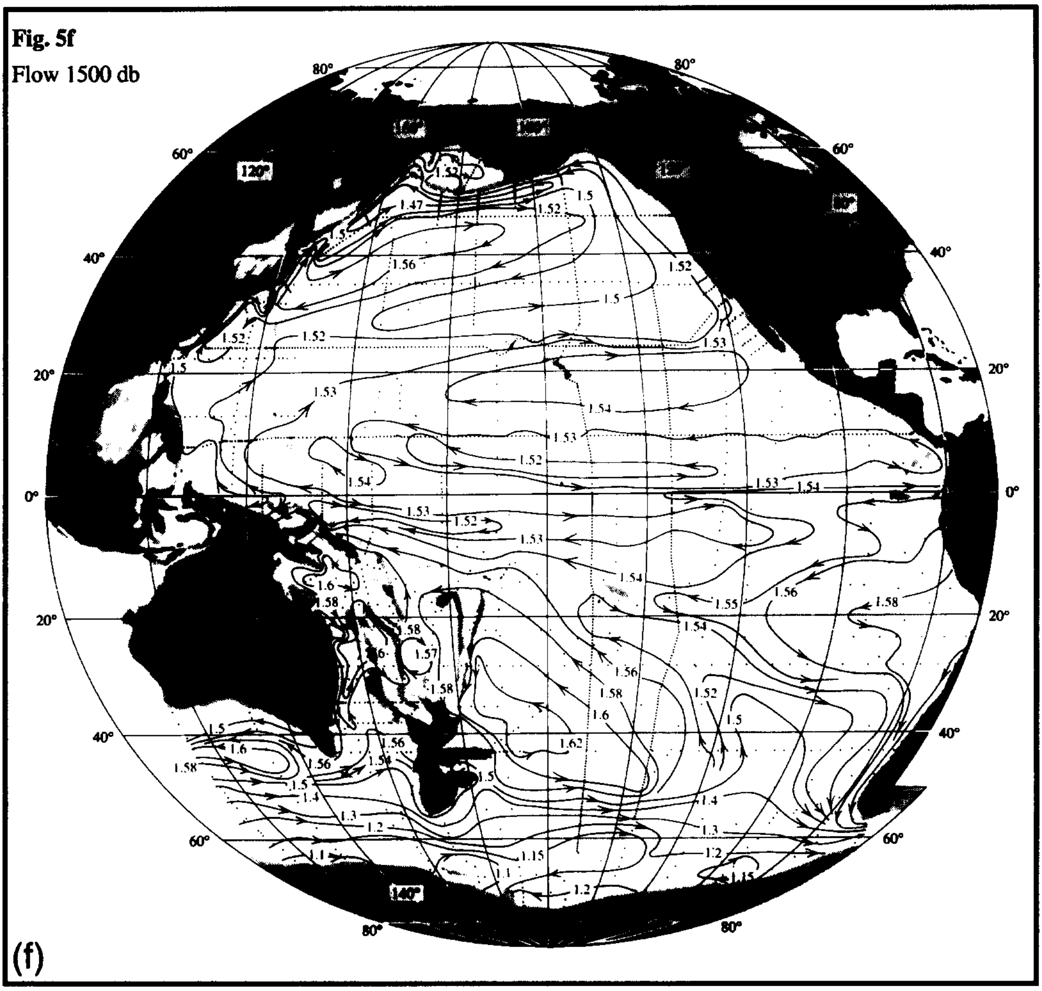

Fig. 5. (f), Adjusted steric height at 1500 db (10 m^2s^{-2} or 10 Jkg^{-1}). Depths less than 1500 m are shaded.

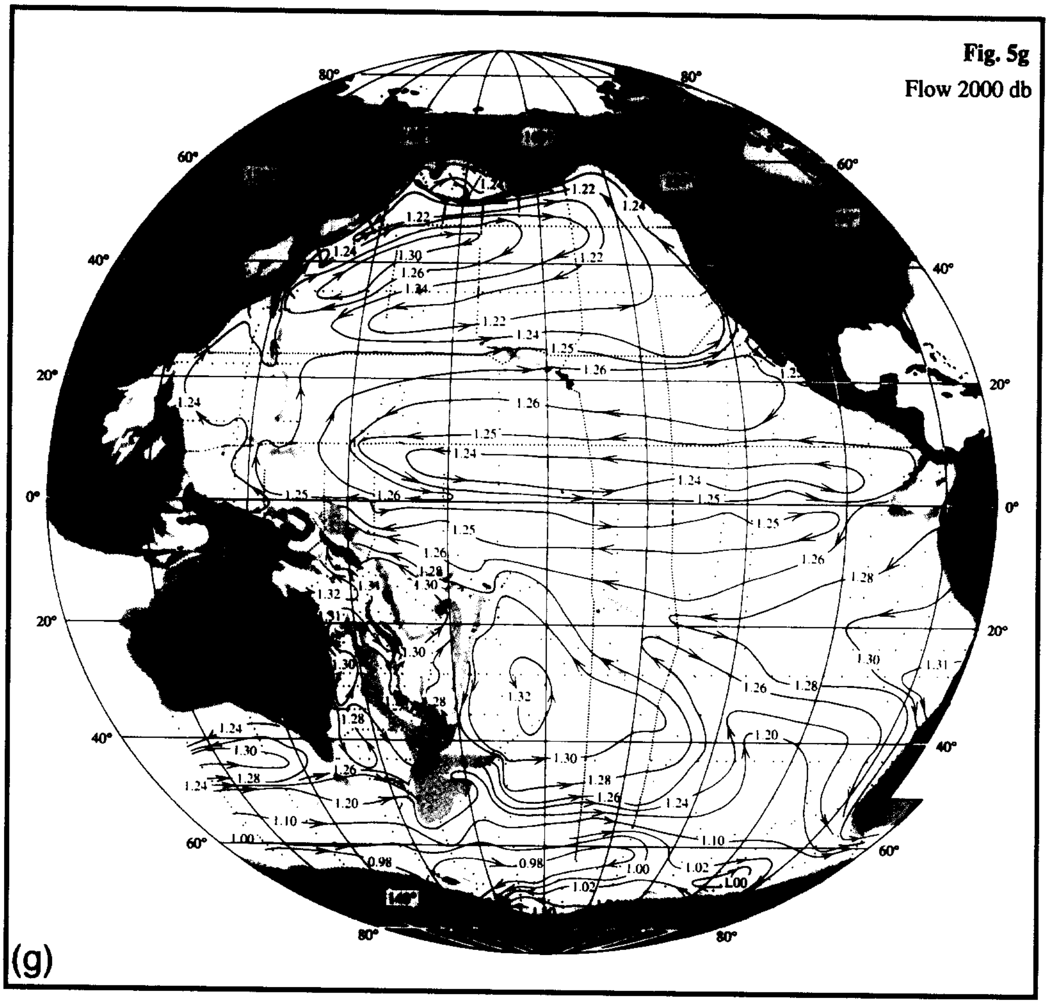

Fig. 5. (g), Adjusted steric height at 2000 db (10 m^2s^{-2} or 10 Jkg^{-1}). Depths less than 2000 m are shaded.

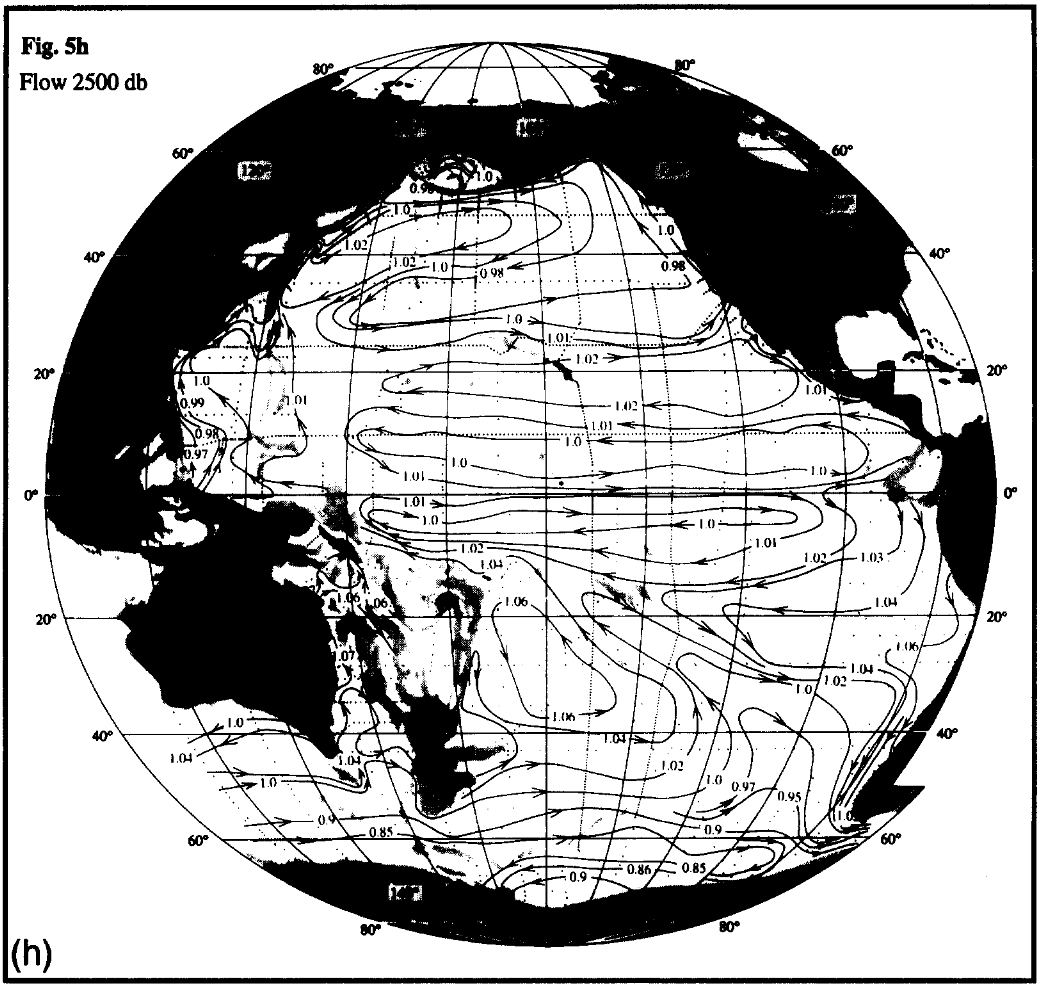

Fig. 5. (h), Adjusted steric height at 2500 db (10 m^2s^{-2} or 10 Jkg^{-1}). Depths less than 2500 m are shaded.

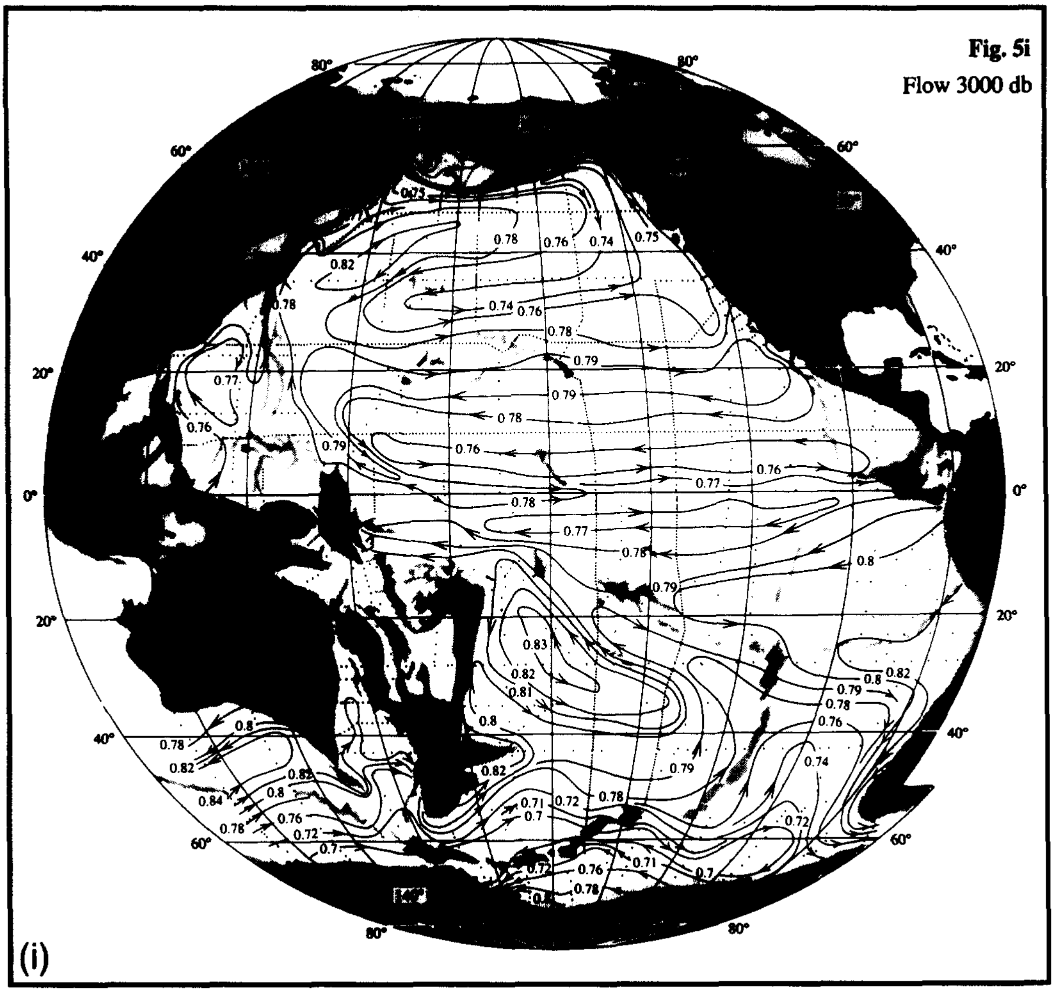

Fig. 5. (i), Adjusted steric height at 3000 db (10 m^2s^{-2} or 10 Jkg^{-1}). Depths less than 3000 m are shaded.

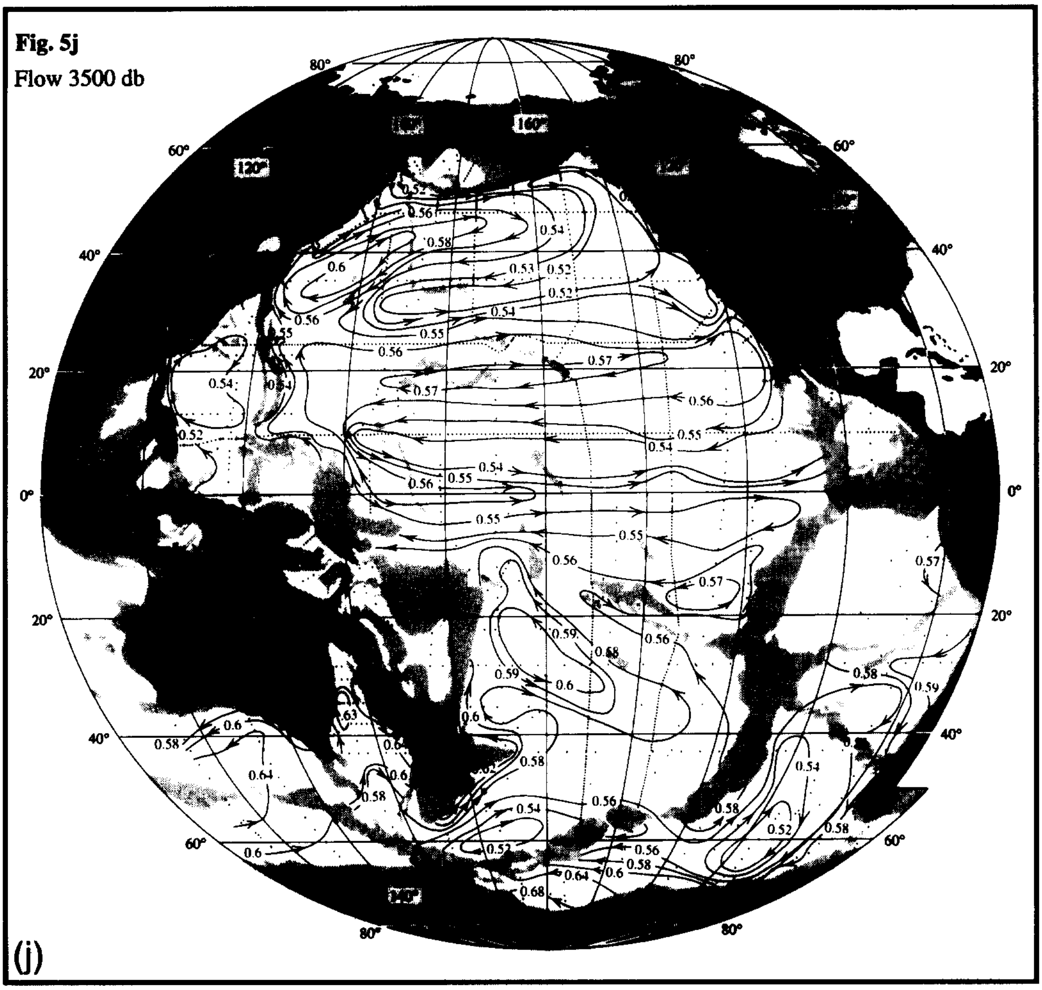

Fig. 5. (j), Adjusted steric height at 3500 db ($10\ m^2s^{-2}$ or $10\ Jkg^{-1}$). Depths less than 3500 m are shaded.

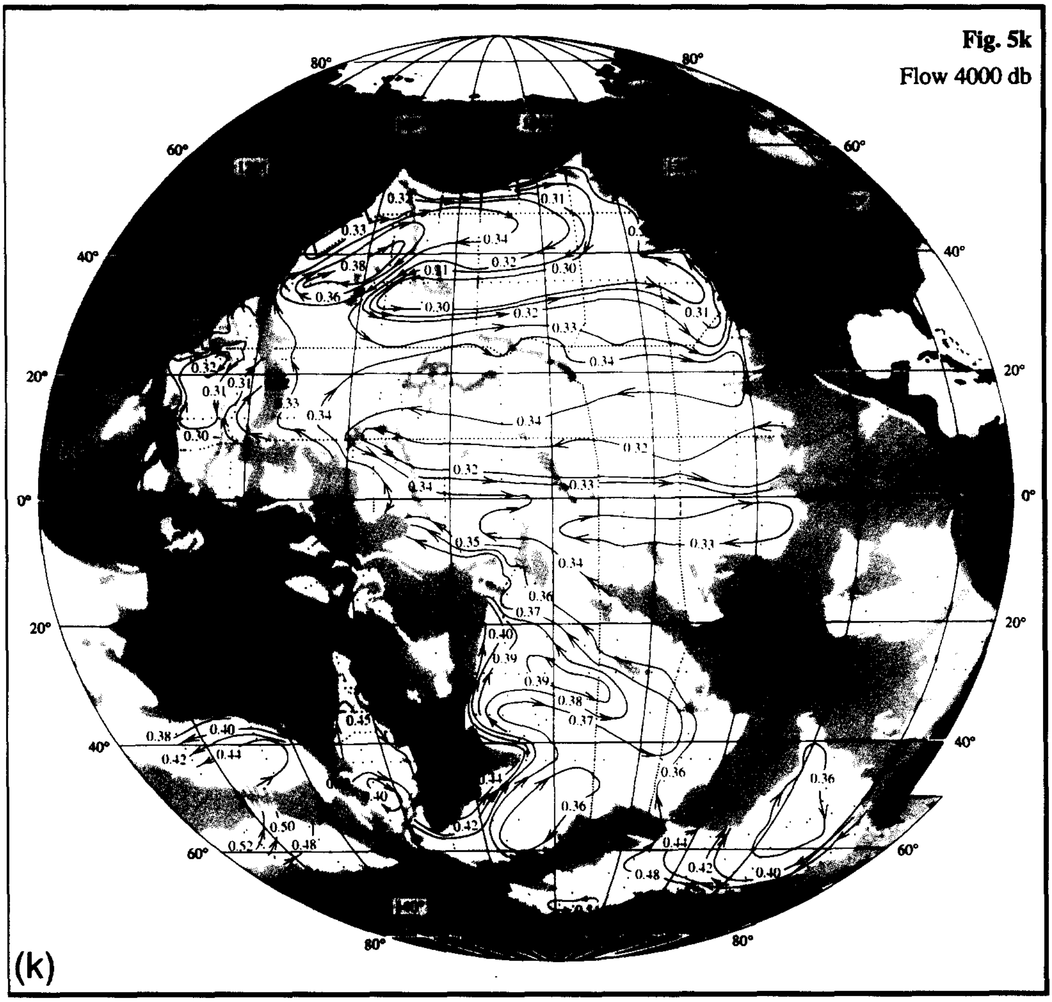

Fig. 5. (k), Adjusted steric height at 4000 db (10 m^2s^{-2} or 10 Jkg^{-1}). Depths less than 4000 m are shaded.

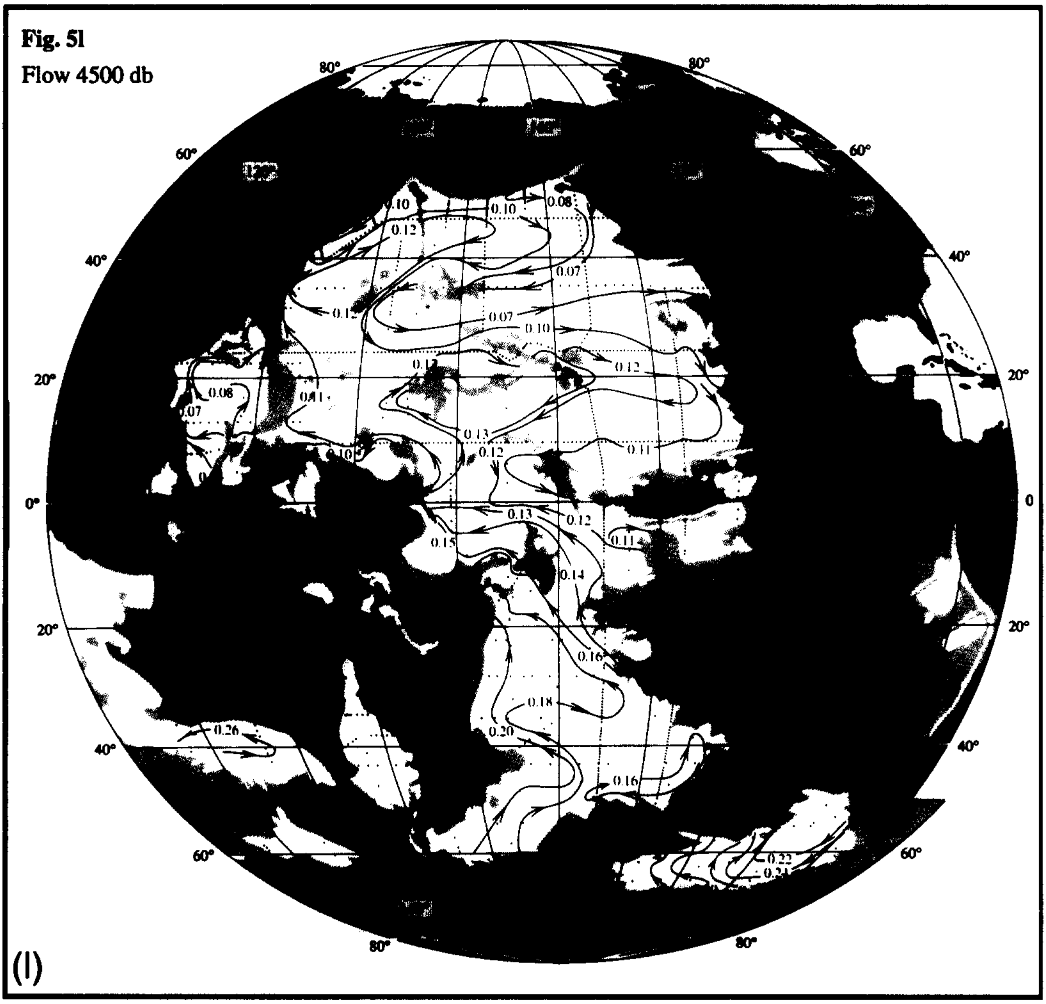

Fig. 5. (l), Adjusted steric height at 4500 db (10 m^2s^{-2} or 10 Jkg^{-1}). Depths less than 4500 m are shaded.

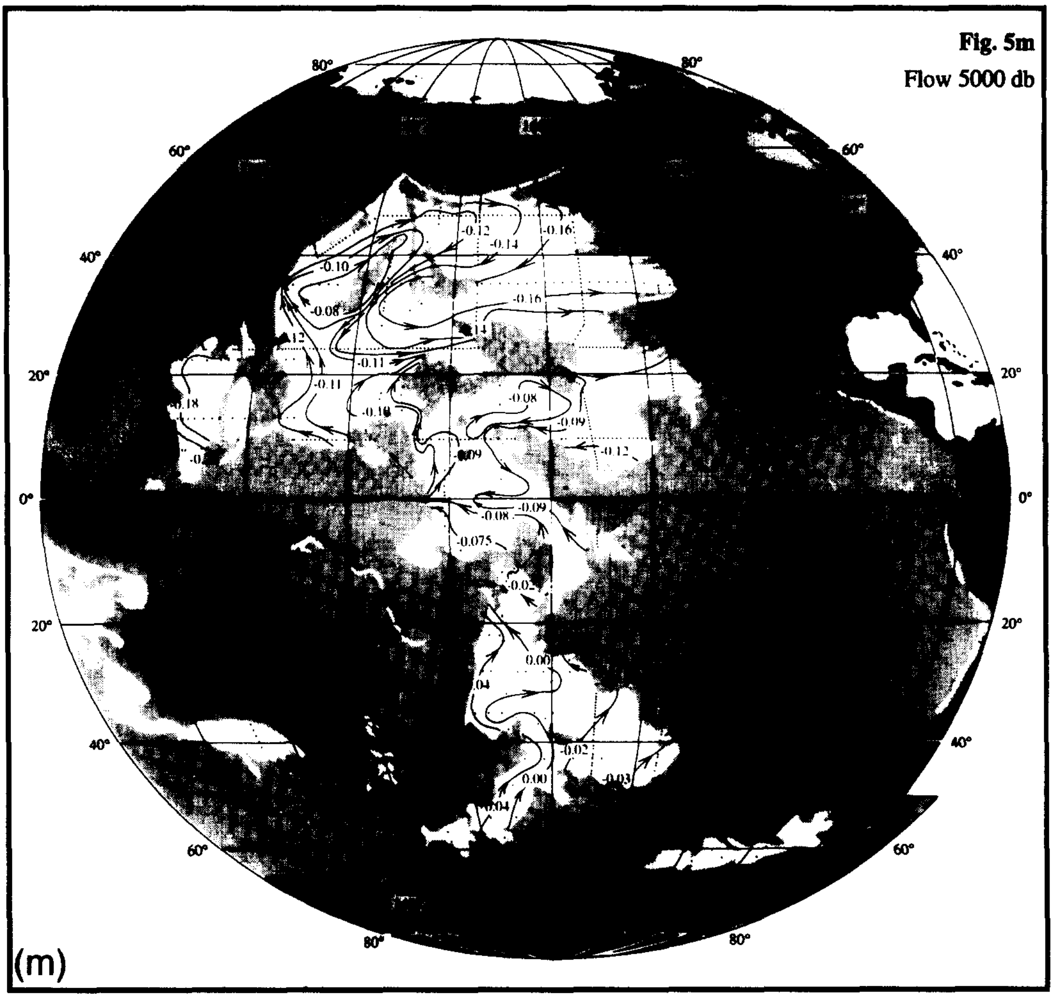

Fig. 5. (m), Adjusted steric height at 5000 db (10 m^2s^{-2} or 10 Jkg^{-1}). Depths less than 5000 m are shaded.

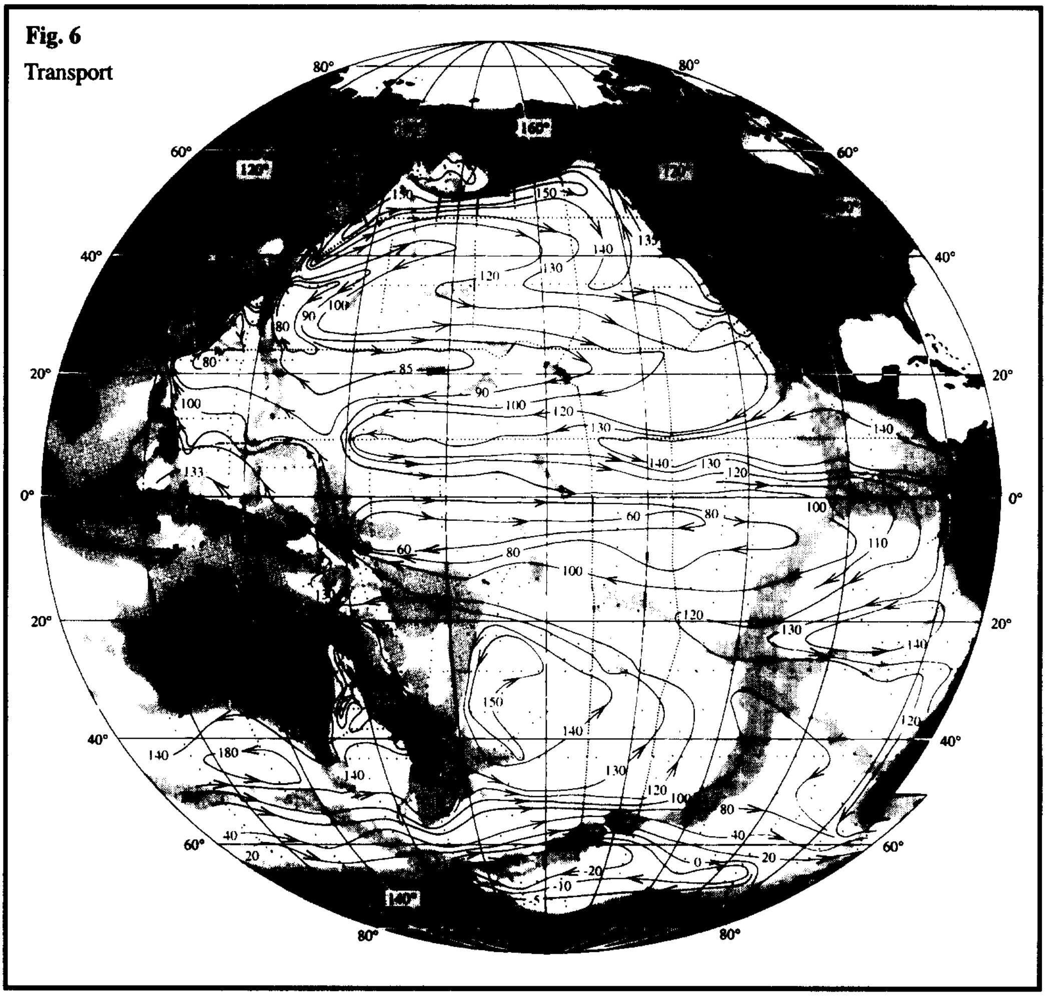

Fig. 6. Transport (10 m^2s^{-2} or $10Jkg^{-1}$). The integration starts from zero along the coast of Antarctica and reaches 135 along the coast of Australia up to the Indonesian Seas, where 3 pass westward to the Indian Ocean. It is 132 from there to the Bering Strait, where 2 pass into the Arctic Ocean, and 130 along the American continents.

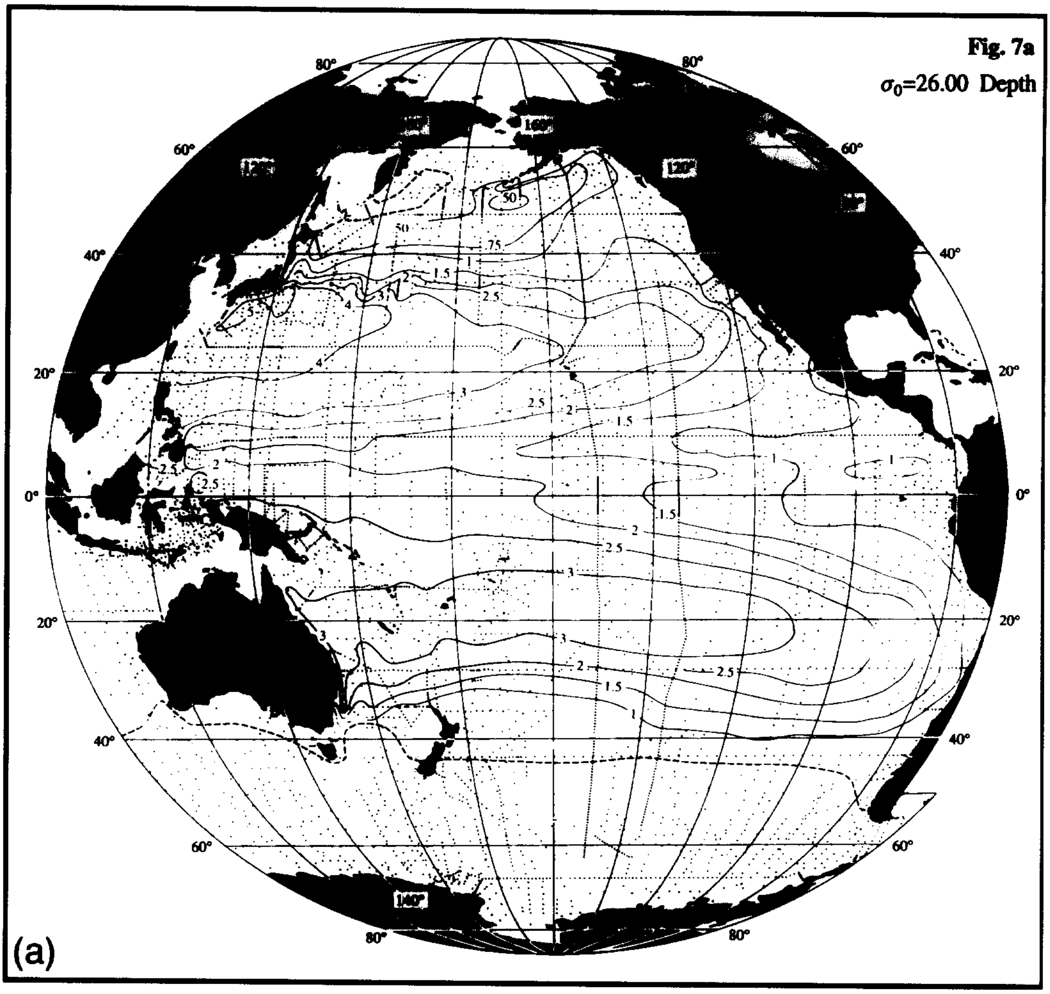

Fig. 7. (a) Depth (hm) of the isopycnal defined by 26.00 in σ_0. On this and all the other isopycnal maps the shaded parts represent areas where all the water is less dense than the isopycnal value and the dashed line indicates the outcrop.

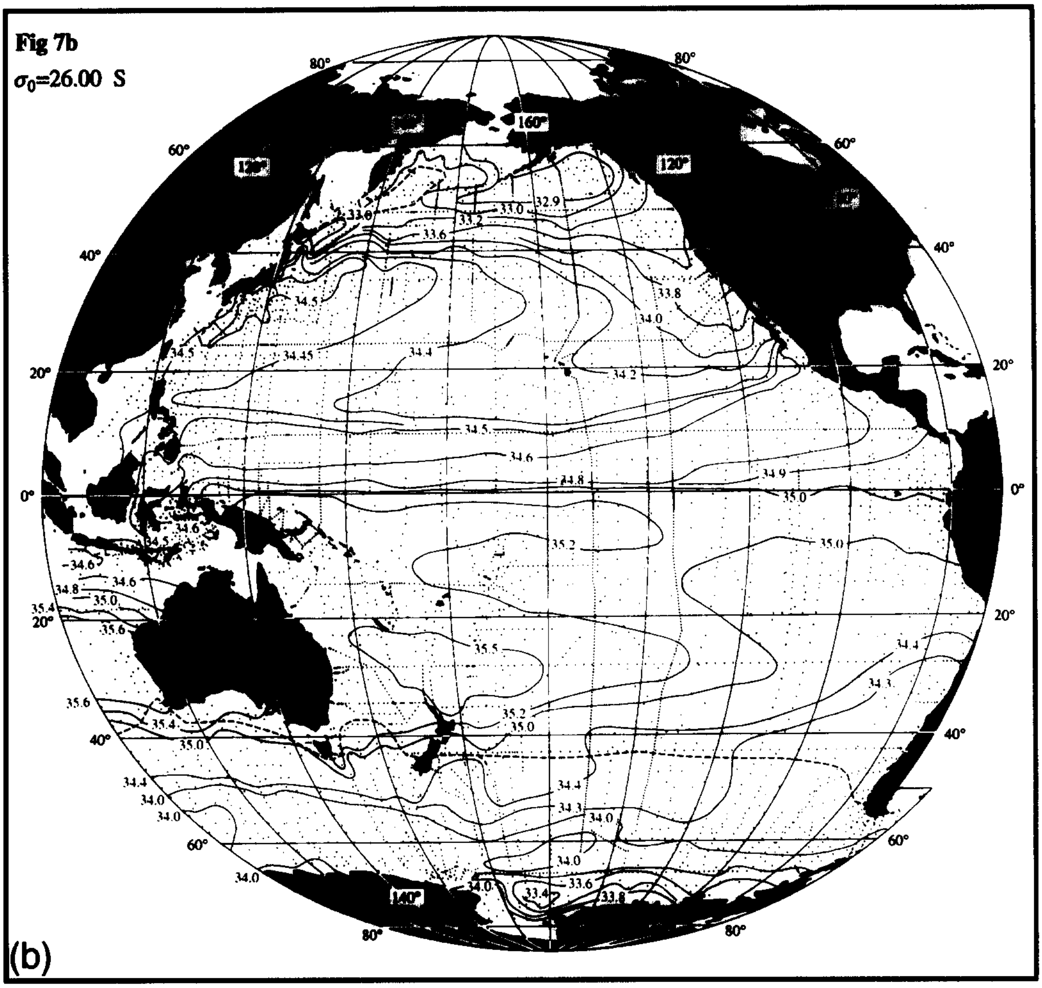

Fig. 7. (b), Salinity on the isopycnal defined by 26.00 in σ_0.

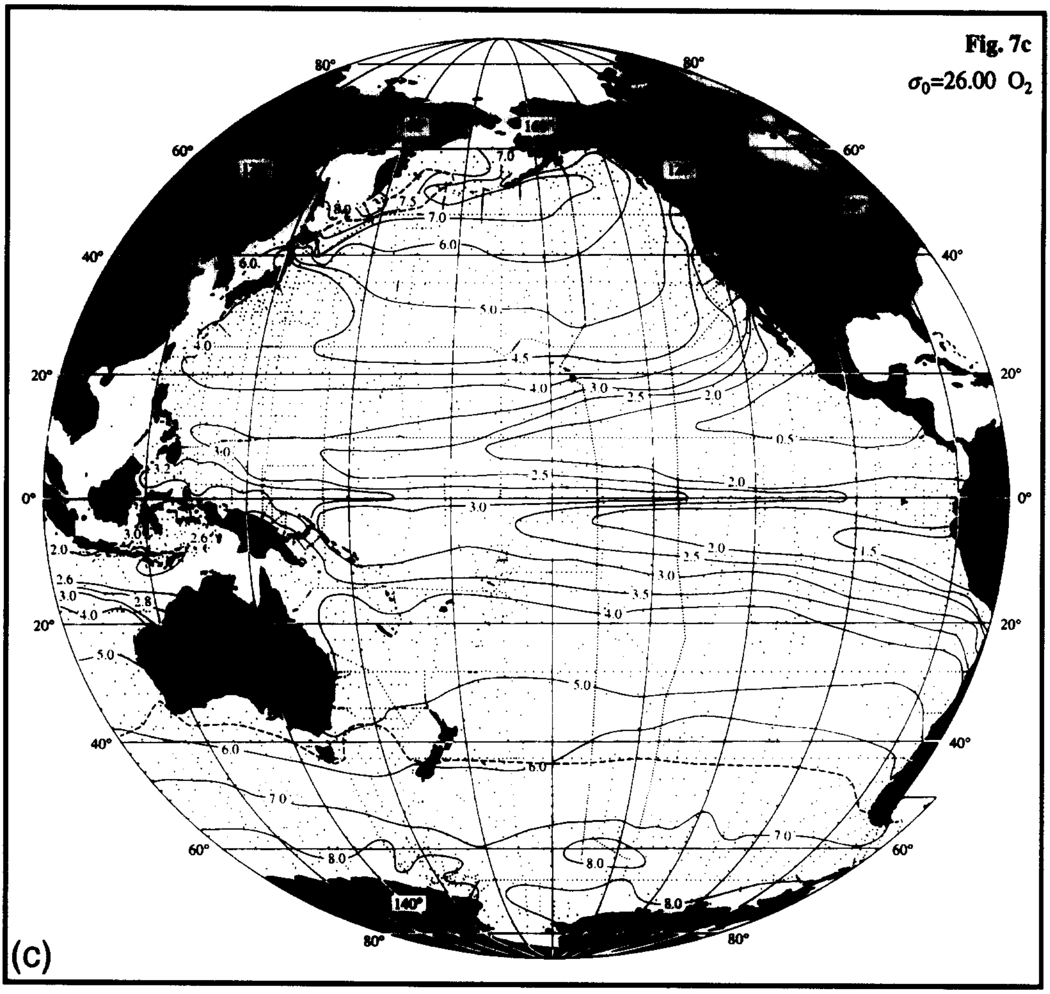

Fig. 7. (c), Oxygen (ml/l) on the isopycnal defined by 26.00 in σ_0.

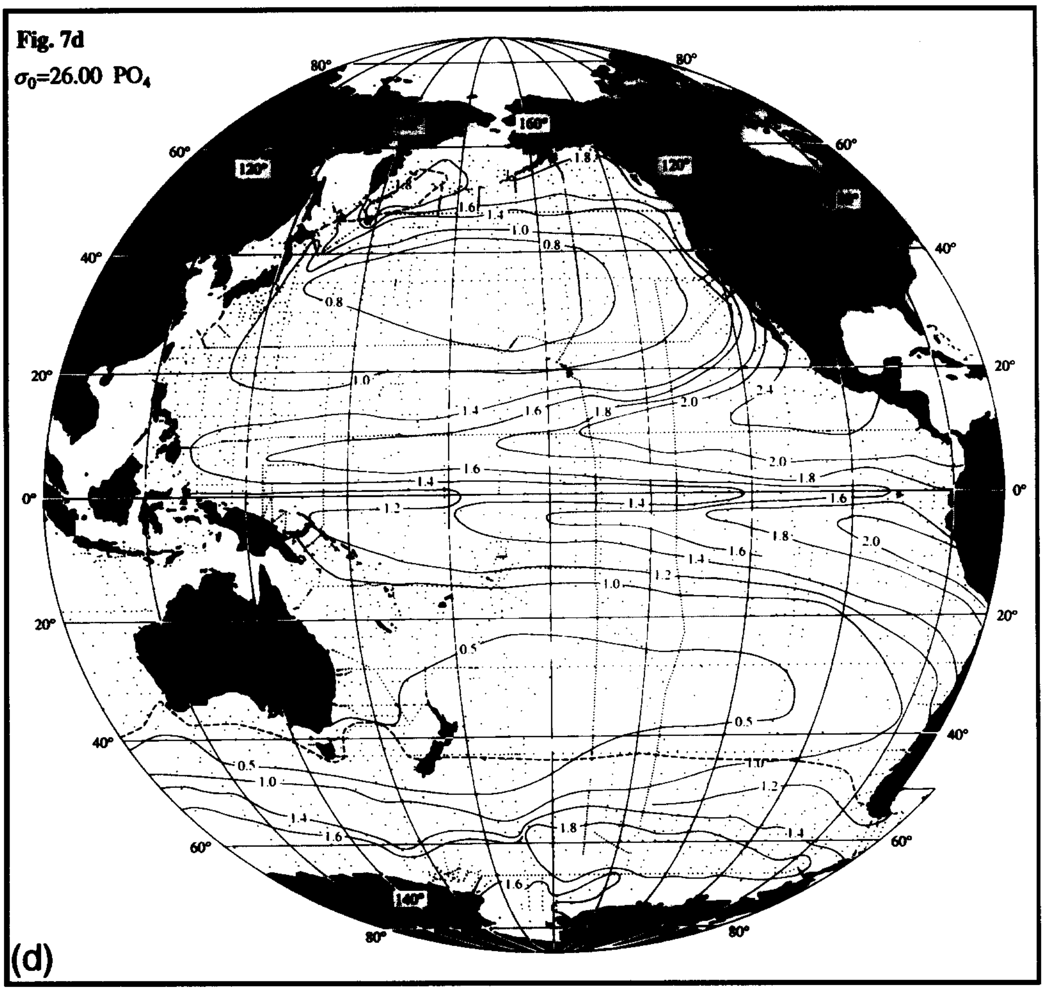

Fig. 7. (d), Phosphate (μm kg^{-1}) on the isopycnal defined by 26.00 in σ_0.

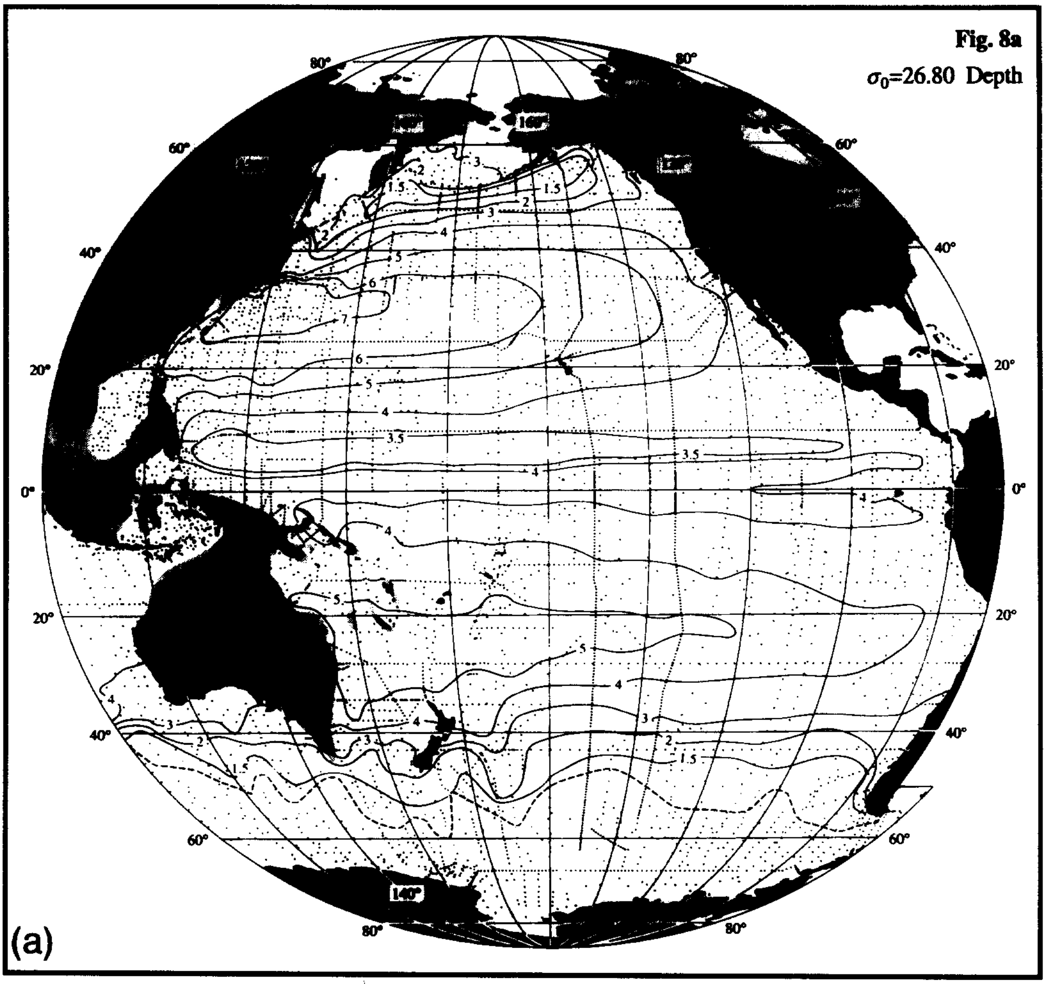

Fig. 8. (a) Depth (hm) of the isopycnal defined by 26.80 in σ_0.

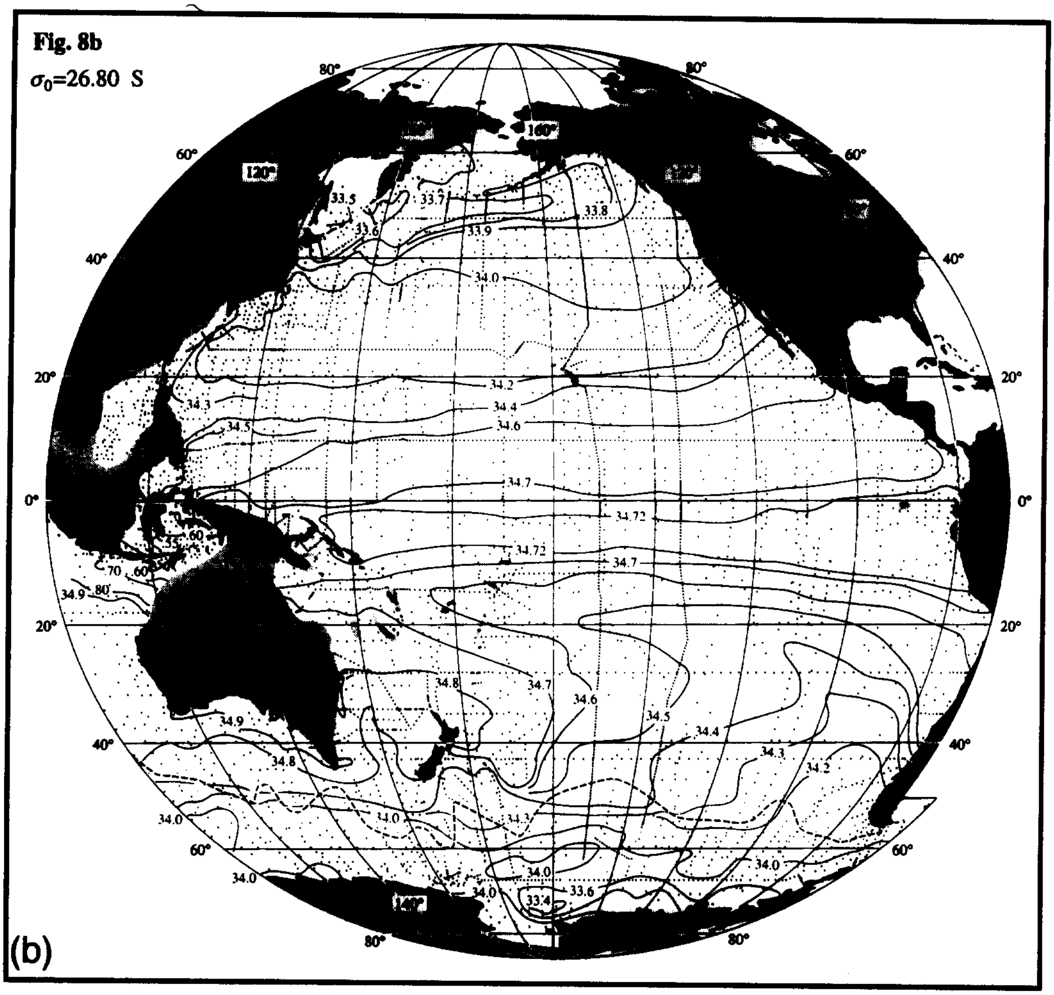

Fig. 8. (b), Salinity on the isopycnal defined by 26.80 in σ_0.

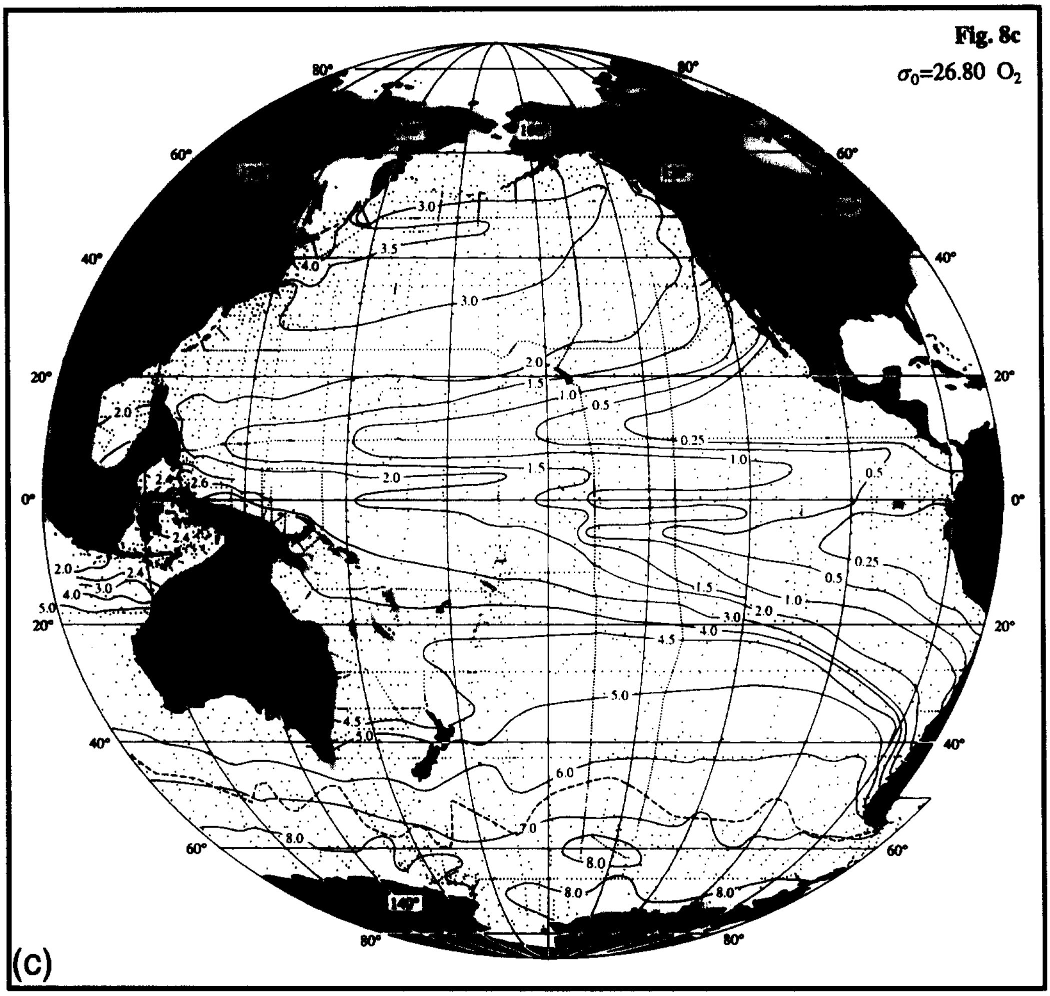

Fig. 8. (c), Oxygen (ml/l) on the isopycnal defined by 26.80 in σ_0.

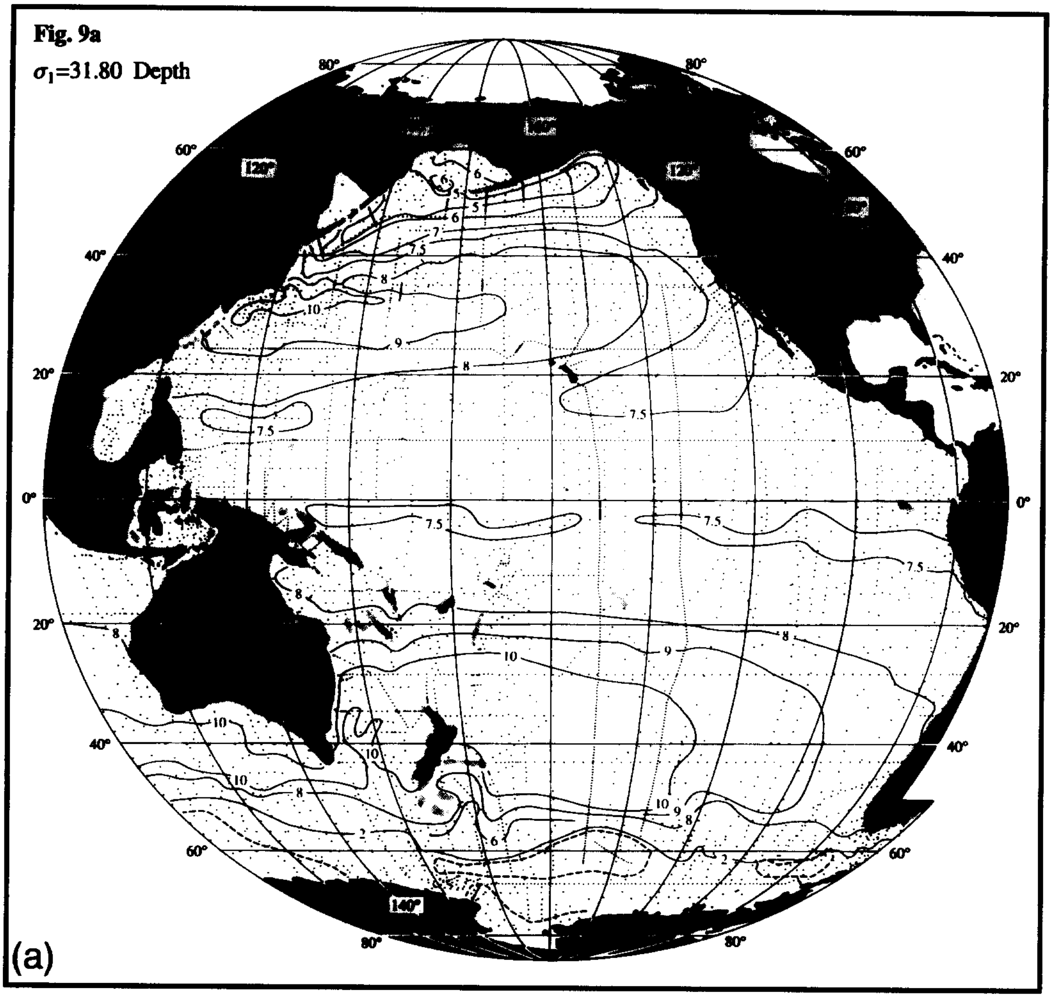

Fig. 9. (a) Depth (hm) of the isopycnal defined by 31.80 in σ_1.

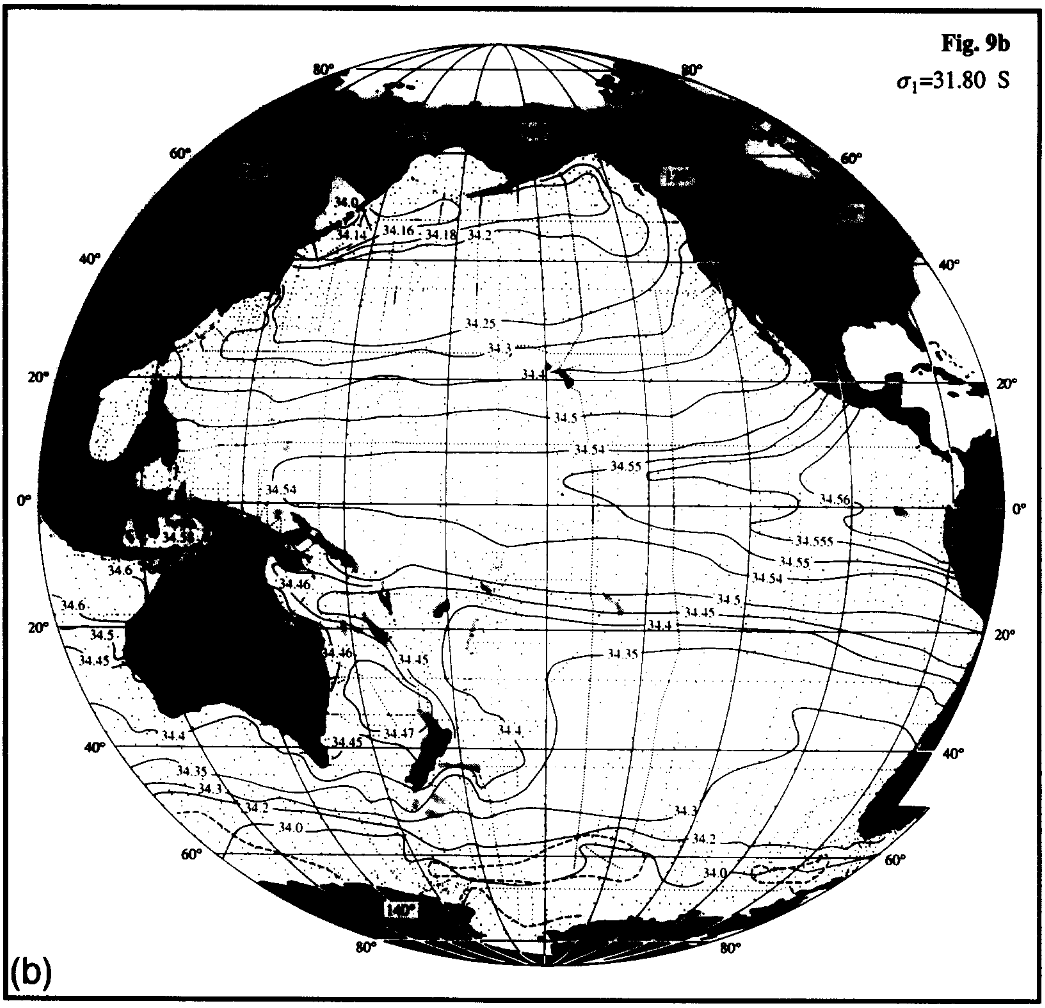

Fig. 9. (b), Salinity on the isopycnal defined by 31.80 in σ_1.

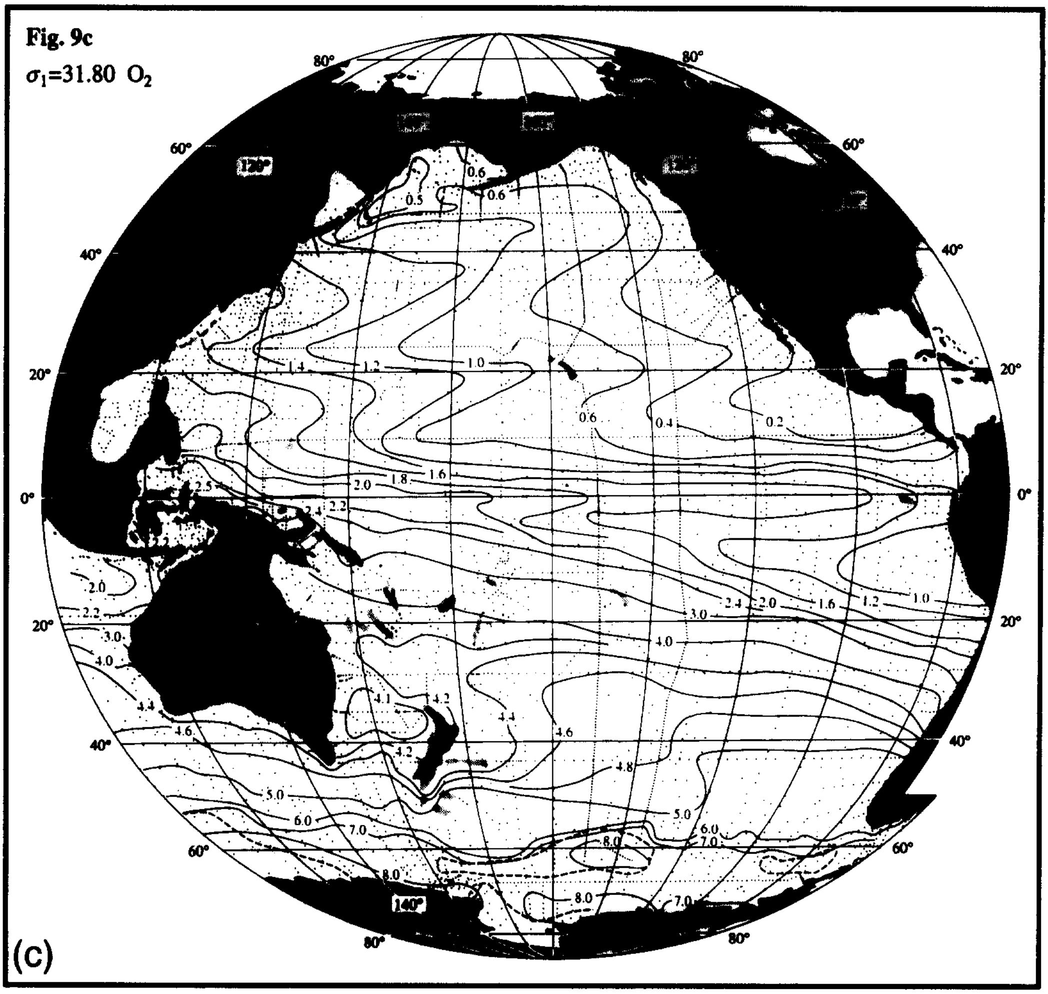

Fig. 9. (c), Oxygen (ml/l) on the isopycnal defined by 31.80 in σ_1.

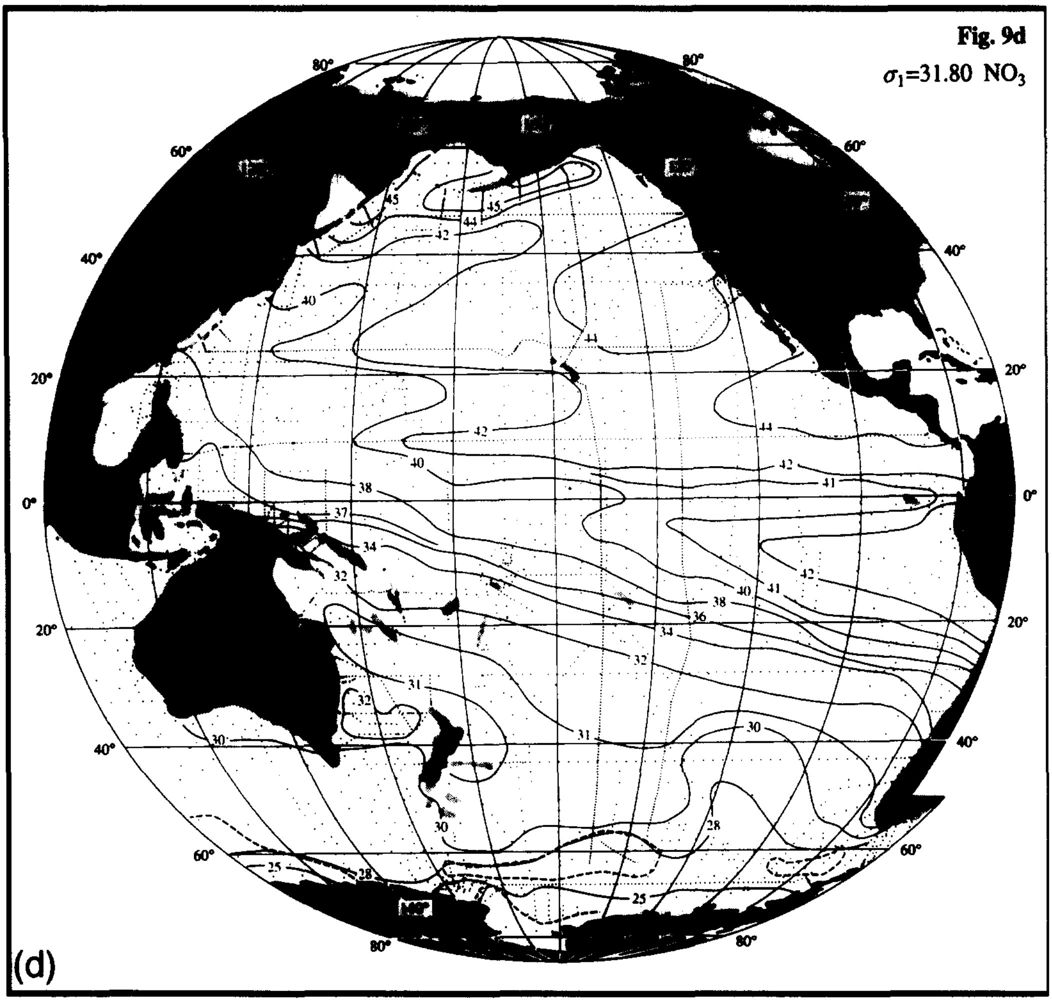

Fig. 9. (d), Nitrate (μm kg^{-1}) on the isopycnal defined by 31.80 in σ_1.

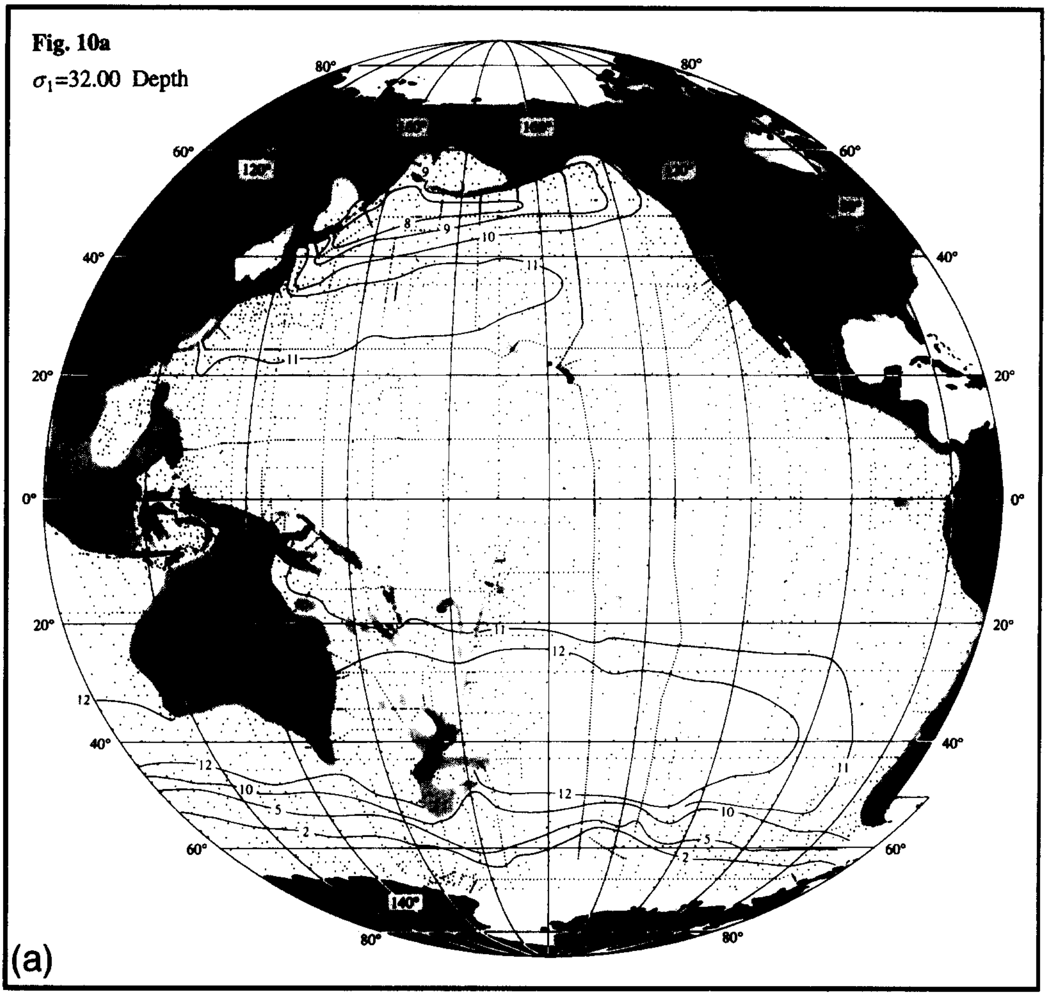

Fig. 10. (a) Depth (hm) of the isopycnal defined by 32.00 in σ_1.

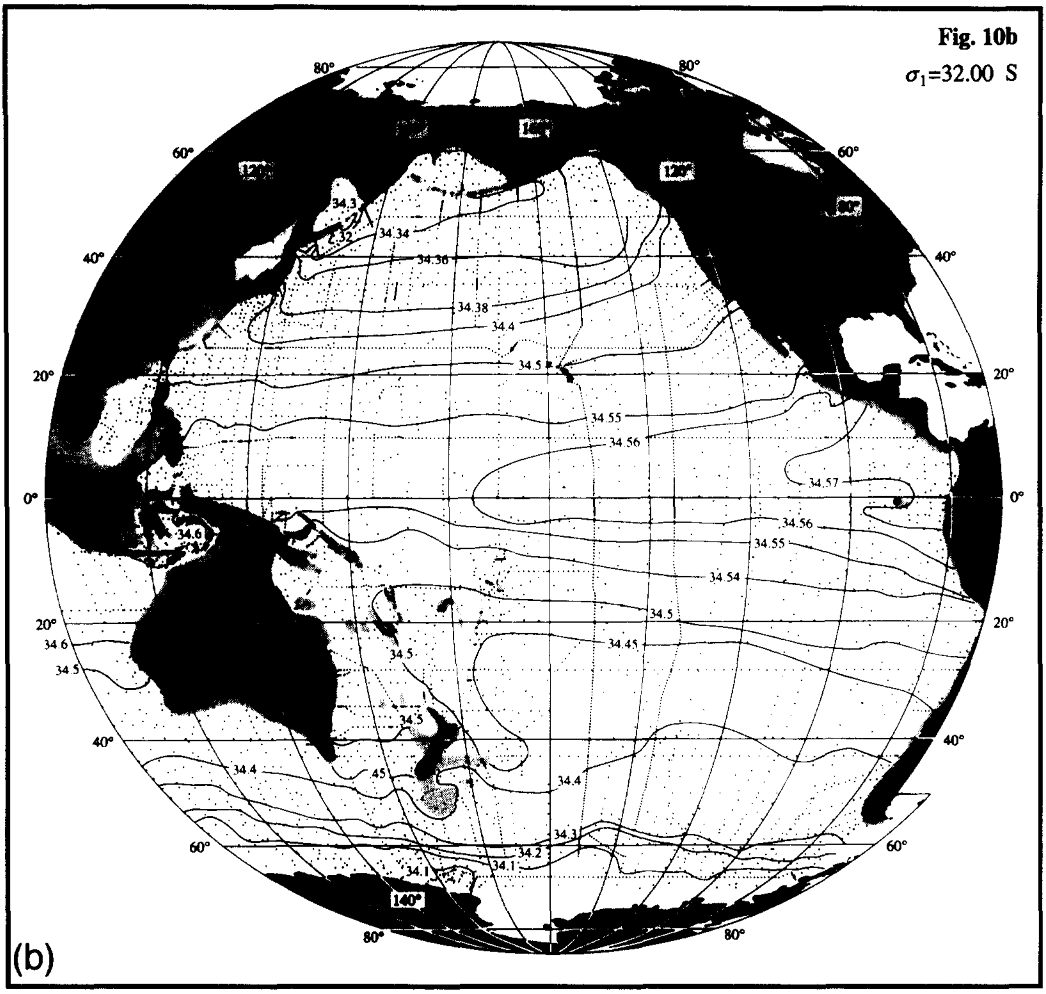

Fig. 10. (b), Salinity on the isopycnal defined by 32.00 in σ_1.

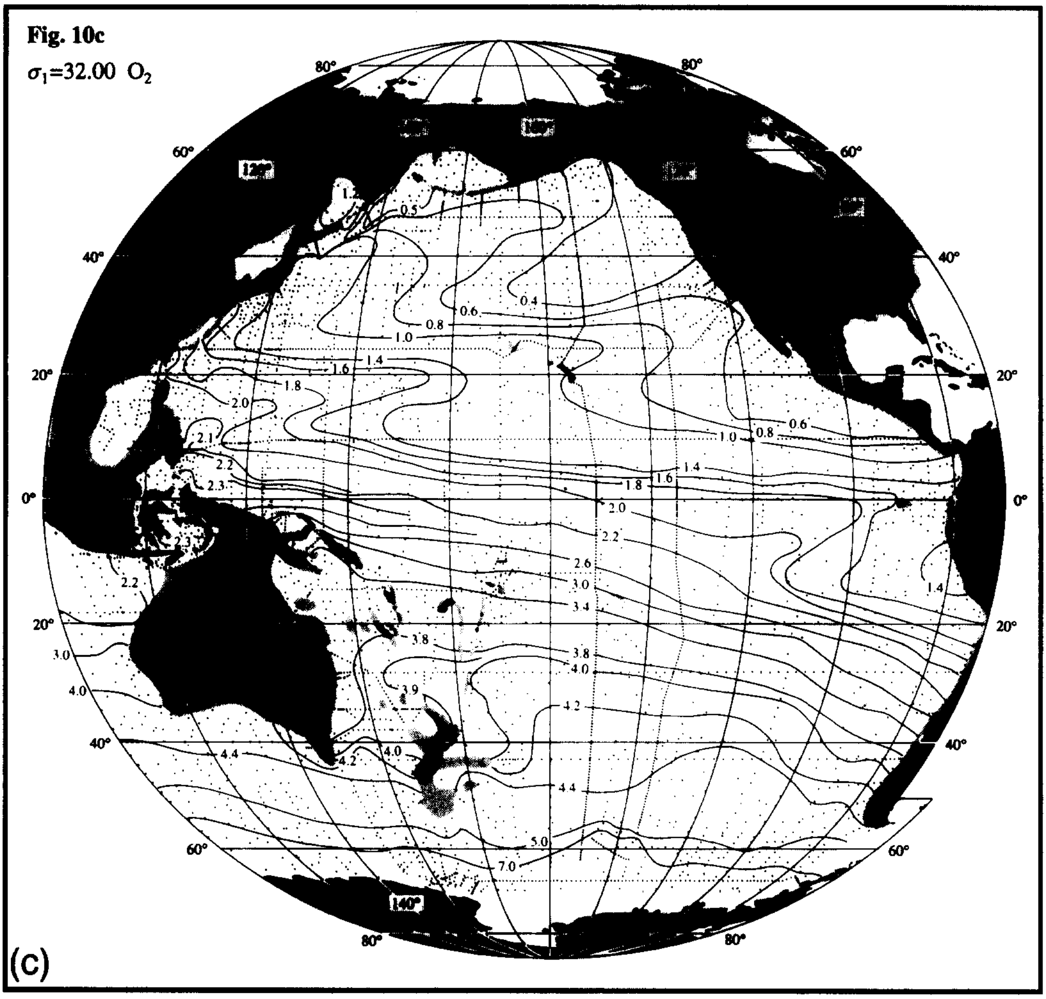

Fig. 10. (c), Oxygen (ml/l) on the isopycnal defined by 32.00 in σ_1.

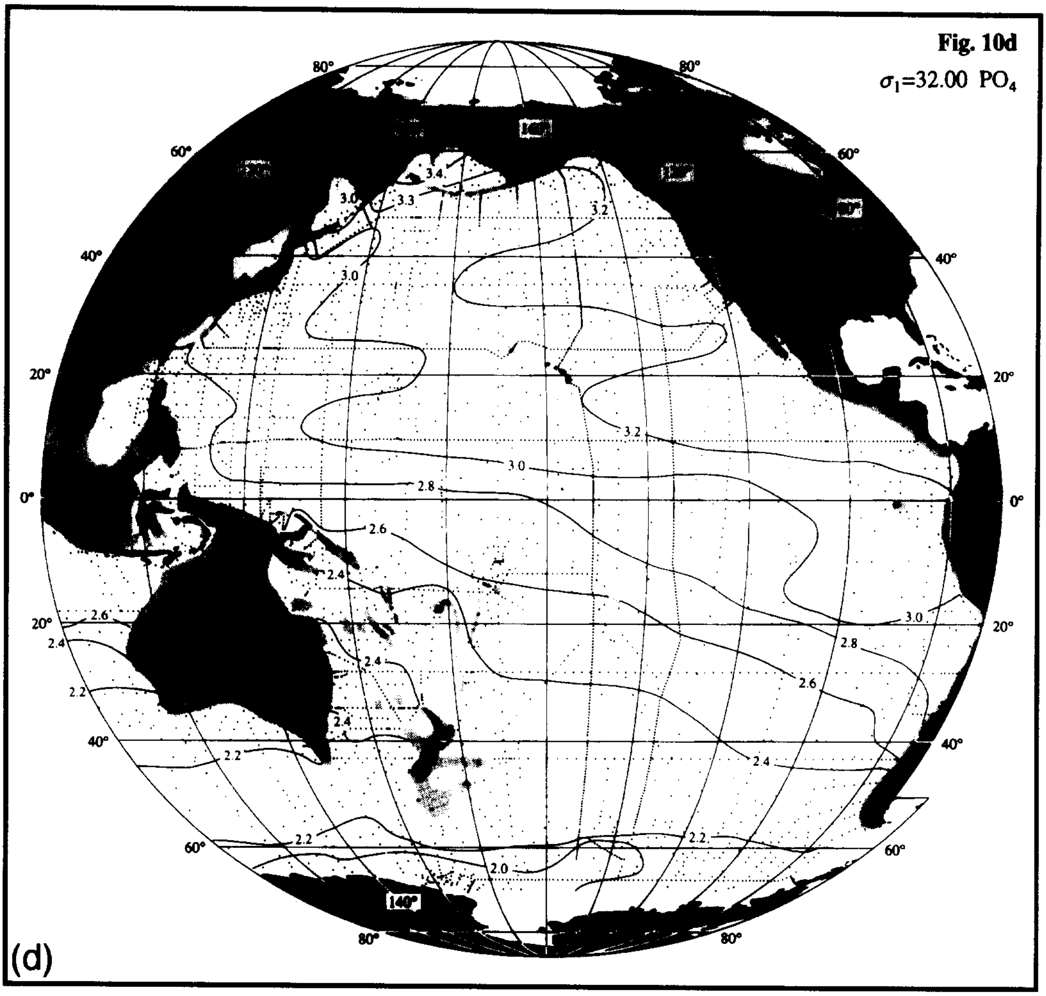

Fig. 10. (d), Phosphate (μm kg^{-1}) on the isopycnal defined by 32.00 in σ_1.

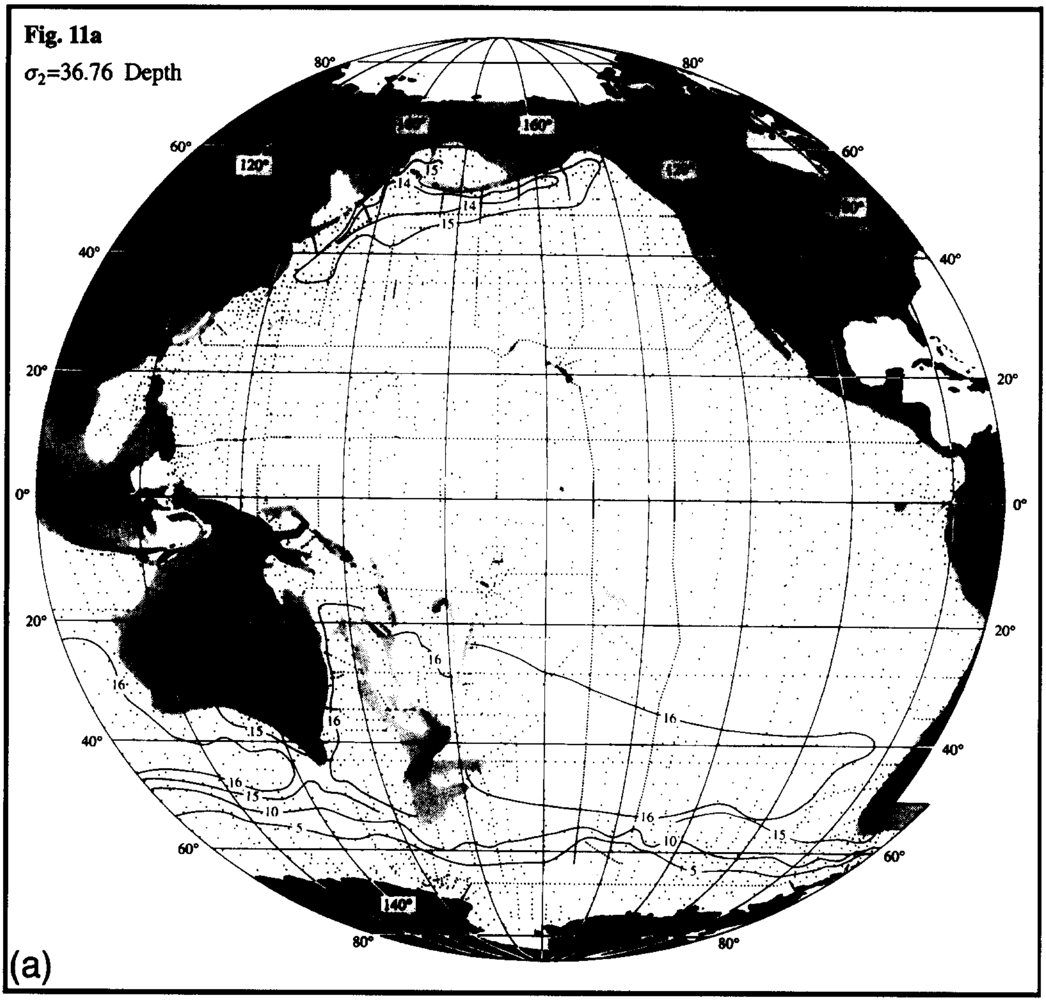

Fig. 11. (a) Depth (hm) of the isopycnal defined by 36.76 in σ_2.

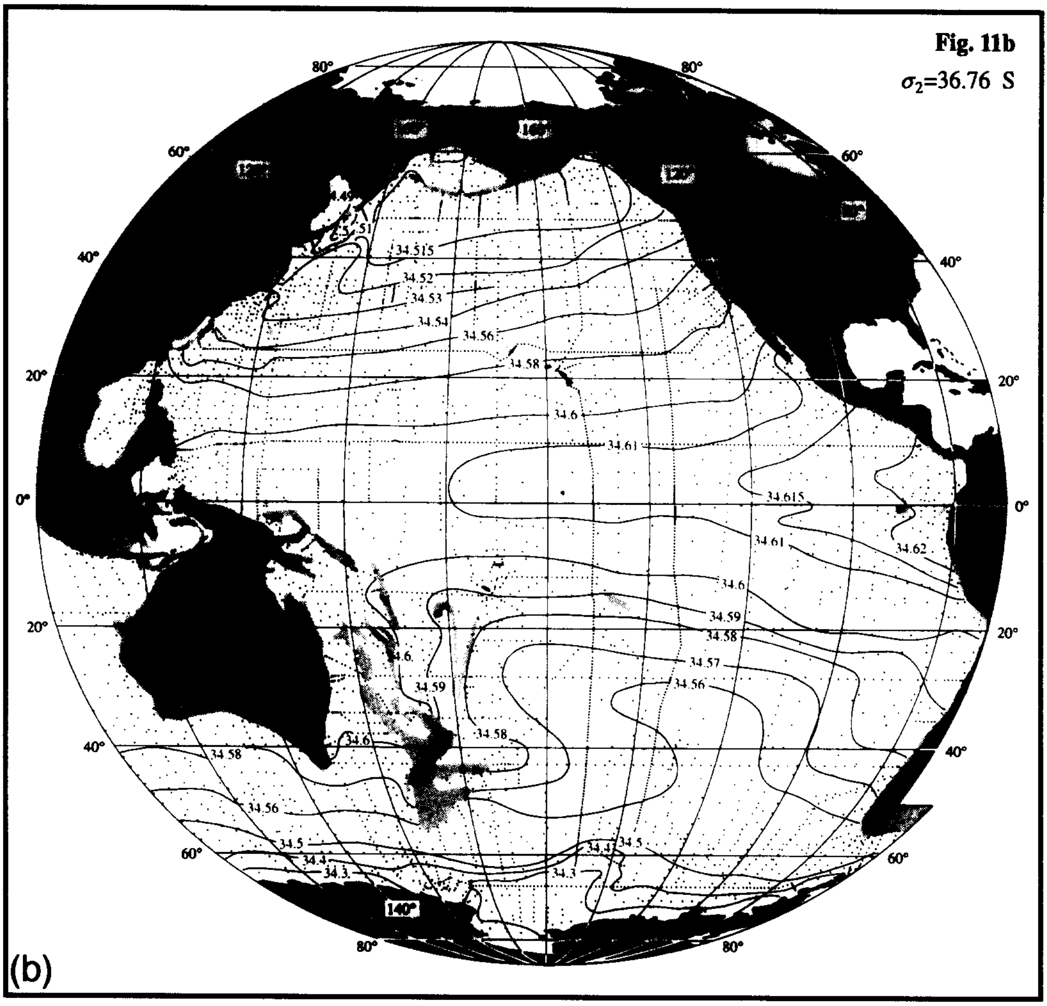

Fig. 11. (b), Salinity on the isopycnal defined by 36.76 in σ_2.

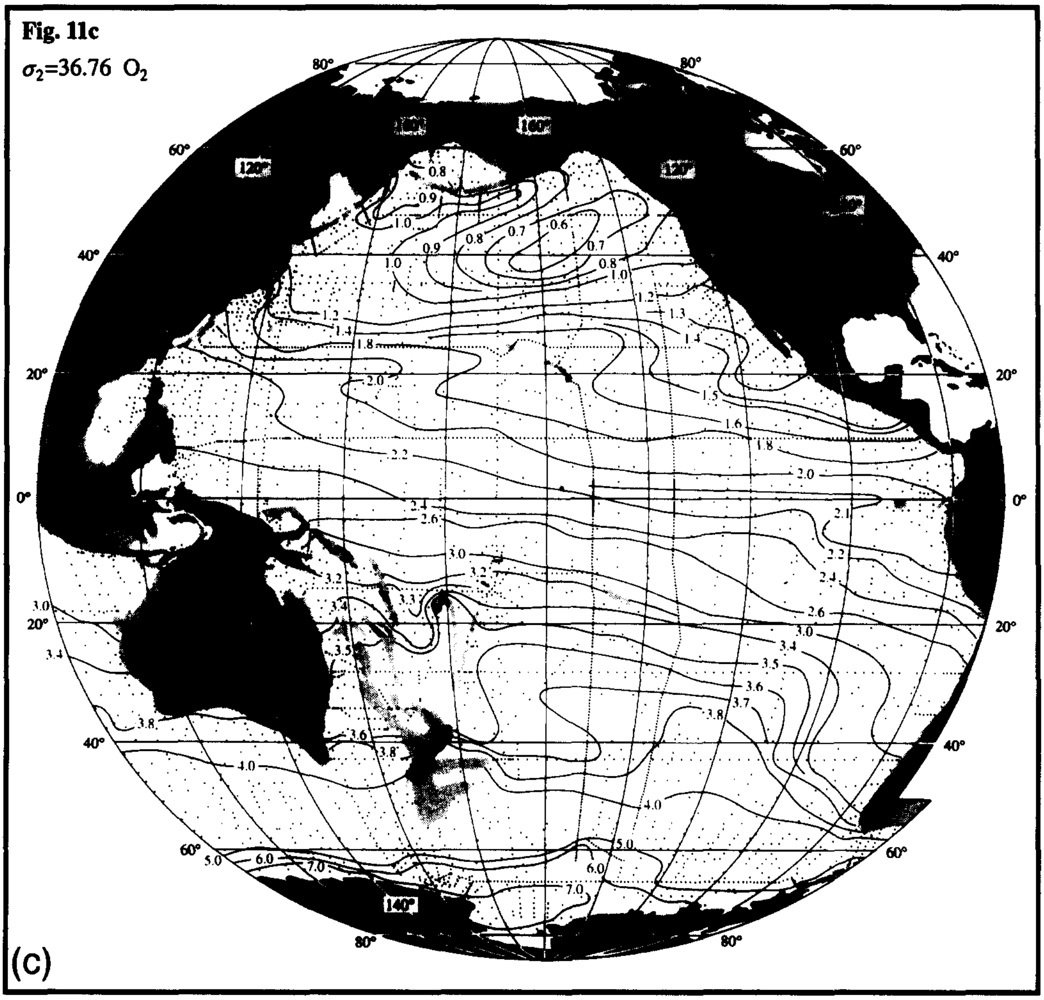

Fig. 11. (c), Oxygen (ml/l) on the isopycnal defined by 36.76 in σ_2.

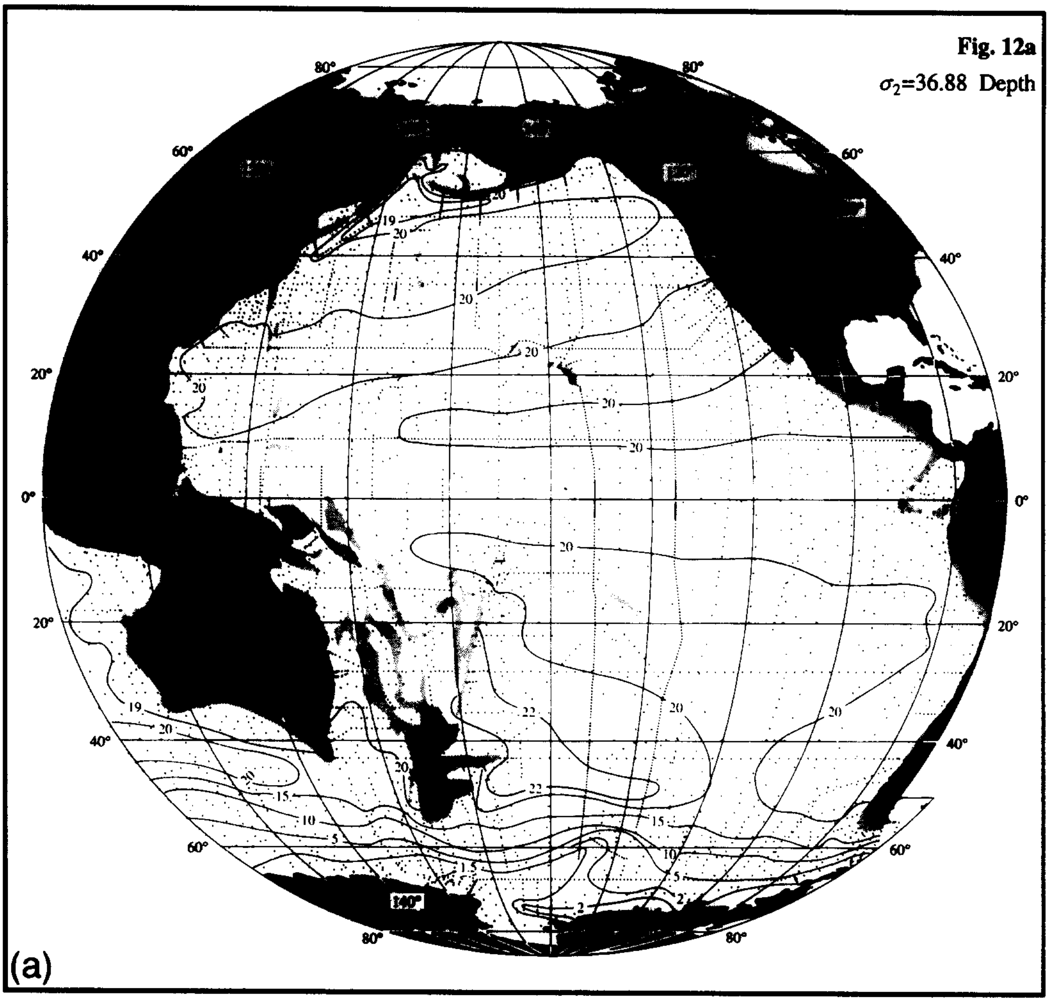

Fig. 12. (a) Depth (hm) of the isopycnal defined by 36.88 in σ_2.

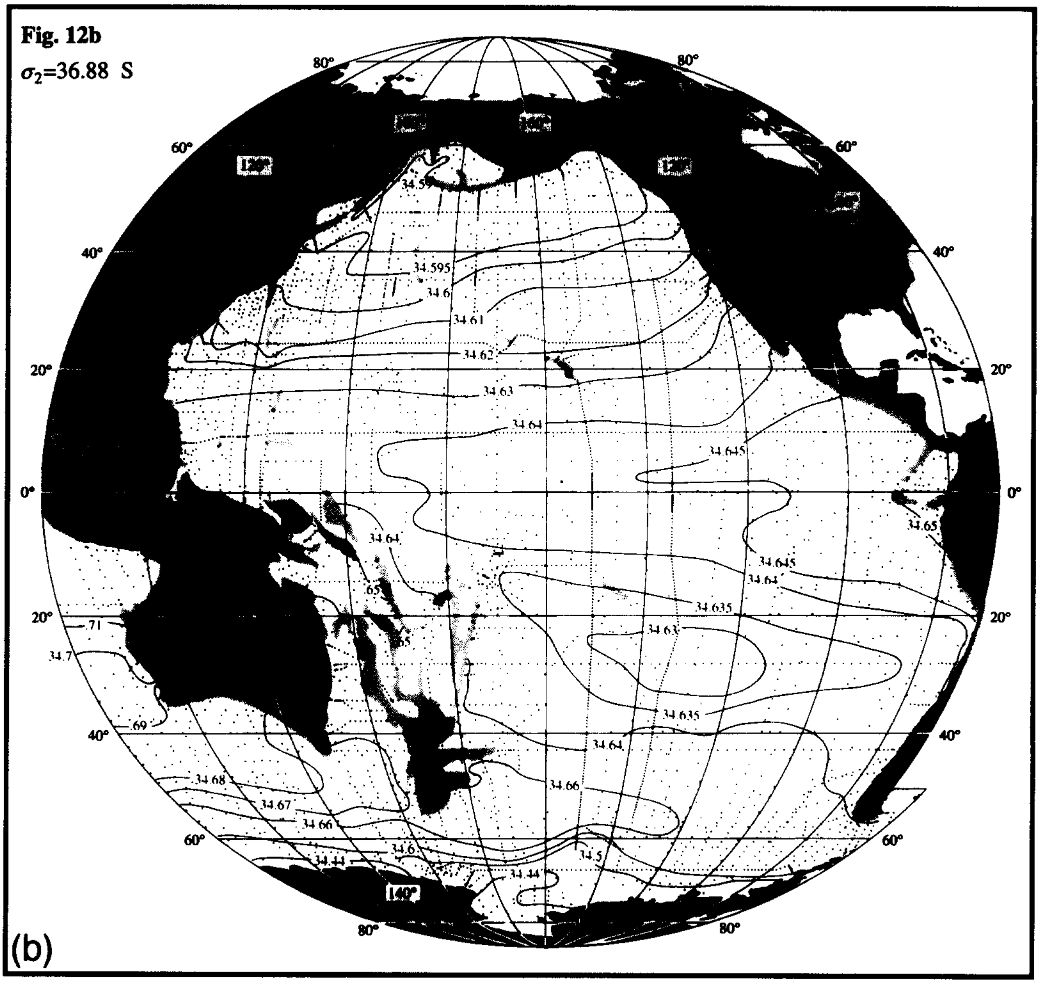

Fig. 12. (b), Salinity on the isopycnal defined by 36.88 in σ_2.

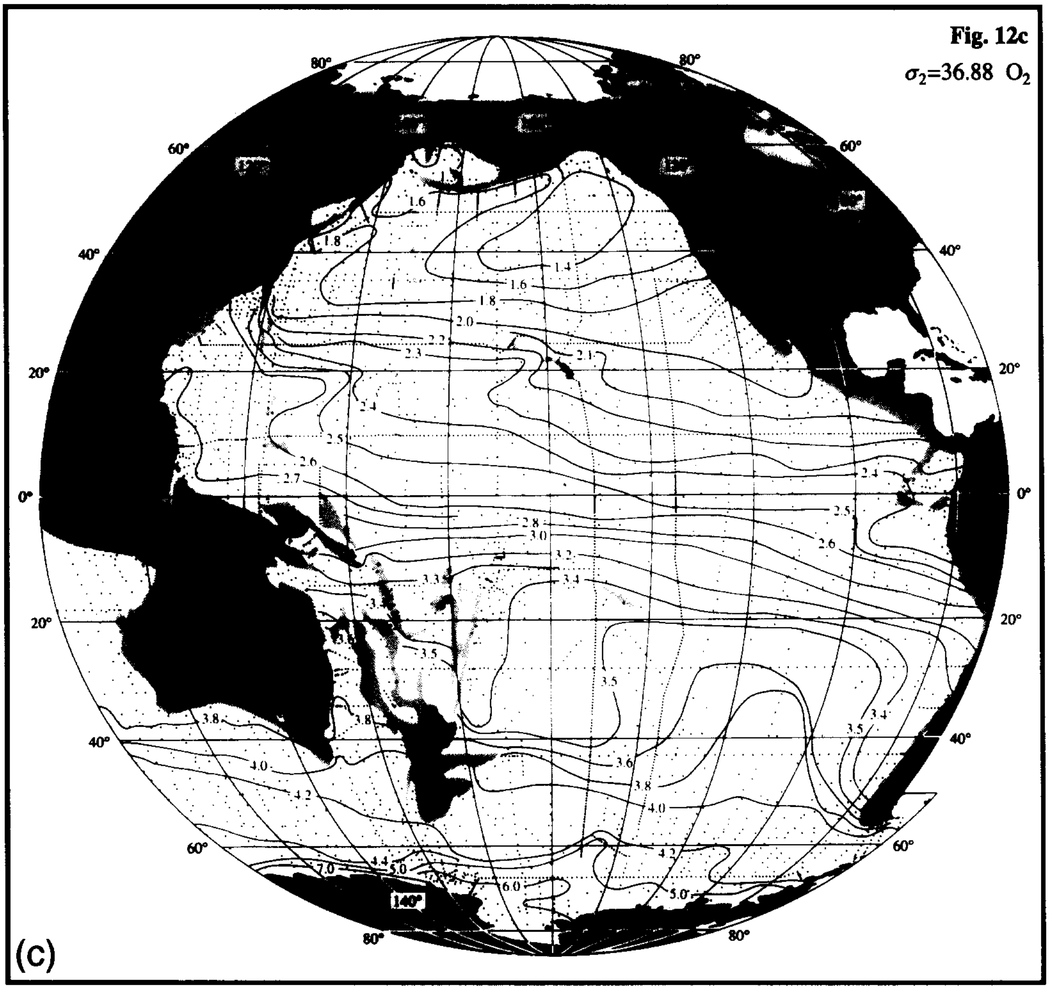

Fig. 12. (c), Oxygen (ml/l) on the isopycnal defined by 36.88 in σ_2.

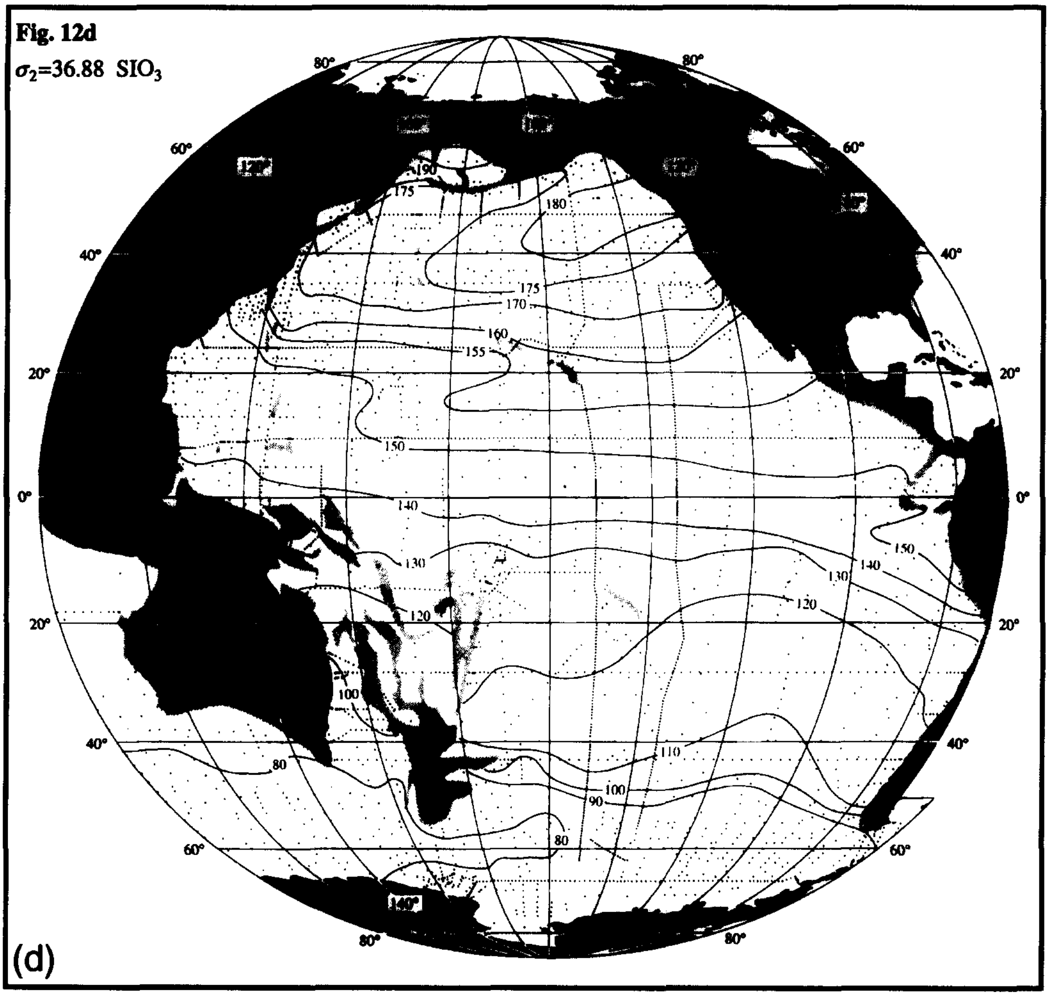

Fig. 12. (d), Silica (μm kg^{-1}) on the isopycnal defined by 36.88 in σ_2.

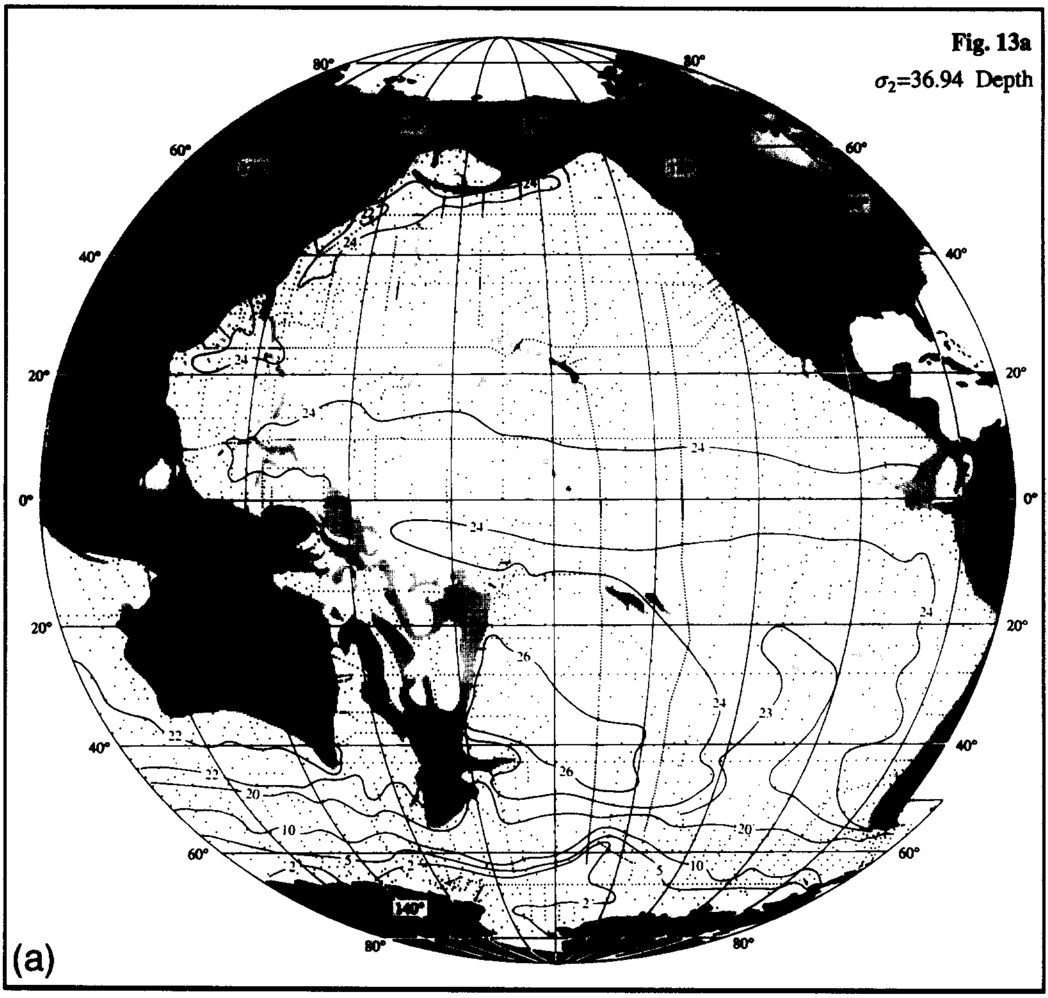

Fig. 13. (a) Depth (hm) of the isopycnal defined by 36.94 in σ_2.

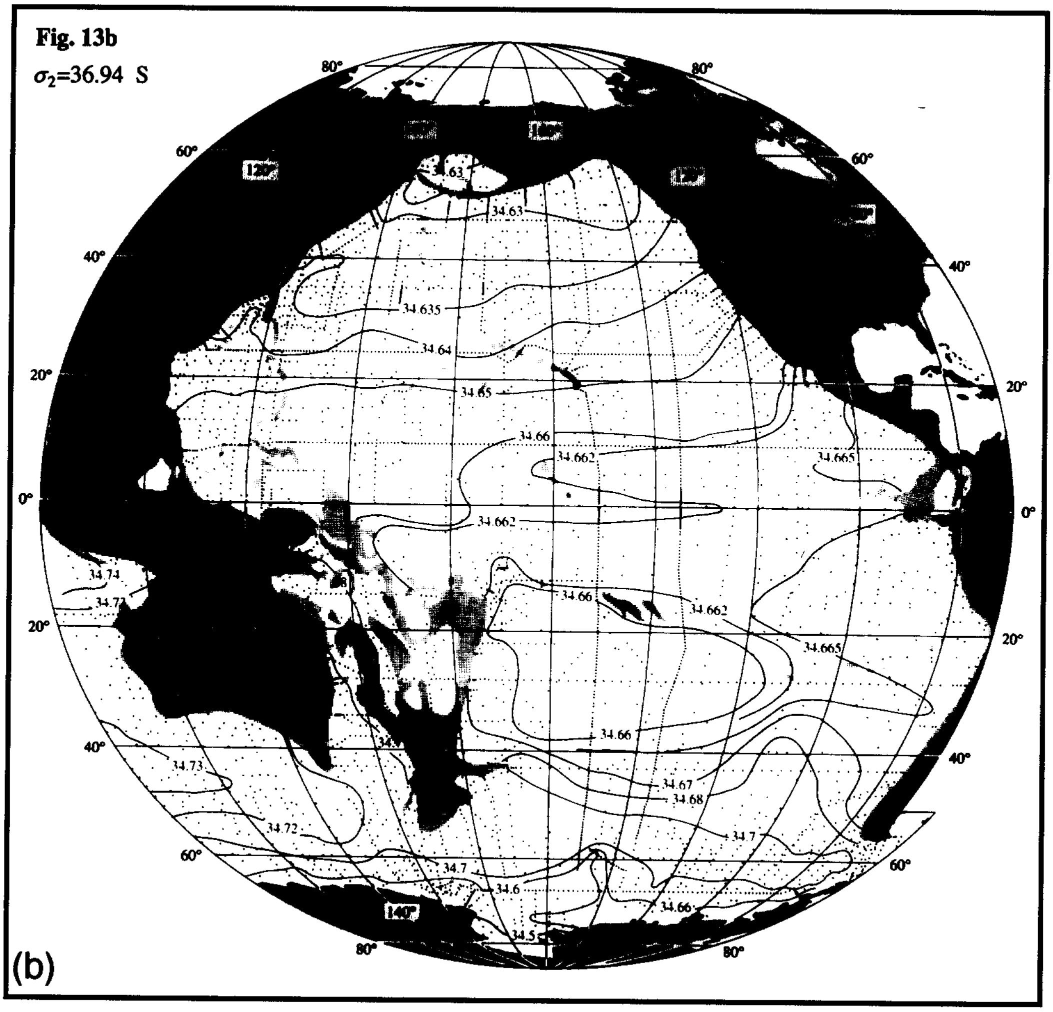

Fig. 13. (b), Salinity on the isopycnal defined by 36.94 in σ_2.

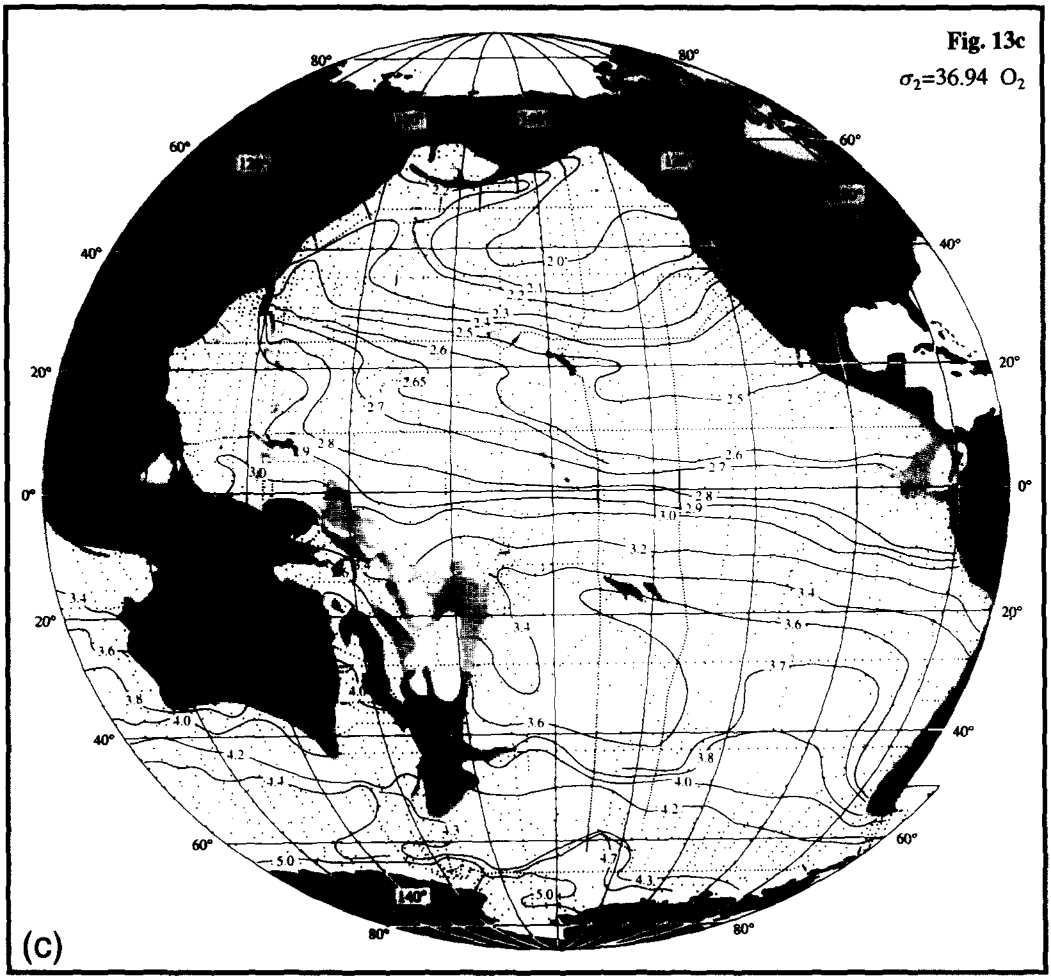

Fig. 13. (c), Oxygen (ml/l) on the isopycnal defined by 36.94 in σ_2.

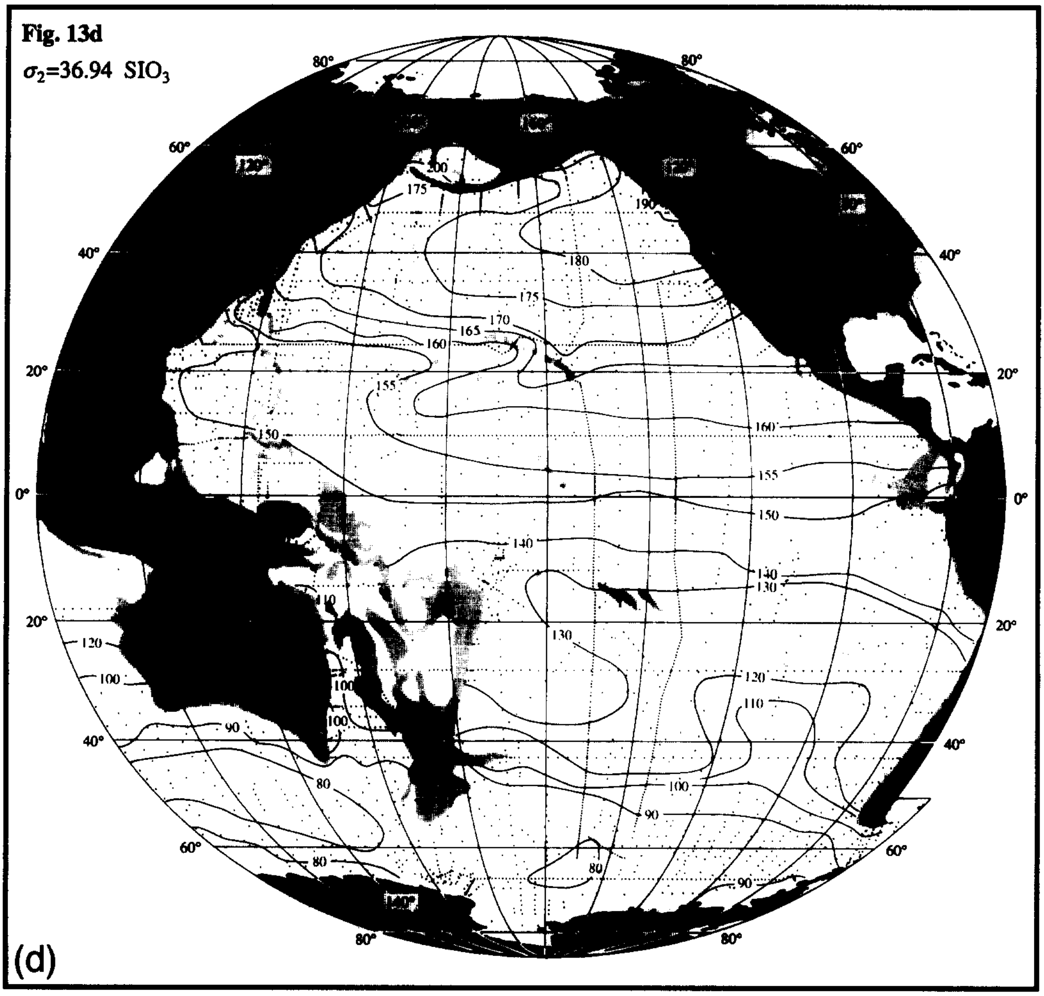

Fig. 13. (d), Silica (μm kg^{-1}) on the isopycnal defined by 36.94 in σ_2.

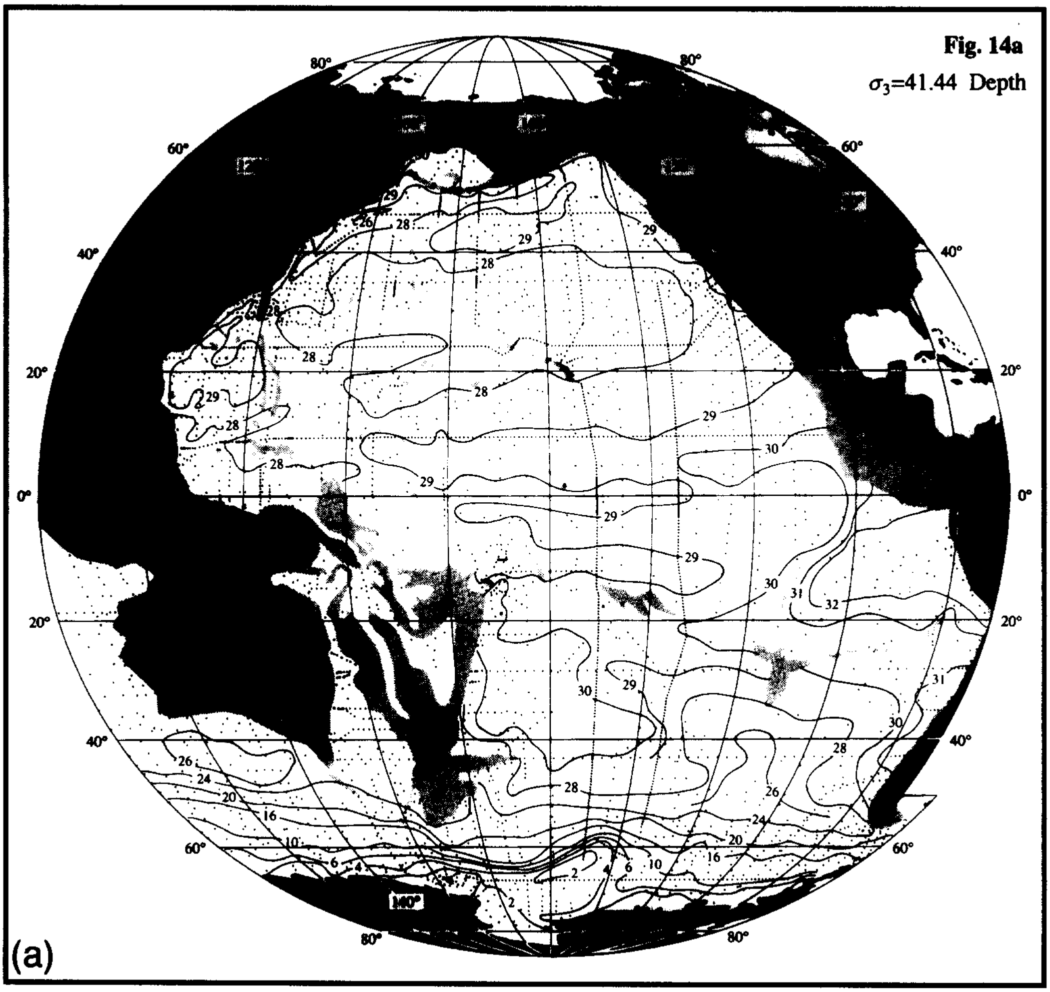

Fig. 14. (a) Depth (hm) of the isopycnal defined by 41.44 in σ_3.

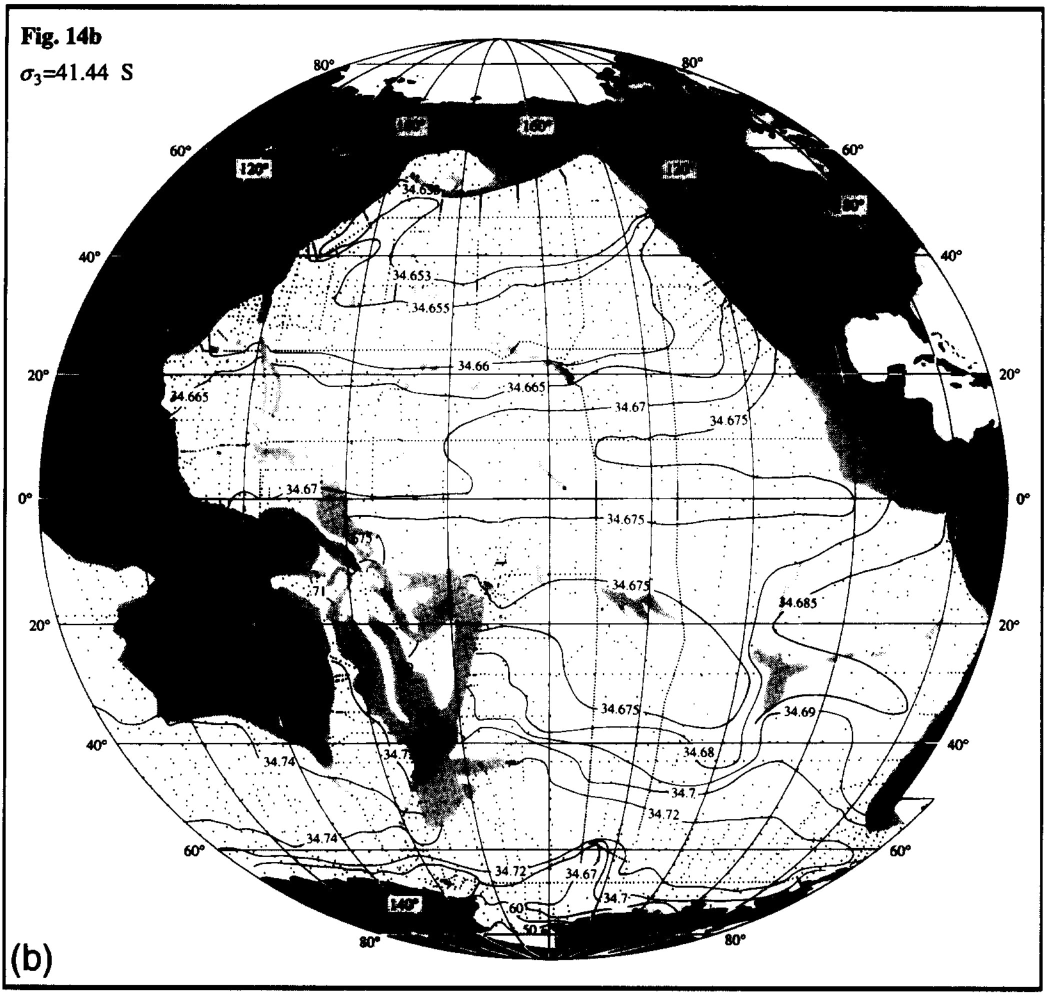

Fig. 14. (b), Salinity on the isopycnal defined by 41.44 in σ_3.

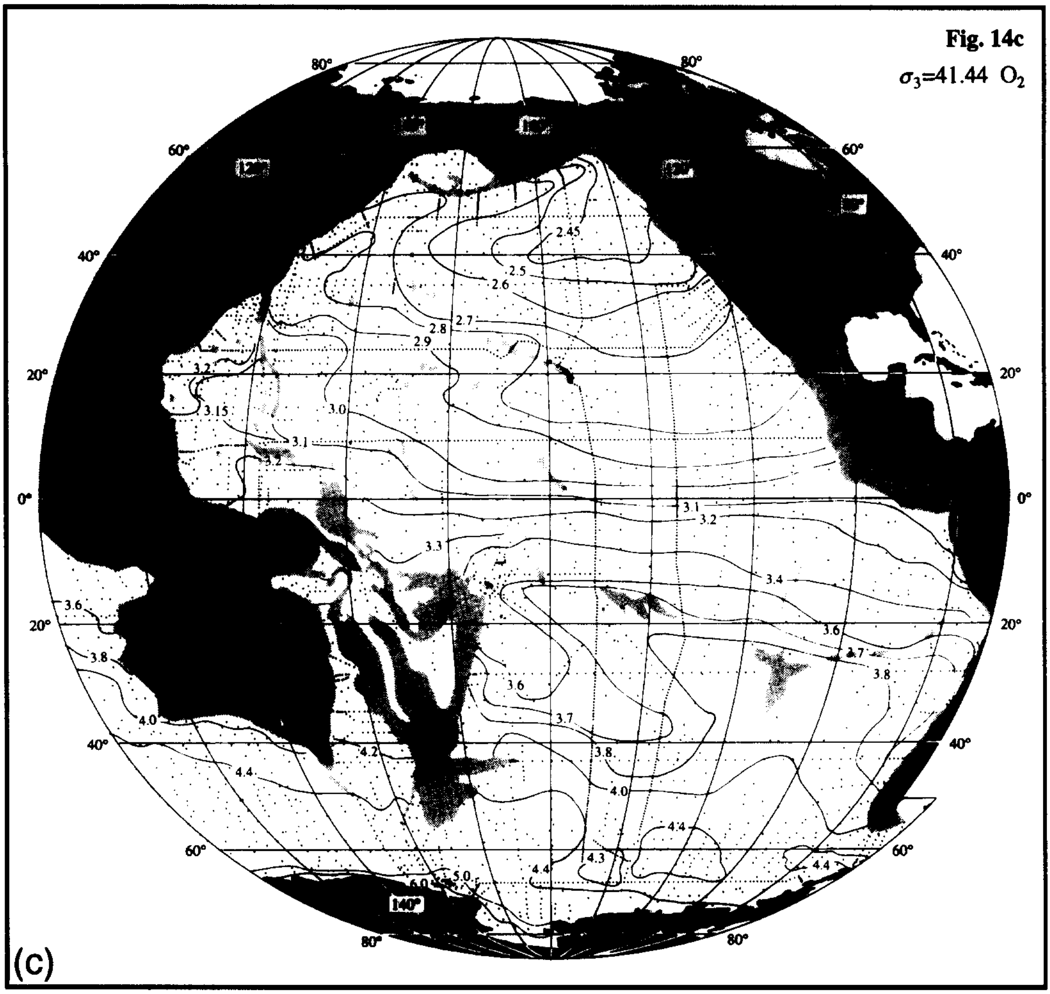

Fig. 14. (c), Oxygen (ml/l) on the isopycnal defined by 41.44 in σ_3.

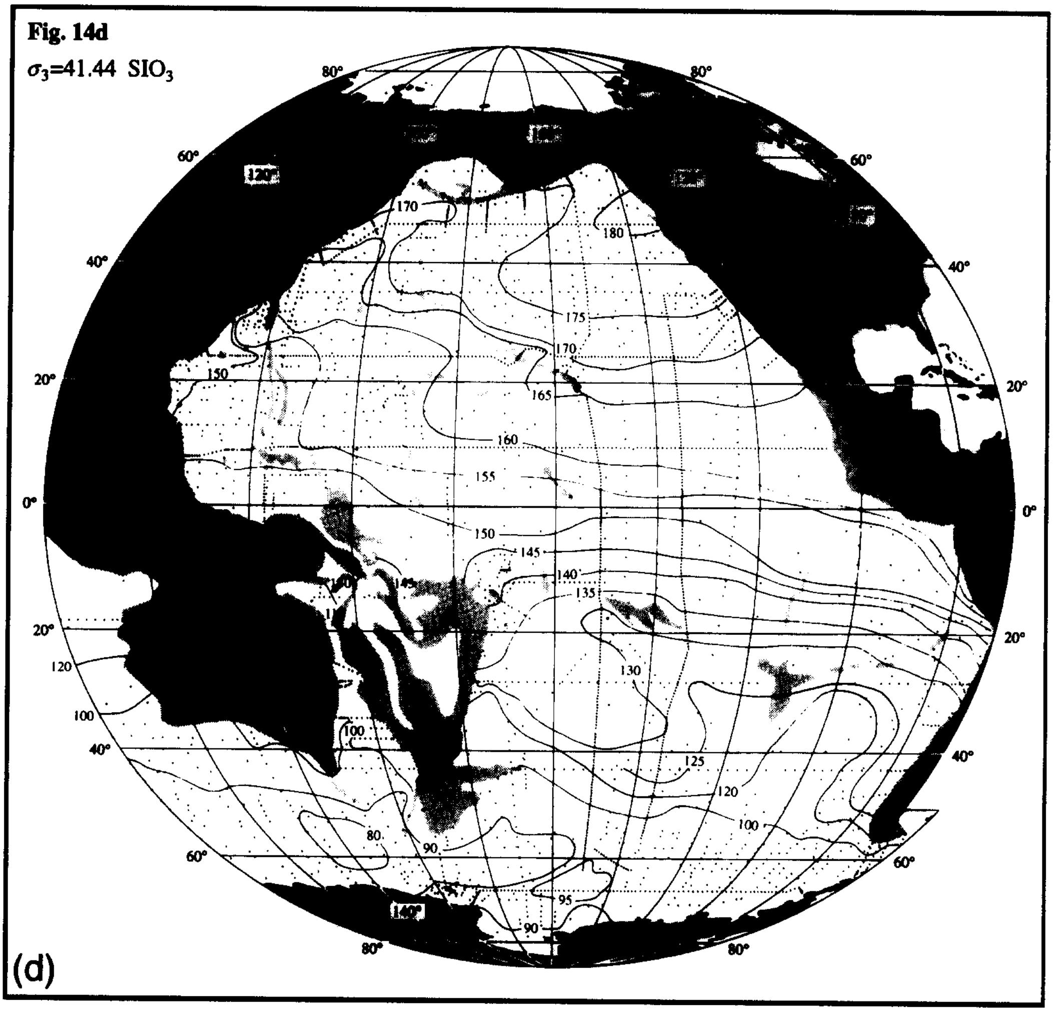

Fig. 14. (d), Silica (μm kg^{-1}) on the isopycnal defined by 41.44 in σ_3.

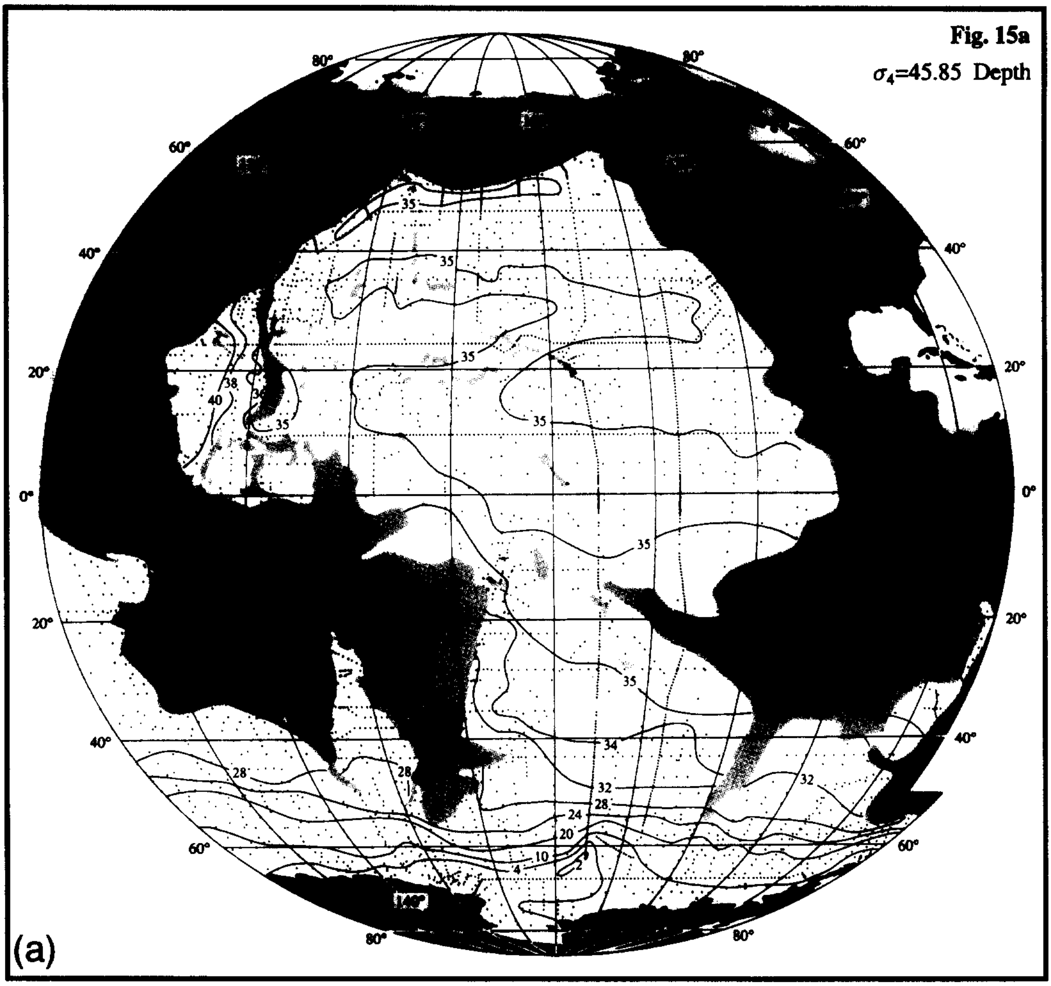

Fig. 15. (a) Depth (hm) of the isopycnal defined by 45.85 in σ_4.

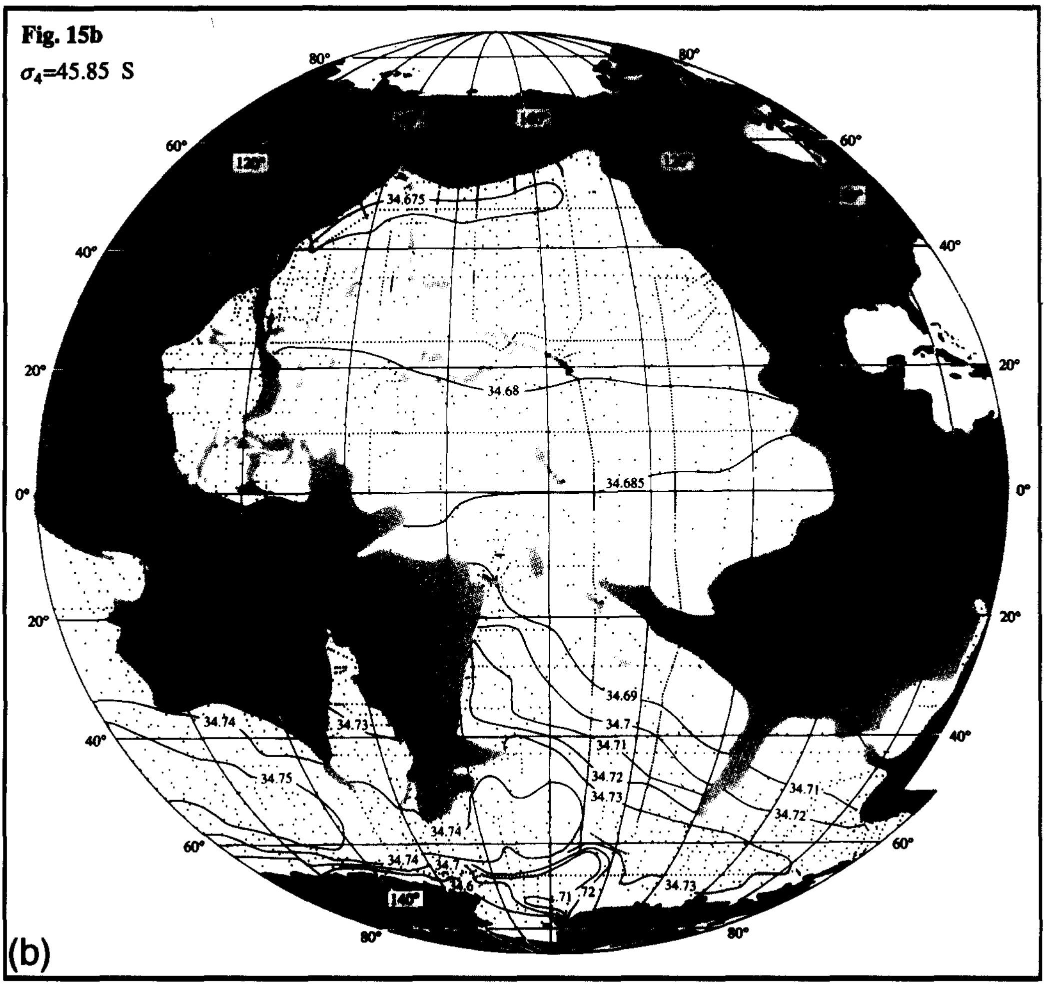

Fig. 15. (b), Salinity on the isopycnal defined by 45.85 in σ_4.

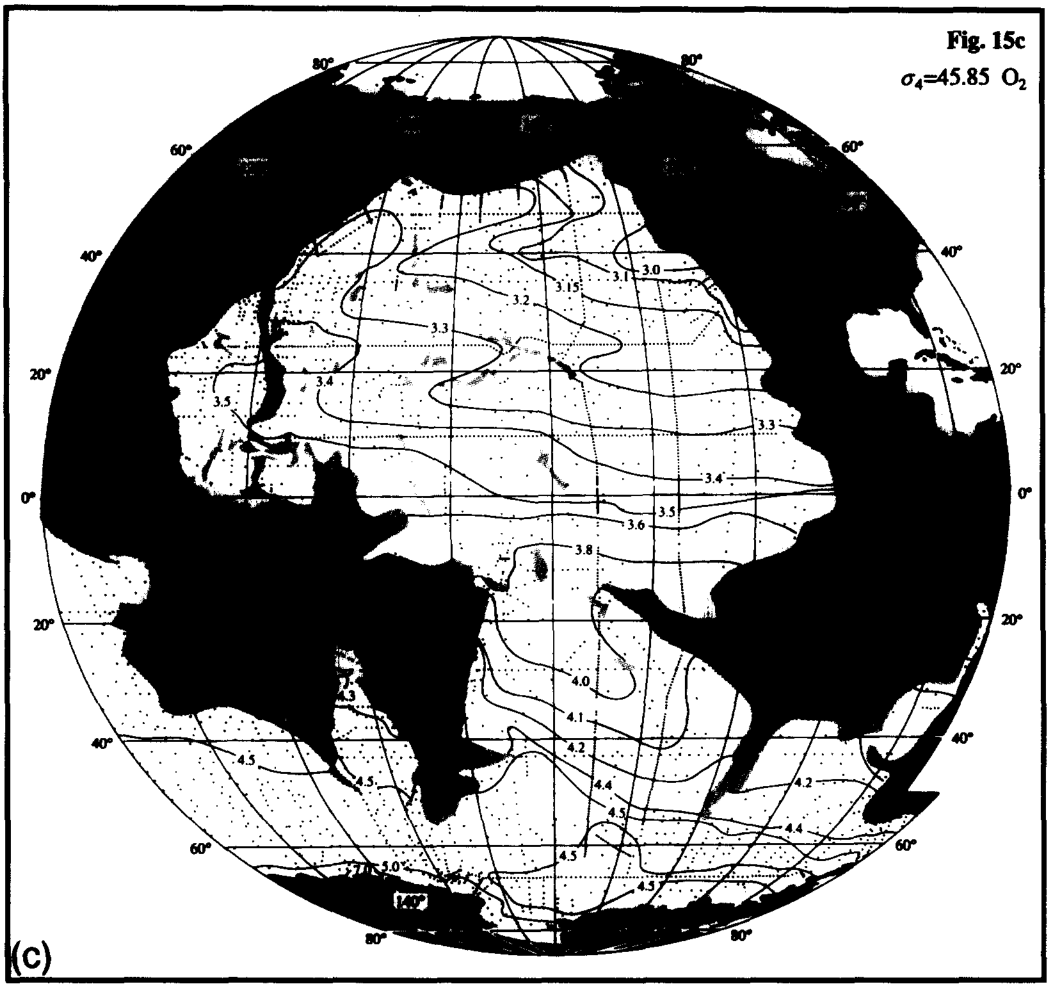

Fig. 15. (c), Oxygen (ml/l) on the isopycnal defined by 45.85 in σ_4.

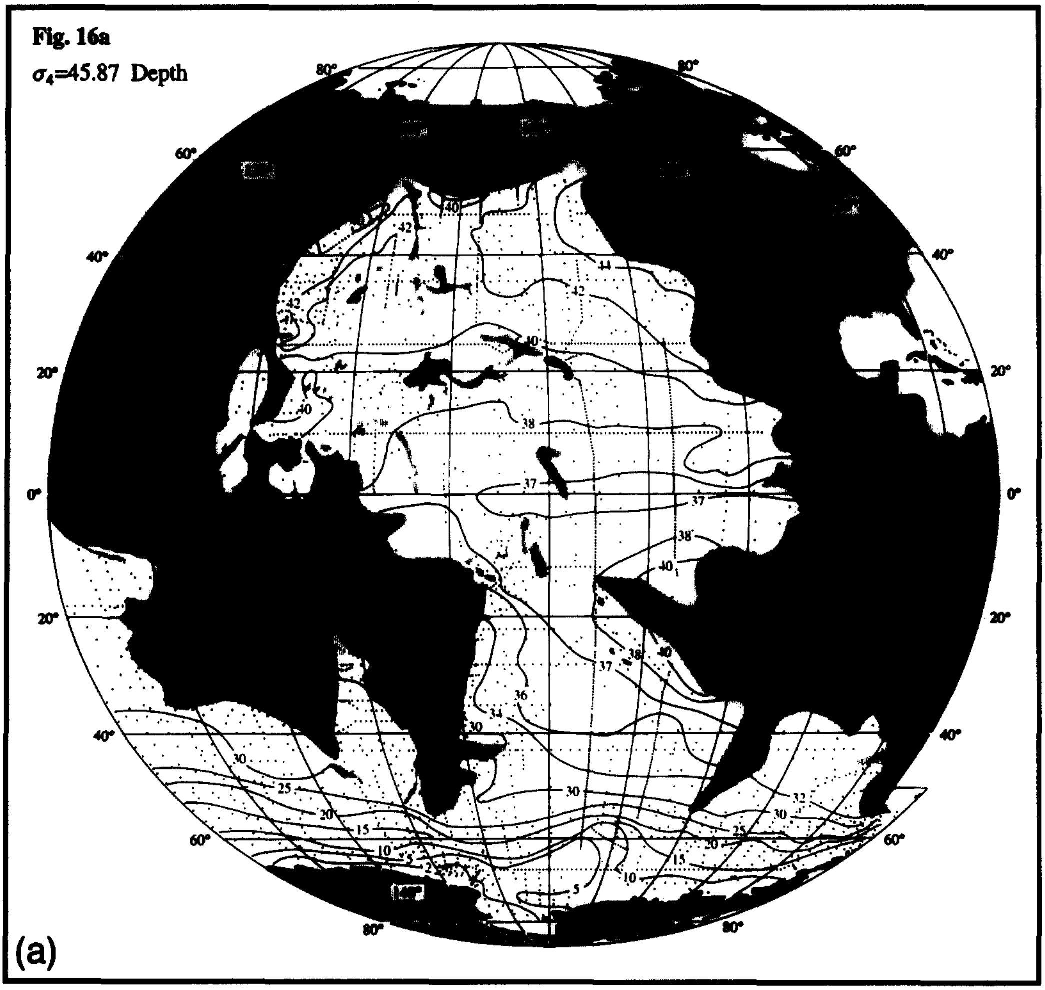

Fig. 16. (a) Depth (hm) of the isopycnal defined by 45.87 in σ_4.

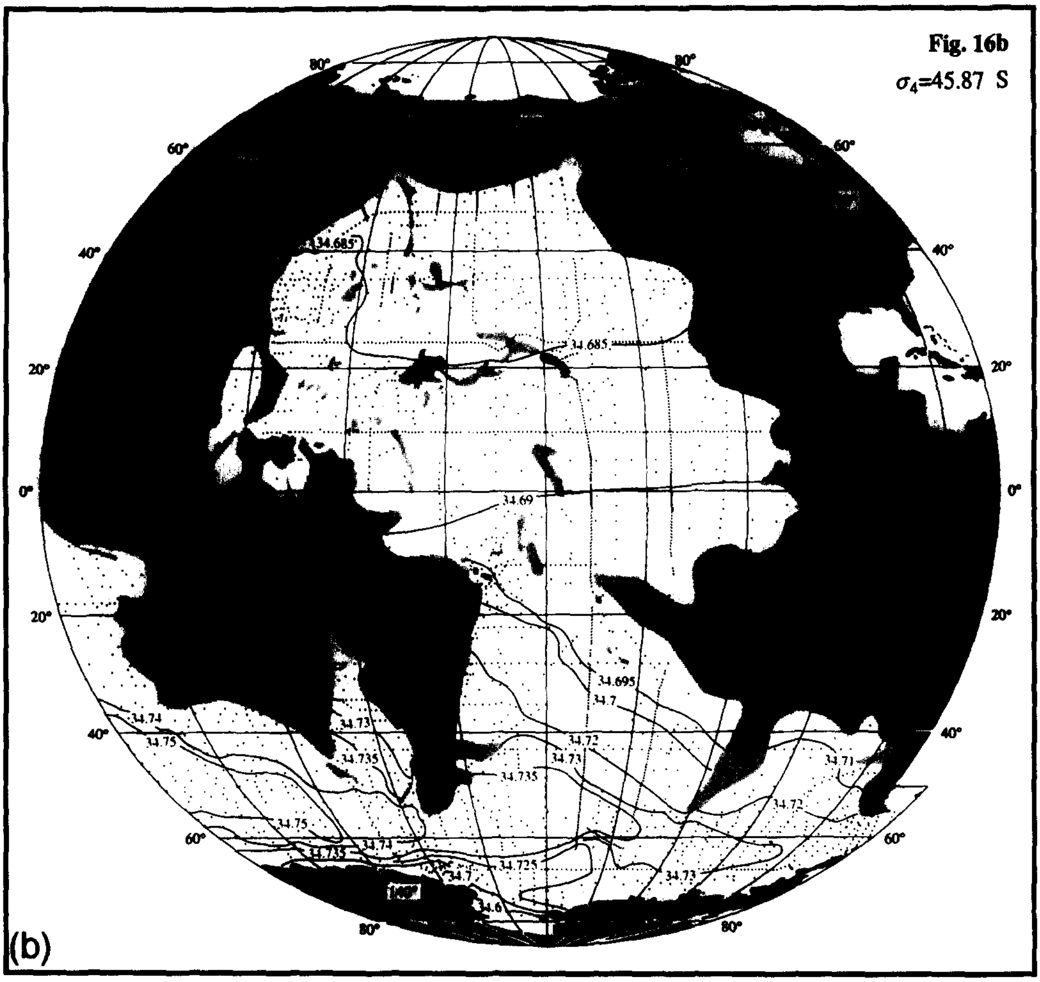

Fig. 16. (b), Salinity on the isopycnal defined by 45.87 in σ_4.

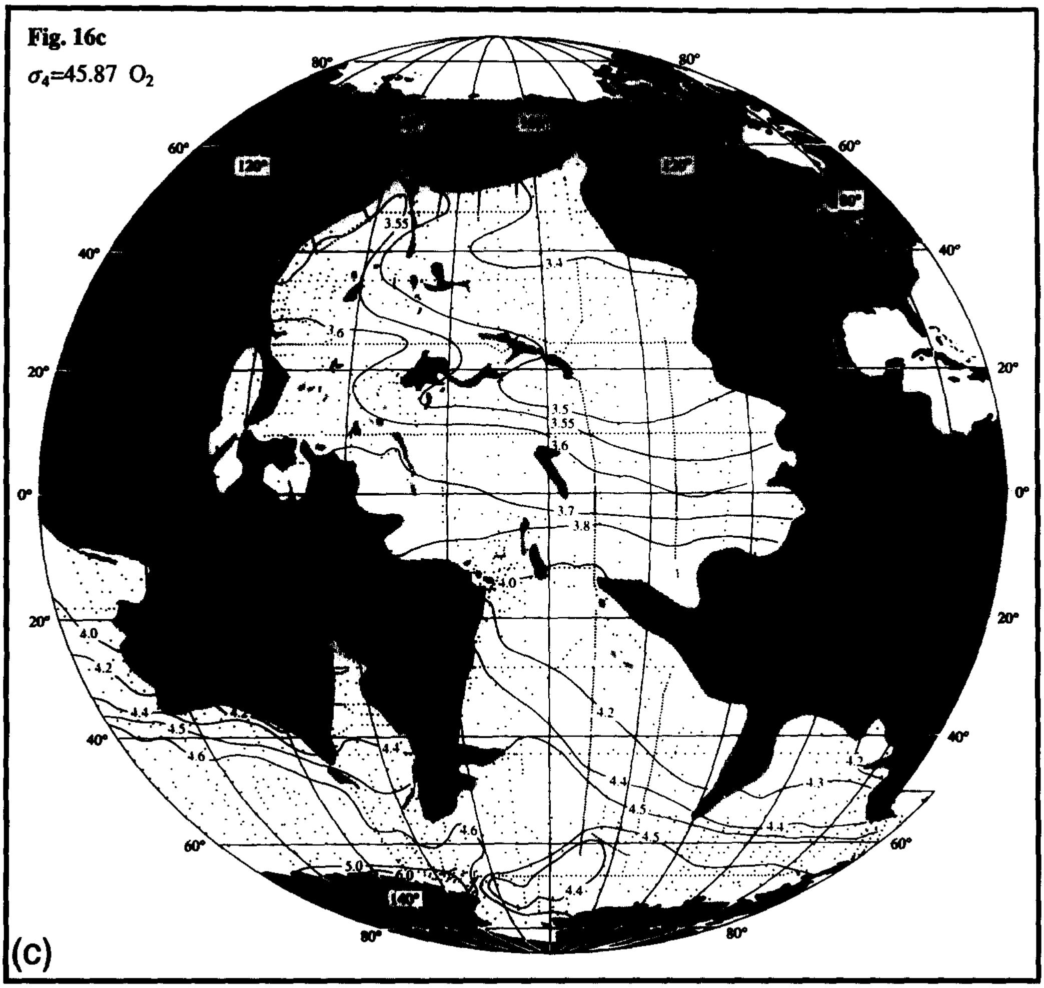

Fig. 16. (c), Oxygen (ml/l) on the isopycnal defined by 45.87 in σ_4.

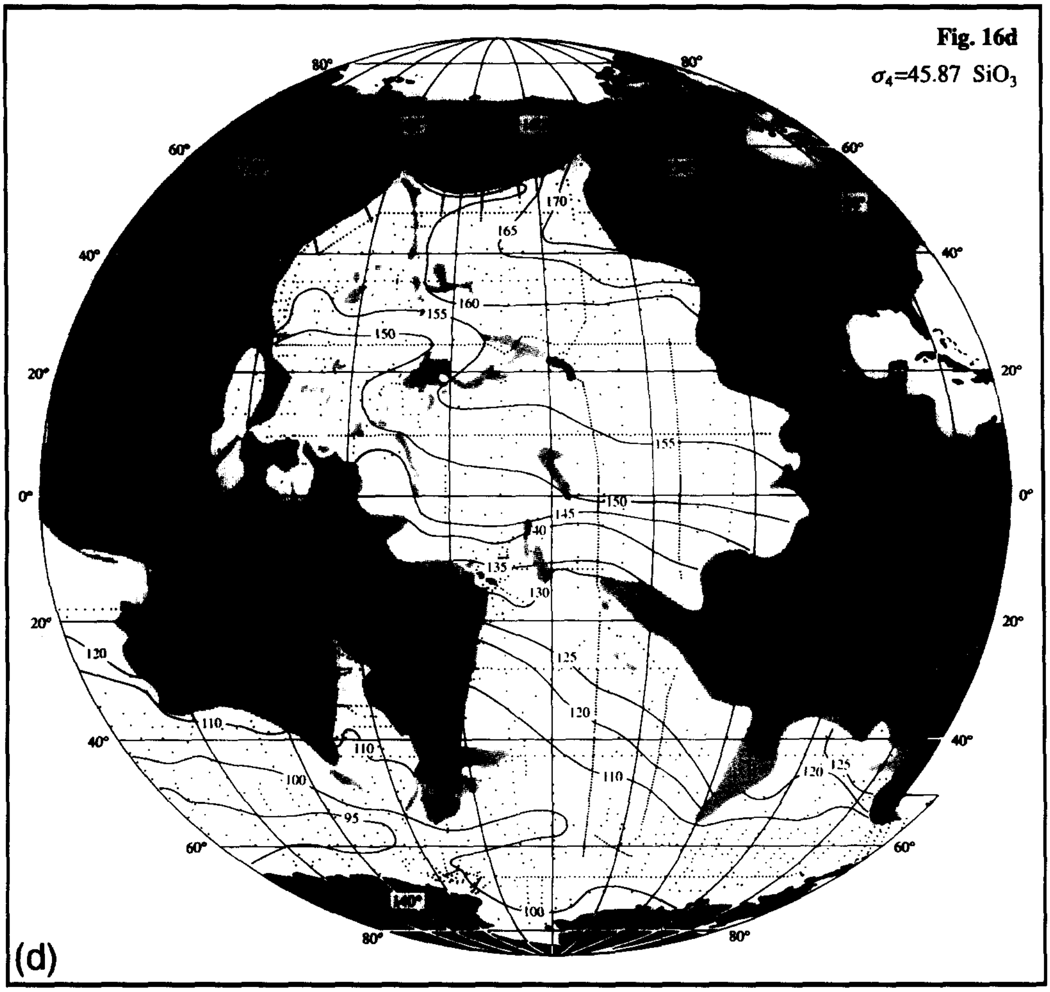

Fig. 16. (d), Silica (μm kg^{-1}) on the isopycnal defined by 45.87 in σ_4.

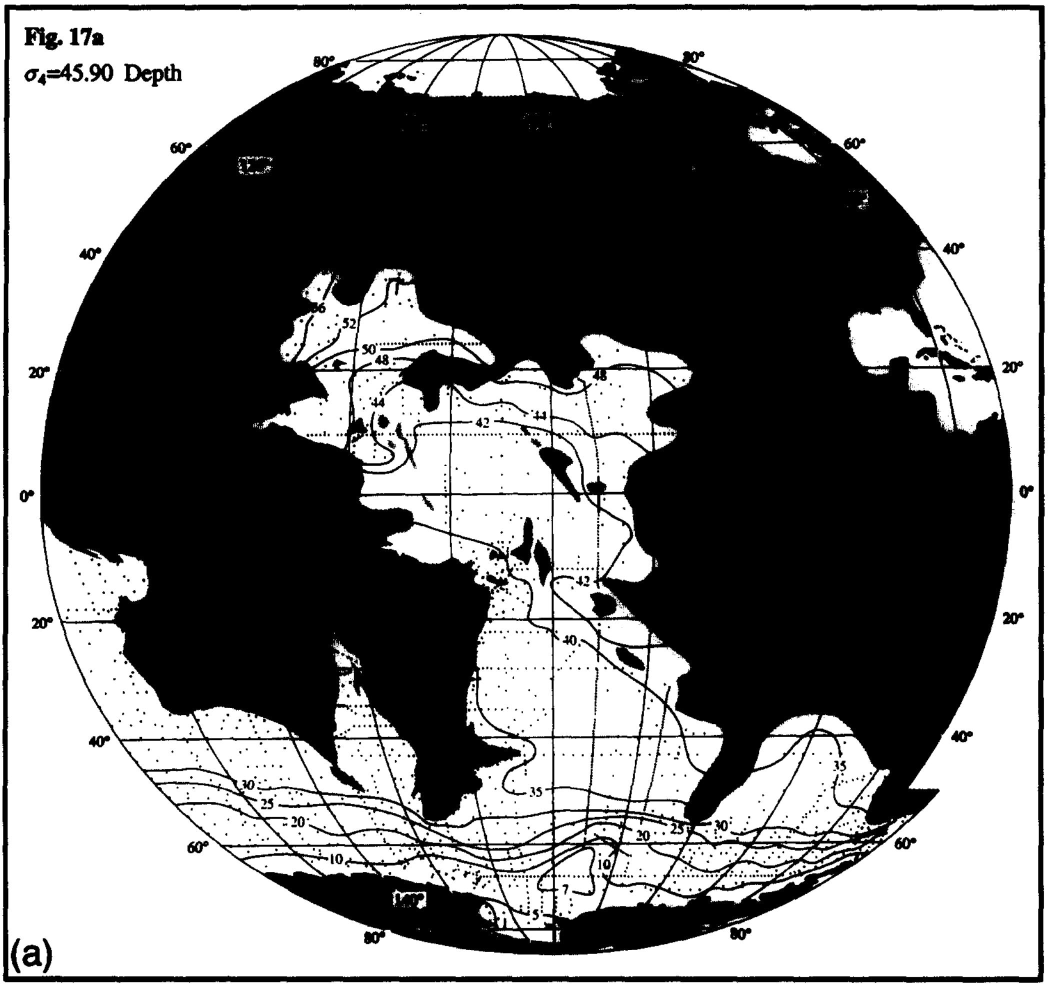

Fig. 17. (a) Depth (hm) of the isopycnal defined by 45.90 in σ_4.

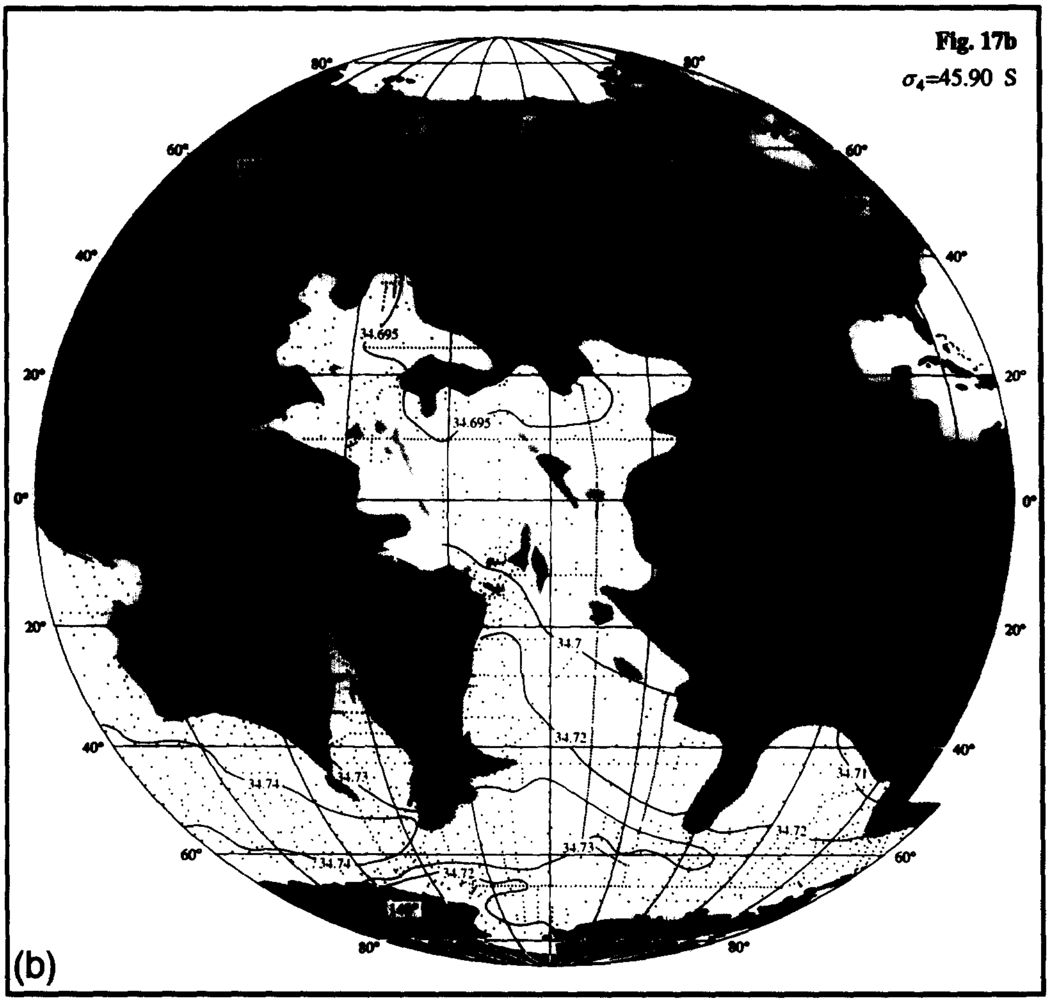

Fig. 17. (b), Salinity on the isopycnal defined by 45.90 in σ_4.

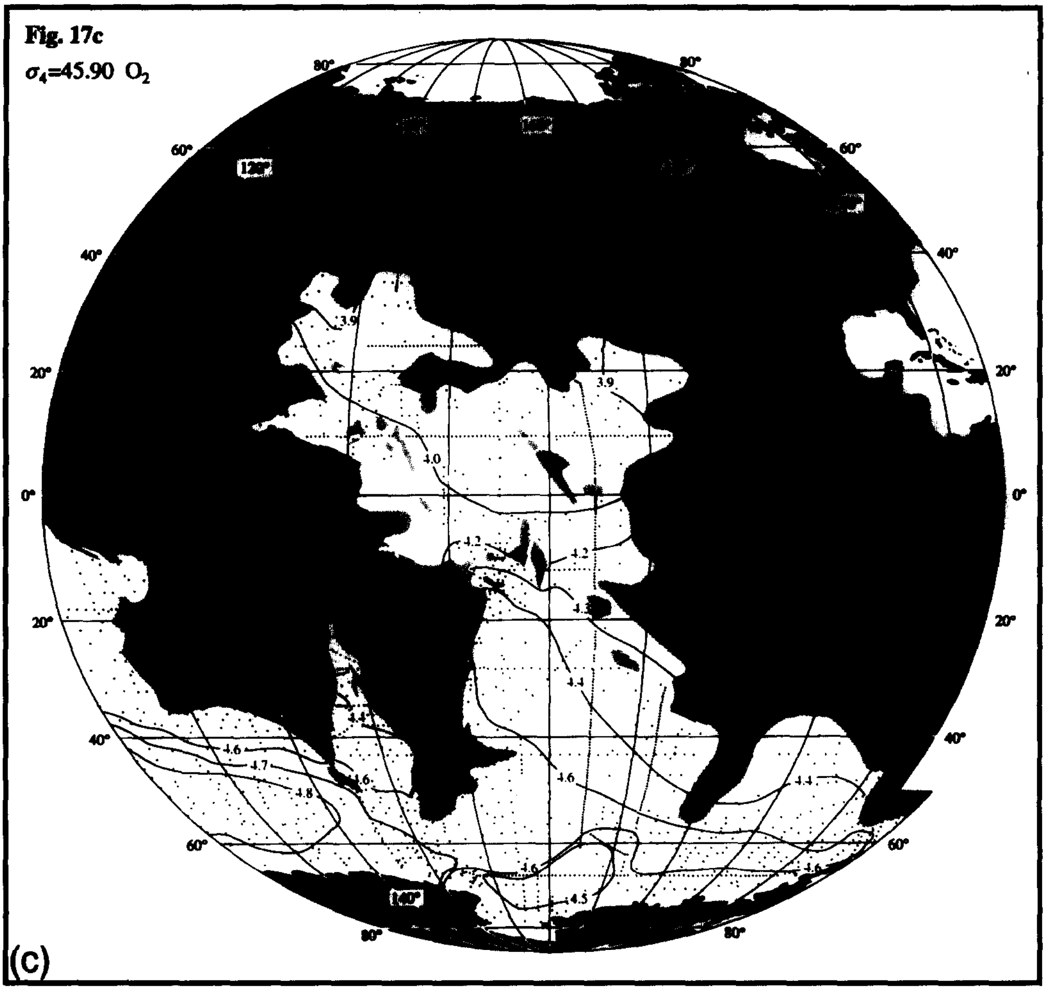

Fig. 17. (c), Oxygen (ml/l) on the isopycnal defined by 45.90 in σ_4.